1521-009X/50/9/1272–1286$35.00
DRUG METABOLISM AND DISPOSITION

dx.doi.org/10.1124/dmd.122.000883
Drug Metab Dispos 50:1272–1286, September 2022

An Improved Method for Cytochrome P450 Reaction Phenotyping Using a Sequential Qualitative-Then-Quantitative Approach

Angela C. Doran, Alyssa L. Dantonio, Gabrielle M. Gualtieri, Amanda Balesano, Connor Landers, Woodrow Burchett, Theunis C. Goosen, and R. Scott Obach

Medicine Design, Pfizer Worldwide Research, Development and Medical, Groton, Connecticut

Received March 2, 2022; accepted May 11, 2022

ABSTRACT

Cytochrome P450 reaction phenotyping to determine the fraction of metabolism (f_m) values for individual enzymes is a standard study in the evaluation of a new drug. However, there are technical challenges in these studies caused by shortcomings in the selectivity of P450 inhibitors and unreliable scaling procedures for recombinant P450 (rCYP) data. In this investigation, a two-step "qualitative-then-quantitative" approach to P450 reaction phenotyping is described. In the first step, each rCYP is tested qualitatively for potential to generate metabolites. In the second step, selective inhibitors for the P450s identified in step 1 are tested for their effects on metabolism using full inhibition curves. Forty-eight drugs were evaluated in step 1 and there were no examples of missing an enzyme important to in vivo clearance. Five drugs (escitalopram, fluvastatin, pioglitazone, propranolol, and risperidone) were selected for full phenotyping in step 2 to determine f_m values, with findings compared with f_m values estimated from single-inhibitor concentration data and rCYP with intersystem extrapolation factor corrections. The two-step approach yielded f_m values for major drug-clearing enzymes that are close to those estimated from clinical data: escitalopram and CYP2C19 (0.42 versus 0.36–0.82), fluvastatin and CYP2C9 (0.76 versus 0.76), pioglitazone and CYP2C8 (0.72 versus 0.73), propranolol and CYP2D6 (0.68 versus 0.37–0.56) and risperidone and CYP2D6 (0.60 versus 0.66–0.88). Reaction phenotyping data generated in this fashion should offer better input to physiologically based pharmacokinetic models for prediction of drug-drug interaction and impact of genetic polymorphisms on drug clearance. The qualitative-then-quantitative approach is proposed as a replacement to standard reaction phenotyping strategies.

SIGNIFICANCE STATEMENT

Cytochrome P450 reaction phenotyping is important for projecting drug-drug interactions and interpatient variability in drug exposure. However, currently recommended practices can frequently fail to provide reliable estimates of fractional contributions to (f_m) of specific P450 enzymes to drug clearance. In this report, we describe a two-step qualitative-then-quantitative reaction phenotyping approach that yields more accurate estimates of f_m.

Introduction

Pharmacokinetic drug-drug interactions (DDI), wherein one drug (the "perpetrator" or "precipitant") alters the clearance of a second drug (the "victim" or "object"), is important in pharmacotherapy and new drug development. This can occur by a variety of mechanisms, but the most common is when an enzyme responsible for metabolism of a victim drug is inhibited or inactivated by a perpetrator drug. The potential magnitude of a DDI depends on the relative fractional contributions of individual enzymes to the metabolic clearance of the victim drug (f_m), as well as concentration and potency of the perpetrator drug, as described in the following equation (Rowland and Matin, 1973):

$$\mathrm{DDI} = \frac{1}{\left(\frac{f_m}{1+\left(\frac{[I]}{K_i}\right)}\right)+(1-f_m)} \quad (1)$$

Thus, the larger the value for f_m, the larger the potential DDI can be. This concept can be extended to pharmacogenetics to understand the potential magnitude of differences in exposure to a drug that is metabolized by a drug-metabolizing enzyme subject to genetic polymorphism. This simple concept can be further complicated by application of the extended clearance concept wherein drug transport processes can have an impact on overall clearance, and thus enhance or temper the magnitude of DDI caused by alterations in metabolism (Yoshida et al., 2013). Nevertheless, the concept of f_m remains important.

In vitro methods to estimate the relative contributions, i.e., f_m values, of specific human cytochrome P450 (P450) enzymes to the overall metabolism of drugs have been applied for over 30 years (Gelboin et al., 1985). The three main tools/approaches to conduct these experiments are 1) individually expressed P450 enzymes, 2) inhibitory antibodies and chemical inhibitors of defined selectivity, and 3) correlation to

This work received no external funding. Authors are employees and shareholders in Pfizer Inc.

No author has an actual or perceived conflict of interest with the contents of this article.

dx.doi.org/10.1124/dmd.122.000883.

S This article has supplemental material available at dmd.aspetjournals.org.

ABBREVIATIONS: DDI, drug-drug interaction; EMA, European Medicines Agency; f_{CL}, fraction of the total metabolism contributed by a metabolic pathway; f_{CONTR}, fraction of metabolic pathway contributed by an isoform; FDA, US Food and Drug Administration; f_m, fraction of metabolism; HPLC, high-performance liquid chromatography; HRMS, high-resolution mass spectrometry; ISEF, intersystem extrapolation factor; P450, cytochrome P450; PPP, 2-phenyl-2-(1-piperidinyl)propane; rP450, recombinant P450; TAO, troleandomycin; UHPLC, ultrahigh pressure liquid chromatography.

P450 marker activities measured in panels of liver microsome lots obtained from individual donors. These became available in the early 1990s and have evolved and improved since that time. Methods became defined by the late 1990s (Parkinson, 1996; Rodrigues, 1999) and were summarized in a cross-pharmaceutical industry position paper (Bjornsson et al., 2003). Despite common and widespread application, these methods suffer some limitations (Bohnert et al., 2016). The use of relative activity factors, relative abundance factors, and intersystem extrapolation factors (ISEFs) for scaling in vitro data gathered in individually expressed P450 enzymes can be confounded by substrate-dependent activity differences (Siu and Lai, 2017; Lindmark et al., 2018; Wang et al., 2019; Dantonio et al., 2022). Inhibitors commonly used as probes do not possess adequate selectivity to their target enzymes, and this can limit accuracy of f_m (Lu et al., 2003; Khojasteh et al., 2011; Nirogi et al., 2015; Doran et al., 2022). Also, correlation analysis does not yield f_m values, and can only be successful when the relative contribution by a P450 enzyme is high. These challenges are all compounded by the possibility of involvement of other non-P450 enzymes, which must also be defined in any given study to define f_m values.

In this work, an alternate methodological approach to P450 reaction phenotyping has been defined. Instead of using two of the three aforementioned approaches in parallel as described in position papers and regulatory guidance documents [Bjornsson et al., 2003; Bohnert et al., 2016; US Food and Drug Administration (FDA), 2020; European Medicines Agency (EMA), 2012] and hoping for results of quantitative concurrence, a sequential qualitative-then-quantitative process (a.k.a., "mapping and detailing") is described that combines modern high-resolution mass spectrometry (HRMS) drug biotransformation experiments in individual P450 enzymes with more thorough chemical inhibition experiments and complex data fitting. In the first step, a drug of interest is incubated with a wide panel of individual P450 enzymes at a high concentration and metabolite profiles are determined using high-performance liquid chromatography UV–HRMS to identify, qualitatively, which P450 enzymes demonstrate any capability for generating metabolites. In the second step, metabolism of the drug of interest is measured quantitatively in pooled human liver microsomes in the presence and absence of inhibitors for P450 enzymes identified in the first step. The range of inhibitor concentrations and number of datapoints in the second step is high in order to delineate inhibition curves that can be reliably fit to complex functions and account for suboptimal inhibitor selectivity (Doran et al., 2022). This approach was evaluated using 48 drugs for step 1 and five of those (shown in Fig. 1) were selected to progress to step 2. Data were compared with clinical observations. This method is proposed as one that yields f_m data of greater confidence and avoids spurious assignments of P450 enzymes that do not have meaningful contributions to the metabolism of individual drugs.

Materials and Methods

Materials. Pooled human liver microsomes (50 donors, mixed sex) were prepared under contract by Xenotech (Lenexa, KS) and were stored in 20% glycerol at 20 mg/mL at −80°C. Individual heterologously expressed human P450 enzymes in the baculosome system, each at 1 nmol P450/mL, were obtained from Corning Life Sciences (Tewksbury, MA). Cryopreserved human hepatocytes were a custom mix of 13 donors of both sexes prepared under contract by BioIVT (Baltimore, MD). The 48 drugs used in this analysis were from either Sigma-Aldrich (St. Louis, MO) or Sequoia Research Products (Pangbourne, UK). Metabolites of escitalopram, fluvastatin, pioglitazone, risperidone, and propranolol used as standards for bioanalysis were prepared by biosynthesis using a previously described method (Walker, et al., 2014), with the exceptions of the following, which were purchased from commercial sources: N-desmethylcitalopram and 5-hydroxypropranolol (Toronto Research Chemicals; North York, Ontario, Canada); 9-hydroxyrisperidone (paliperidone, USP; North Bethesda, MD); and 4-hydroxypropranolol, N-desiospropylpropranolol; and 6-fluoro-3-(4-piperidinyl)-1,2-benzisoxazole (Sigma-Aldrich). NADPH (tetrasodium salt) was from Sigma-Aldrich. Williams E medium was from Thermo Fisher (Waltham, MA).

Metabolite Profiles in Recombinant P450 Enzymes. Drugs (10 μM) were incubated with 17 individually expressed P450 enzymes (100 pmol/mL) or human liver microsomes (2 mg/mL) and NADPH (1.3 mM) in 0.2 mL of potassium phosphate buffer (100 mM, pH 7.5) containing $MgCl_2$ (3.3 mM). The recombinant P450s (rP450s) evaluated were CYP1A1, CYP1A2, CYP1B1, CYP2A6, CYP2B6, CYP2C8, CYP2C9, CYP2C18, CYP2C19, CYP2D6, CYP2E1, CYP2J2, CYP3A4, CYP3A5, CYP3A7, CYP4A11, and CYP4F2, all wild type. Incubations were initiated with the addition of enzymes and conducted for 1 hour at 37°C in a shaking water bath. Incubations were terminated with the addition of acetonitrile (0.6 mL) and spun in a centrifuge at 1800*g* for 6 minutes. Supernatants (0.6 mL) were transferred to limited-volume glass inserts and subjected to vacuum centrifugation to remove the liquid. The residues were reconstituted in 0.1 mL 20% acetonitrile in water, spun at 1800*g* for 5 minutes for analysis by ultrahigh pressure liquid chromatography (UHPLC)–UV-HRMS.

The UHPLC-UV-HRMS system consisted of a Thermo Fisher Vanquish quaternary pumping system, with the autoinjector maintained at 10°C, column heater held at 45°C, and diode array UV detector operated at a wavelength range of 200–500 nm at 4 nm intervals at 50 Hz, in line with a Thermo Fisher Elite Orbitrap mass spectrometer. Separations were affected on a Phenomenex Kinetex XB-C18 column (2.3 × 100 mm; 2.6 μ) using one of two mobile phases—acidic or neutral—at a flow rate of 0.4 mL/min. The acidic mobile phase was 0.1% formic acid in water and acetonitrile and the neutral mobile phase was 10 mM ammonium acetate in water and acetonitrile. Mobile phase gradients were adjusted to optimize separations for each drug and its metabolites. The eluent was introduced into a heated electrospray ionization source on the mass spectrometer operated in the positive ion mode. Source settings were 4 kV for potential; 375°C and 275°C for source and capillary temperatures; and flows of 50, 20, and 2 for sheath, auxiliary, and sweep gas, respectively (arbitrary units). The orbitrap was set to scan a range of 100–1000 *m/z* at a resolution setting of 30000.

The data were interrogated first by visual inspection of the UV data using an extracted wavelength maximum for the parent drug and comparing data from P450-containing incubations to those in an incubation that contained

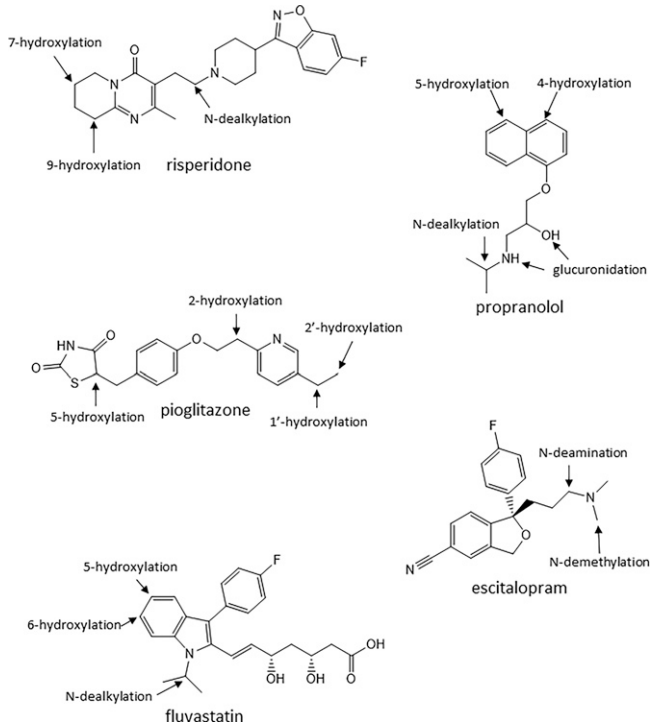

Fig. 1. Metabolism of escitalopram, fluvastatin, pioglitazone, propranolol, and risperidone.

microsomes from nontransfected control. They were then interrogated similarly by visual inspection of total ion current, and ultimately ion current of extracted ions of likely P450 biotransformation products (e.g., hydroxylation, heteroatom dealkylation, etc.) at a resolution of 5 ppm. A positive response was considered as a peak that had a height that was twice the background in the control incubation.

Enzyme Kinetics in Human Liver Microsomes and Human Hepatocytes. To select an appropriate sub-K_M concentration for subsequent inhibition experiments, the enzyme kinetics for the metabolism of escitalopram, fluvastatin, pioglitazone, propranolol, and risperidone were determined in either pooled human liver microsomes or pooled human hepatocytes using previously determined time and optimized protein or cell density linear conditions. In general, for human liver microsome incubations, substrates were incubated in 100 mM potassium phosphate buffer (pH 7.4) containing $MgCl_2$ (3.3 mM) and NADPH (1.3 mM) at 37°C. Incubations were terminated with the addition of acetonitrile containing internal standard. In general, for human hepatocyte incubations, substrates were incubated in a custom formula of William's E Medium supplemented with 26 mM $NaHCO_3$ in an incubator set to 37°C with 5% CO_2 and 75% relative humidity. Incubations were commenced with the addition of substrate and terminated with the addition of acetonitrile containing internal standard. Details of the incubation conditions for each of the five substrates are listed in Supplemental Tables 1–3, and the bioanalytical methods used for each are listed in Supplemental Tables 4 and 5. Experiments were run in triplicate. Enzyme kinetic parameters were determined as described below.

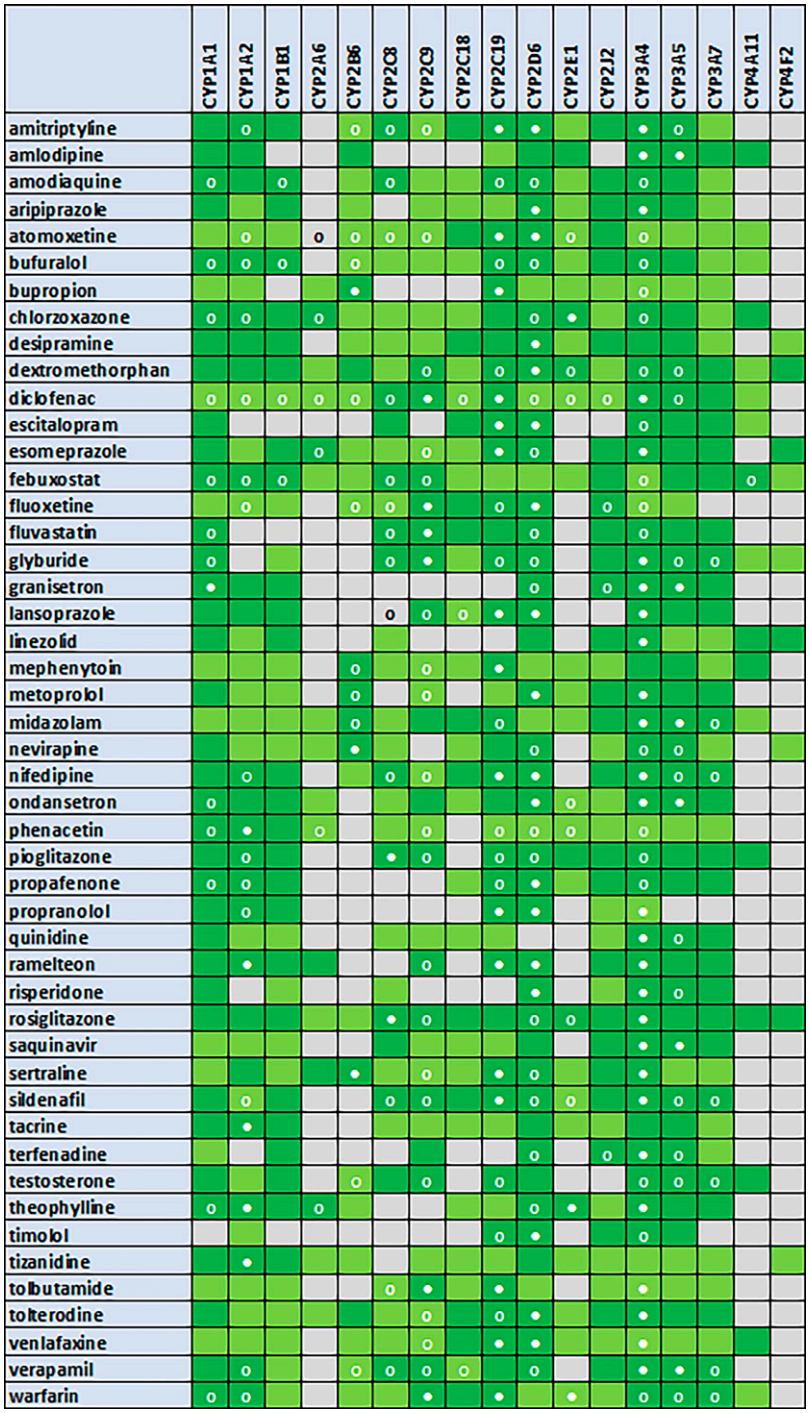

Fig. 2. Summary of metabolism of 48 drugs by 17 rCYP enzymes. Dark green boxes indicate the observation of metabolites by HPLC-UV and mass spectrometry. Pale green boxes indicate the observation of metabolites only by mass spectrometry. Gray boxes indicate that no metabolism was observed. The presence of a solid circle indicates that there is clinical and in vitro evidence for the involvement of an enzyme in the metabolism of the drug, while an open circle indicates that there is only in vitro evidence for the involvement of an enzyme in the metabolism of the drug. A list of the literature references supporting the placement of solid and open circles is in the Supplemental Information.

TABLE 1

Enzyme kinetics and calculated f_{CL} values for the metabolism of escitalopram, fluvastatin, pioglitazone, propranolol, and risperidone.

Values for V_{max} and K_M are mean (S.E.). Velocity units are in pmol/min/mg microsomal protein for fluvastatin, pioglitazone, and risperidone. Units are in pmol/min/million cells for escitalopram and propranolol. Intrinsic clearance units are μL/min/mg for fluvastatin, pioglitazone, and risperidone and μL/min/million cells for escitalopram and propranolol. Units for KM are in uM.

Drug/Reaction	V_{max} (1)	K_M (1)	CL_{int} (1)	V_{max} (2)	K_M (2)	CL_{int} (2)	Total CL_{int}	Pathway f_{CL}
Escitalopram[a]								
N-demethylation	30.6 (2.34)	46.9 (6.63)	0.652	—	—	—	0.652	0.80
N-deamination	12.1 (0.82)	76.2 (9.63)	0.159	—	—	—	0.159	0.20
Fluvastatin								
5-hydroxylation	6.53 (0.26)	0.326 (0.026)	20.0	4.11 (0.22)	11.6 (2.3)	0.35	20.4	0.36
6-hydroxylation	499 (5)	20.9 (0.5)	23.9	—	—	—	23.9	0.42
N-dealkylation	3.76 (0.08)	0.318 (0.015)	11.8	4.61 (0.07)	18.1 (1.3)	0.26	12.1	0.21
Pioglitazone[b]								
1'-hydroxylation	214 (10.2)	9.22 (0.8)	23.2	—	—	—	23.2	0.45
2-hydroxylation	29.6 (1.0)	4.90 (0.3)	6.05	—	—	—	6.05	0.12
2'-hydroxylation	26.3 (1.1)	1.83 (0.2)	14.4	—	—	—	14.4	0.28
5-hydroxylation	484 (37)	61.6 (5.9)	7.85	—	—	—	7.85	0.15
Propranolol[a]								
Glucuronidation 1	30.6 (10.3)	15.2 (5.3)	2.01	47.6 (5.5)	177 (114)	0.269	2.28	0.075
Glucuronidation 2	33.9 (15.5)	13.0 (5.5)	2.61	35.3 (11.7)	106 (90)	0.333	2.94	0.097
4-hydroxylation	33.9 (1.2)	1.46 (0.10)	22.6	35.6 (2.0)	113 (25)	0.315	22.9	0.77
5-hydroxylation	0.57 (0.1)	5.06 (1.08)	0.113	—	—	0.013	0.126	0.004
N-dealkylation	16.0 (2.4)	11.7 (3.0)	1.37	—	—	0.176	1.55	0.051
Risperidone								
7-hydroxylation	16.2 (1.4)	10.5 (2.3)	1.54	—	—	0.063 (0.005)	1.61	0.16
9-hydroxylation	170 (23)	27.3 (7.2)	6.23	—	—	0.59 (0.07)	6.82	0.67
N-dealkylation	92.1 (4.1)	57.5 (3.7)	1.60	—	—	0.14 (0.01)	1.74	0.17

[a]Data for escitalopram and propranolol are from pooled human hepatocytes.
[b]Pioglitazone enzyme kinetics best fit a model that also included substrate inhibition with K_s values of 65.4, 67.2, 76.5, and 23.5 μM for 1', 2, 2', and 5-hydroxylation pathways, respectively.

Inhibition of P450 Activity in Human Liver Microsomes. Inhibition experiments were conducted using the same incubation conditions listed for each substrate in Supplemental Tables 1 and 2. Fixed substrate concentrations were used: escitalopram (4 μM), fluvastatin (0.1 μM), pioglitazone (0.3 μM), propranolol (0.5 μM), and risperidone (1.0 μM). P450-selective inhibitors were evaluated at both single concentrations and >18-point concentration curves. The concentration ranges used for each were: furafylline for CYP1A2 (0.01–20 μM or 100 μM), phenylethylpiperidine (PPP) for

TABLE 2

Single-inhibitor concentration data for the metabolism of escitalopram, fluvastatin, pioglitazone, propranolol, and risperidone and estimates of f_m.

Percent inhibition data are mean (S.E.); values labeled with an asterisk (*) are statistically significant. Estimated f_m calculated only from enzymes with statistically significant outcomes. The single concentrations of inhibitors used for these estimates are listed in Supplemental Table 9.

	f_{CL}	CYP1A2	CYP2B6	CYP2C8	CYP2C9	CYP2C19	CYP2D6	CYP3A	Sum
Escitalopram									
N-demethylation	0.80	7.3 (5.7)	15.6 (3.7)*	34.2 (2.5)*	6.7 (10.0)	31.3 (1.6)*[a]	10.3 (6.5)	43.3 (2.5)*	
N-deamination	0.20	ND[c]	ND[c]	ND[c]	ND[c]	89.0 (1.4)*[a]	ND[c]	ND[c]	
Estimated f_m			0.13	0.28		0.43		0.35	1.19
Fluvastatin									
5-hydroxylation	0.36	<0[b]	<0[b]	<0[b]	95.0 (0.4)*	11.9 (1.4)*	3.7 (3.9)	23.9 (2.3)*	
6-hydroxylation	0.42	<0[b]	<0[b]	0.5 (6.9)	61.2 (1.4)*	10.5 (2.6)*	<0[b]	31.5 (1.4)*	
N-dealkylation	0.21	<0[b]	<0[b]	<0[b]	96.6 (1.4)*	10.2 (2.6)*	2.8 (2.6)	9.8 (1.3)*	
Estimated f_m					0.81	0.11		0.24	1.16
Pioglitazone									
1'-hydroxylation	0.45	<0[b]	1.2 (1.4)	76.3 (4.0)*	<0[b]	<0[b]	<0[b]	<0[b]	
2-hydroxylation	0.12	<0[b]	0.4 (4.1)	52.4 (4.3)*	31.5 (6.4)*	<0[b]	<0[b]	<0[b]	
2'-hydroxylation	0.28	<0[b]	<0[b]	69.1 (5.3)*	<0[b]	<0[b]	<0[b]	<0[b]	
5-hydroxylation	0.15	29.2 (5.8)*	2.3 (6.3)	4.5 (13.2)	5.4 (9.1)	<0[b]	<0[b]	24.3 (1.9)*	
Estimated f_m		0.04		0.60	0.04			0.04	0.72
Propranolol[d]									
4-hydroxylation	0.77	0.6 (14.9)	11.7 (10.0)	19.0 (9.7)	3.5 (6.4)	1.1 (8.8)	91.1 (11.6)*	0.93 (4.5)	
5-hydroxylation	0.004	<0[b]	16.4 (17.7)	24.4 (17.0)	11.4 (9.9)	11.9 (12.6)	88.5 (10.2)*	<0[b]	
N-dealkylation	0.05	70.2 (5.0)*	3.3 (10.5)	28.0 (7.9)	23.3 (8.7)	16.7 (8.8)	35.3 (7.3)*	0.56 (2.1)	
Estimated f_m		0.04					0.73		0.77
Risperidone									
7-hydroxylation	0.16	<0[b]	12.9 (7.3)	22.2 (5.5)*	12.9 (7.3)	<0[b]	87.4 (2.3)*	<0[b]	
9-hydroxylation	0.67	<0[b]	13.4 (14.5)	23.2 (5.3)	16.8 (11.6)	7.4 (7.3)	62.4 (4.2)*	25.8 (1.6)*	
N-dealkylation	0.17	<0[b]	39.2 (17.1)	30.8 (7.0)	39.2 (17.1)	24.0 (6.8)*	19.7 (8.1)	90.4 (7.9)*	
Estimated f_m				0.04		0.04	0.56	0.33	0.97

[a]Data for CYP2C19 catalyzed escitalopram metabolism were from esomeprazole in human hepatocytes.
[b]Rates in inhibited incubation were greater than in the control incubation.
[c]ND, not determined.
[d]f_{CL} excludes the contribution of glucuronidation determined in human hepatocyte kinetics reported in Table 1.

CYP2B6 (0.01–100 μM), montelukast for CYP2C8 (0.001–10 μM), sulfaphenazole for CYP2C9 (0.01–100 μM), N-benzylnirvanol for CYP2C19 (0.005–50 μM), quinidine for CYP2D6 (0.0001–10 μM), and troleandomycin for CYP3A (0.01–100 μM). Since furafylline, troleandomycin (TAO), and PPP are time-dependent inhibitors, these were each preincubated for 10 minutes with microsomes and NADPH prior to addition of substrate. Positive control substrate reactions for each inhibitor were included using a previously established method (Supplemental Tables 6 and 7) and nonspecific binding of the inhibitors to microsomes was corrected based on previously determined values (Supplemental Table 8; Doran et al., 2022).

The percent activity remaining was obtained by normalizing metabolite concentration data to the averaged solvent controls. The inhibitory profiles were generated using GraphPad Prism for Windows (version 9). In general, nonlinear regression of the data were conducted using the log [I] versus normalized response with variable slope model to better fit the data, which uses the following inhibitory equation (referred to as the "four-parameter fit"):

$$Y = \text{Bottom} + \frac{\text{Top} - \text{Bottom}}{1 + e^{h(\ln x - \ln IC_{50})}} \quad (2)$$

where Y is the percent of control activity remaining and x is the inhibitor concentration. The four parameters in the model are the IC^{50}, which represents the inhibitor concentration that yields a response halfway between the upper and lower asymptotes; the hill slope (h), which represents the steepness of the curve; and the upper and lower asymptotes (Top and Bottom, respectively), which represent the maximum and minimum possible responses. The maximal contribution of a P450 was determined by the span or the difference between the fitted upper and lower asymptotes:

$$\text{span} = \text{Top} - \text{Bottom} \quad (3)$$

In certain instances, the above equation was not able to fit the data, and the equation below was used to fit the data (referred to as the "six-parameter fit"):

$$Y = I_{max} - MAX_A + \left(\frac{MAX_A}{1 + e^{h(\ln x - \ln IC_{50}A)}}\right) - MAX_B + \left(\frac{MAX_B}{1 + e^{h(\ln x - \ln IC_{50}B)}}\right) \quad (4)$$

where Y is the percent control activity remaining and x is the inhibitor concentration. The six parameters in the model are MAX_A and MAX_B, which represent the maximum contribution of enzymes A and B, respectively; IC_{50A} and IC_{50B}, which are the inflection points for the inhibitor on enzymes A and B, respectively; the hill slope (h), which represents the steepness of the curve for enzymes A and B; and I_{max}, which represents the maximum possible response (Doran et al., 2022).

Rates of Metabolism in rP450 Enzymes. The metabolism of the five drugs was measured in seven major hepatically expressed rCYP enzymes. Specifics for each drug are listed in Supplemental Table 3. In general, each drug was incubated with 1, 10, and 100 pmol P450/mL in 100 mM potassium phosphate buffer containing $MgCl_2$ (3.3 mM) and NADPH (1.3 mM). Incubations were commenced with the addition of NADPH and carried out at 37°C. At various times up to 60 minutes, aliquots were removed and reactions terminated by addition to four volumes of acetonitrile containing internal standard. Substrate concentrations were below K_M values that had been determined in either human liver microsomes or human hepatocytes. Reaction velocities were determined from the product formed versus time plots at the incubation condition that yielded linear product formation over the longest incubation time and at the lowest enzyme concentration.

Estimation of f_m Values. Estimations of f_m values were made as follows. Enzyme kinetic data were used to calculate intrinsic clearance (CL_{int}) for each metabolic pathway in pooled human liver microsomes:

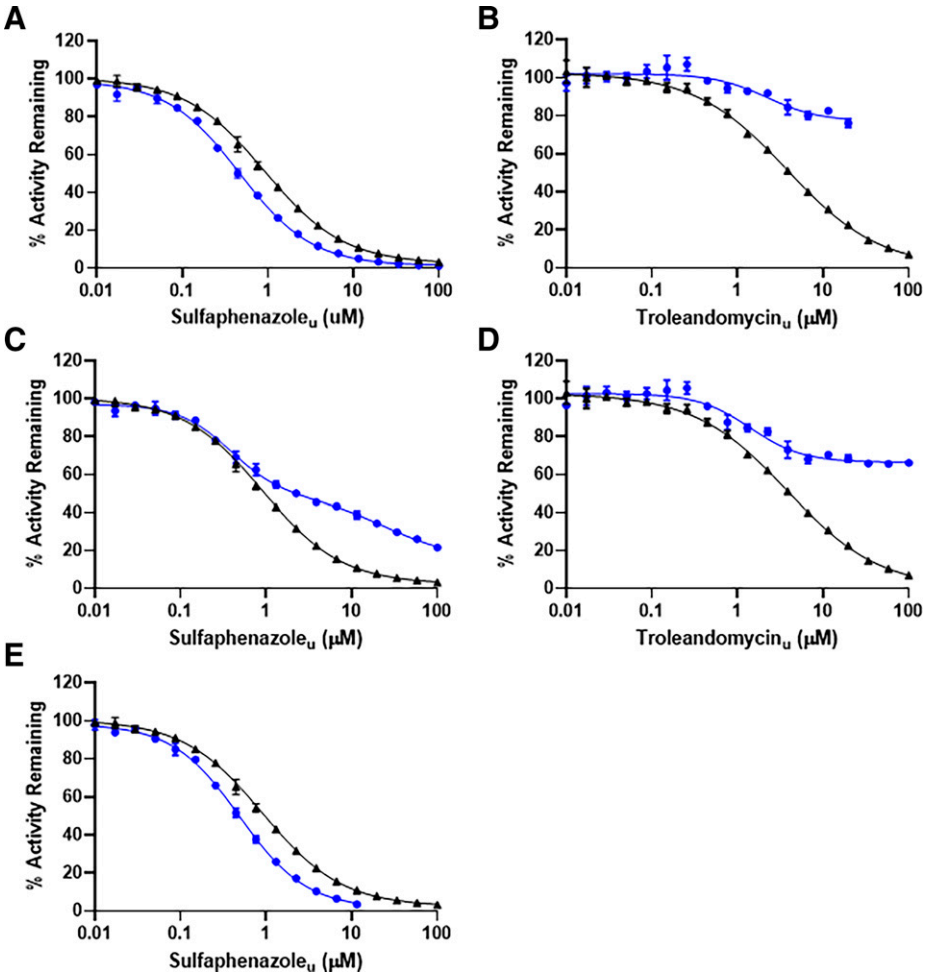

Fig. 3. Inhibition curves for metabolism of fluvastatin. (A and B) Effect of sulfaphenazole and troleandomycin on 5-hydroxylation. (C and D) Effect of sulfaphenazole and troleandomycin on 6-hydroxlation. (E) Effect of sulfaphenazole on N-dealkylation. Blue curves represent fluvastatin metabolism and black curves represent the positive control reactions for CYP2C9 (diclofenac 4'-hydroxylation) and CYP3A (midazolam 1'-hydroxylation).

TABLE 3

Maximum percentage inhibition values (MAX_A) from multiple concentration inhibition experiments for the metabolism of escitalopram, fluvastatin, pioglitazone, propranolol, and risperidone and estimates of f_m.

Maximum percentage inhibition data are mean (SE). All unbound IC_{50} values are listed in Supplemental Table 11.

	Pathway f_{CL}[a]	Enzyme							Sum f_m
		CYP1A2	CYP2B6	CYP2C8	CYP2C9	CYP2C19	CYP2D6	CYP3A	
Escitalopram									
N-demethylation	0.80	—	—	24.3 (7.1)	—	28.3 (1.7)[b]	19.5 (2.01)	36.0 (3.1)	
N-deamination	0.20	—	—	—	—	97.1 (5.2)[b]	—	—	
Estimated f_m		—	—	0.20	—	0.42	0.16	0.29	1.07
Fluvastatin									
5-hydroxylation	0.36	—	—	—	98.0 (0.9)	—	—	—	
6-hydroxylation	0.42	—	—	—	47.7 (2.7)	—	—	36.3 (1.7)	
N-dealkylation	0.21	—	—	—	97.2 (1.5)	—	—	—	
Estimated f_m		—	—	—	0.77	—	—	0.15	0.92
Pioglitazone									
1'-hydroxylation	0.45	—	—	85.1 (2.2)	—	—	—	—	
2-hydroxylation	0.12	—	—	44.9 (7.6)	31.4 (2.7)	—	—	—	
2'-hydroxylation	0.28	—	—	100 (5.8)	—	—	—	—	
5-hydroxylation	0.15	—	—	—	—	—	—	32.8 (2.4)	
Estimated f_m		—	—	0.72	0.04	—	—	0.05	0.81
Propranolol[c]									
4-hydroxylation	0.77	—	—	—	—	—	86.0 (3.5)	—	
5-hydroxylation	0.004	—	—	—	—	—	76.1 (2.8)	—	
N-dealkylation	0.05	68.9 (4.8)	33.6 (6.0)	—	—	—	17.5 (2.0)	—	
Estimated f_m		0.03	0.02	—	—	—	0.68	—	0.73
Risperidone									
7-hydroxylation	0.16	—	—	—	—	—	91.4 (2.9)	—	
9-hydroxylation	0.67	—	—	—	—	—	67.1 (4.1)	24.9 (2.7)	
N-dealkylation	0.17	—	—	—	—	—	—	99.1 (7.1)	
Estimated f_m		—	—	—	—	—	0.60	0.34	0.94

[a]Human hepatocyte-derived f_{CL} values for escitalopram and propranolol, all others in human liver microsomes.
[b]From chemical inhibition conducted in human hepatocytes.
[c]f_{CL} excludes the contribution of UGT metabolism determined in human hepatocyte kinetics reported in Table 1.

$$CL_{int,\,pathwayX} = \frac{V_{max}}{K_M}(\text{one} - \text{enzyme model}) \quad (5)$$

or

$$CL_{int,\,pathwayX} = \frac{V_{max(1)}}{K_{M(1)}} + CL_{int(2)}(\text{two} - \text{enzyme model}) \quad (6)$$

in which $CL_{int,pathwayX}$ refers to the intrinsic clearance for a specific metabolic pathway, V_{max} and K_M are the maximum reaction velocity and Michaelis constant for that pathway, and, when necessary, $CL_{int(2)}$ represents a high capacity/high K_M enzyme activity wherein the K_M was greater than the highest substrate concentration evaluated.

TABLE 4

ISEF adjusted rCYP rate data for escitalopram, fluvastatin, pioglitazone, propranolol, and risperidone.

Rate data are expressed in intrinsic clearance terms (v/[S]) and are in units of μL/min/mg microsomes. Values represent the measured rates from Supplemental Table 10 multiplied by the P450-specific ISEF and P450 abundance in human liver microsomes.

	CYP1A2	CYP2B6	CYP2C8	CYP2C9	CYP2C19	CYP2D6	CYP3A4
ISEF	0.052	1.3	1.8	0.38	0.33	0.054	0.19
P450 abundance[a]	52	17	24	73	14	8	137
Escitalopram							
N-demethylation	0.00124	—	1.60	—	0.246	3.44	0.567
N-deamination	—	—	—	—	0.016	—	—
Fluvastatin							
5-hydroxylation	—	—	—	6.57	—	—	—
6-hydroxylation	—	—	2.85	5.27	—	0.016	16.8
N-dealkylation	—	—	—	0.591	—	—	—
Pioglitazone							
1'-hydroxylation	0.133	—	10.3	0.407	0.083	0.024	0.097
2-hydroxylation	—	—	1.09	0.366	—	—	–
2'-hydroxylation	—	—	1.88	—	—	—	–
5-hydroxylation	—	—	0.209	—	—	—	0.802
Propranolol							
4-hydroxylation	1.60	0.00171	0.0619	0.00566	0.00444	7.15	1.44
5-hydroxylation	0.340	—	0.00753	0.00971	—	0.630	0.0256
N-dealkylation	3.16	0.0544	0.0243	0.0189	0.635	0.753	0.118
Risperidone							
7-hydroxylation	—	—	0.0372	—	0.00517	0.0791	0.0113
9-hydroxylation	—	—	0.165	—	0.0223	0.566	3.28
N-dealkylation	—	—	—	—	—	—	19.9

[a]Units of pmol P450/mg human liver microsomal protein.

TABLE 5

Percent contribution and f_m values estimated from rCYP rate data for escitalopram, fluvastatin, pioglitazone, propranolol, and risperidone.

Individual metabolic pathway enzyme f_m values represent the ISEF-adjusted rates for each enzyme divided by the sum of rates across all enzymes (Table 4). f_{CL} derived from enzyme kinetic parameters (Table 1). Final f_m values for each enzyme are sums of the products of individual pathway f_m values and f_{CL} values.

		Isoform Contribution by Pathway (Percent)						
	Pathway f_{CL}[a]	CYP1A2	CYP2B6	CYP2C8	CYP2C9	CYP2C19	CYP2D6	CYP3A4
Escitalopram								
N-demethylation	0.80	0.021	—	27.3	—	4.21	58.8	9.68
N-deamination	0.20	—	—	—	—	100	—	—
Total enzyme f_m		<0.01		0.22		0.23	0.47	0.08
Fluvastatin								
5-hydroxylation	0.36	—	—	—	100	—	—	—
6-hydroxylation	0.42	—	—	11	21	—	0.065	67
N-dealkylation	0.21	—	—	—	100	—	—	—
Total enzyme f_m				0.05	0.67		< 0.01	0.29
Pioglitazone								
1'-hydroxylation	0.45	1.2	—	93	3.7	0.76	0.22	0.88
2-hydroxylation	0.12	—	—	75	25	—	—	—
2'-hydroxylation	0.28	—	—	100	—	—	—	—
5-hydroxylation	0.15	—	—	21	—	—	—	79
Total Enzyme f_m		<0.01		0.82	0.05	<0.01	<0.01	0.13
Propranolol[b]								
4-hydroxylation	0.77	16	0.017	0.60	0.055	0.043	70	14
5-hydroxylation	0.004	34	—	0.74	1.0	—	62	2.5
N-dealkylation	0.05	66	1.1	0.51	0.40	13	16	2.5
Total enzyme f_m		0.16	<0.01	<0.01	<0.01	<0.01	0.55	0.11
Risperidone								
7-hydroxylation	0.16	—	—	2.8	—	3.9	60	8.6
9-hydroxylation	0.67	—	—	4.1	—	0.55	14	81
N-dealkylation	0.17	—	—	—	—	—	—	100
Total enzyme f_m				0.07		0.01	0.19	0.73

[a]Human hepatocyte-derived f_{CL} values for escitalopram and propranolol, all others in human liver microsomes.
[b]f_{CL} excludes the contribution of UGT metabolism determined in HHEP kinetics reported in Table 1.

These CL_{int} values were used to calculate the fraction of metabolic clearance proceeding through a pathway (f_{CL}) by dividing the CL_{int} for the pathway of interest by the sum of CL_{int} values of all pathways:

$$f_{CL,pathwayX} = \frac{CL_{int,pathwayX}}{\mathrm{CL_{int,\,all\ \ pathways}}} \tag{7}$$

The fractional clearance values for each pathway were scaled to the respective isoform contributions to determine the fraction metabolized using the following general equation:

$$\mathrm{f_{m,\,CYPA}} = (\mathrm{f_{CL,\,pathwayX}} \cdot \mathrm{f_{CONTR,\,CYPA,\,pathwayX}}) + (\mathrm{f_{CL,\,pathwayY}} \cdot \mathrm{f_{CONTR,\,CYPA,\,pathwayY}}) + (\mathrm{f_{CL,\,pathwayZ}} \cdot \mathrm{f_{CONTR,\,CYPA,\,pathwayZ}}) \tag{8}$$

where the term $f_{CONTR,CYPA,pathwayX}$ refers to the inhibition of metabolic pathway X in human liver microsomes by an inhibitor selective for CYPA. This was calculated in two ways:

For single-concentration inhibition experiments:

$$\mathrm{f_{CONTR,\,CYPA,\,pathwayX}} = \frac{\%\ \mathrm{inhibition_{CYPA,\,pathwayX}}}{100} \tag{9}$$

or for multiple-point inhibition experiments:

$$\mathrm{f_{CONTR,\,CYPA,\,pathwayX}} = \frac{\mathrm{span_{CYPA,\,pathwayX}}}{100} \tag{10}$$

$$\mathrm{f_{CONTR,\,CYPA,\,pathwayX}} = \frac{MAX_{\mathrm{A,\,CYPA,\,pathwayX}}}{100} \tag{11}$$

for the four-parameter and six-parameter inhibition models, respectively.

For data from heterologously expressed P450 enzymes, f_m values were calculated as follows. Reaction velocities for each metabolic pathway for each P450 enzyme were divided by the substrate concentration evaluated in the assay to yield v/[S] values in units of μL/min/pmol P450. These values were converted to estimated values for each P450 enzyme in each metabolic pathway in pooled human liver microsomes:

$$\left(\frac{v}{[S]}\right)_{CYPA,\,pathwayX,\,HLM} = \left(\frac{v}{[S]}\right)_{CYPA,\,pathwayX} \cdot ISEF_{CYPA} \cdot \frac{pmoles\ \ of\ \ CYPA}{mg\ \ microsomal\ \ protein} \tag{12}$$

The ISEF values were determined from marker substrate activities and were 0.052, 1.30, 1.80, 0.38, 0.33, 0.054, and 0.19 for CYP1A2, CYP2B6, CYP2C8, CYP2C9, CYP2C19, CYP2D6, and CYP3A4, respectively. The values for abundance of each P450 enzyme in liver microsomes were 52, 17, 24, 73, 14, 8, and 137 pmol P450/mg protein for CYP1A2, CYP2B6, CYP2C8, CYP2C9, CYP2C19, CYP2D6, and CYP3A4, respectively. The f_m values for each P450 on an individual metabolic pathway were determined as:

$$\mathrm{f_{m,\,CYPA,\,pathwayX}} = \frac{\left(\frac{v}{[S]}\right)_{\mathrm{CYPA,\,pathwayX,\,HLM}}}{\sum\left(\frac{v}{[S]}\right)_{\mathrm{all\ \ CYP,\,pathwayX,\,HLM}}} \tag{13}$$

The contribution of a specific P450 enzyme to the total metabolism was calculated as:

$$\mathrm{f_{m,\,CYPA}} = \mathrm{f_{m,\,CYPA,\,pathwayX}} + \mathrm{f_{m,\,CYPA,\,pathwayY}} + \mathrm{f_{m,\,CYPA,\,pathwayZ}} \tag{14}$$

Statistical Treatment of Data. For enzyme kinetic parameter determination, data were first plotted on Eadie-Hofstee plots for potential model assignment and then the v versus v/[S] data were fit in GraphPad Prism for Windows (version 9) to various models with selection of a model other than Michaelis-Menten based on the Akaike Information Criterion (Nagar et al., 2014). Single-point inhibition data were evaluated using Welch's unpaired two-sample *t* test with unequal variances and a significance threshold of 0.05 as described elsewhere (Doran et al., 2022). Full curve dose-response inhibition data from test compounds were fit using either the four-parameter, single IC_{50} dose-response model or the six-parameter, double IC_{50} dose-response model, using an extra

TABLE 6

Summary comparison of in vitro f_m data for escitalopram, fluvastatin, pioglitazone, propranolol, and risperidone to in vivo f_m values estimated from DDI or pharmacogenetic data.

		Estimate of f_m From:					
Drug	Enzyme	rP450s and ISEF	Single Point Inhibition	Inhibition Curves	In Vivo	PGX or DDI	In Vivo References
Escitalopram	CYP2B6	—	0.13	—	ND		
	CYP2C8	0.22	0.28	0.20	ND		
	CYP2C19	0.23	0.43	0.42	0.36	PGX	Herrlin et al., 2003;
					0.45		Rudberg et al., 2009;
					0.82		Rudberg et al., 2008;
					0.72		Waade et al., 2014;
					0.69		Jukić et al., 2018;
					0.43		Tsuchimine et al., 2018
	CYP2D6	0.47	—	0.16	<0.01	PGX	Herrlin et al., 2003
	CYP3A4	0.08	0.35	0.29	0.08	DDI	Gutierrez et al., 2003
Fluvastatin	CYP2C8	0.05	—	—	0.06	DDI	Spence et al., 1995
	CYP2C9	0.67	0.81	0.76	0.76	PGX	Kirchheiner et al., 2003
	CYP2C19	—	0.11	—	ND		
	CYP2D6	<0.01	—	—	ND		
	CYP3A4	0.29	0.24	0.15	0.12	DDI	Kivisto et al., 1998
Pioglitazone	CYP1A2	—	0.04	—	ND		
	CYP2C8	0.82	0.60	0.72	0.73	DDI	Aquilante et al., 2013
	CYP2C9	0.05	0.04	0.04	ND		
	CYP3A4	0.13	0.04	0.05	0.08	DDI	Jaakkola et al., 2005
Propranolol[a]	CYP1A2	0.16	0.04	0.03	ND		Byrne et al., 1984;
							McLean et al., 1980
	CYP2B6	<0.01	—	0.02	ND		
	CYP2C8	<0.01	—	—	ND		
	CYP2C9	<0.01	—	—	ND		
	CYP2C19	<0.01	—	—	0.25	PGX	Ward et al., 1989
	CYP2D6	0.55	0.72	0.68	0.00	PGX	Lennard et al., 1984
					0.37		Raghuram et al., 1984
					0.55	DDI	Zhou et al., 1990
					0.56		Yasuhara et al., 1990
	CYP3A4	0.11	—	—	0.39	DDI	McCourty et al., 1988
					0.33		Tateishi et al., 1992
					0.32		Tateishi et al., 1989
					0.17		Dimmitt et al., 1991
Risperidone	CYP2C8	0.07	0.04	—	ND		
	CYP2C19	0.01	0.04	—	ND		
	CYP2D6	0.19	0.56	0.60	0.66	PGX	Gasso et al., 2014
					0.88		Cabaleiro et al., 2014
	CYP3A4	0.73	0.32	0.34	0.36	DDI	Mahatthanatrakul et al., 2012

ND, no in vivo data reported for these enzymes; PGX, pharmacogenetic data.
[a]f_{CL} excludes the contribution of UGT metabolism determined in HHEP kinetics reported in Table 1.

sum-of-squares F-test to select the model that best fit the data. After fitting the dose-response curves to the test compound data, a two-one-sided *t* test equivalence procedure was used to determine if the IC_{50} for the test compound was significantly within fivefold of the IC_{50} for the probe substrate (Doran et al., 2022). When the six-parameter model was selected, the IC_{50} of the first phase (IC_{50A}) of the curve was compared with the IC_{50} of the probe substrate. If significant fivefold equivalence in IC_{50} values between the test compound and probe was established, the reduction in percent activity of the test compound was compared with zero. For the four-parameter model, the span parameter (difference between upper asymptote and lower asymptote) needed to be significantly greater than zero, while the MAX_A parameter needed to be significantly greater than zero for the six-parameter model. If both the equivalence test passed and the decrease in activity was significantly greater than zero, then the inhibition of the target enzyme was reported.

Results

Metabolite Profiling in Individual P450 Enzymes. The metabolic profiles for 48 drugs were evaluated in 17 individual P450 enzymes using UHPLC-UV-HRMS (Fig. 2). This represents the first, "qualitative" step in the process, wherein any P450 enzymes with the capability to generate metabolites for a given drug are identified. For each drug, the enzymes were classified into one of three groups: 1) metabolites were generated and observed in the UV chromatogram, 2) metabolites were generated but only observed in the HRMS data, and 3) no metabolites were detected. Depicted in Fig. 2 are dark green boxes that indicate the generation of metabolites observed in the UV data (which are also observed in the more sensitive HRMS data) and pale green boxes that indicate the observation of metabolites observed only in the HRMS data. Within the entries on Fig. 2 are solid circles, which indicate that a particular P450 enzyme has been demonstrated to be involved in the clearance of the drug based on clinical pharmacokinetic data (either DDI data with a well-established P450-selective inhibitor or a difference in pharmacokinetics observed in subjects possessing different genetic polymorphisms for P450 enzymes). Among the 48 drugs evaluated, there were 87 instances of clinical evidence supporting meaningful contributions of specific P450 enzymes to the metabolism of a drug. In 84 of these cases, metabolites were observed in the UV data, and in the other three, metabolites were observed, but only in the HRMS data. In these latter three cases, the contributions are minor (CYP3A4 contributions to tolbutamide and venlafaxine clearance and CYP2E1 to warfarin clearance; O'Reilly, 1973; Krishnaiah et al., 1994; Lindh et al., 2003). Thus, there are no false negatives, i.e., every enzyme demonstrated to be contributing to the clearance of a drug in a clinically meaningful manner is identified in this approach.

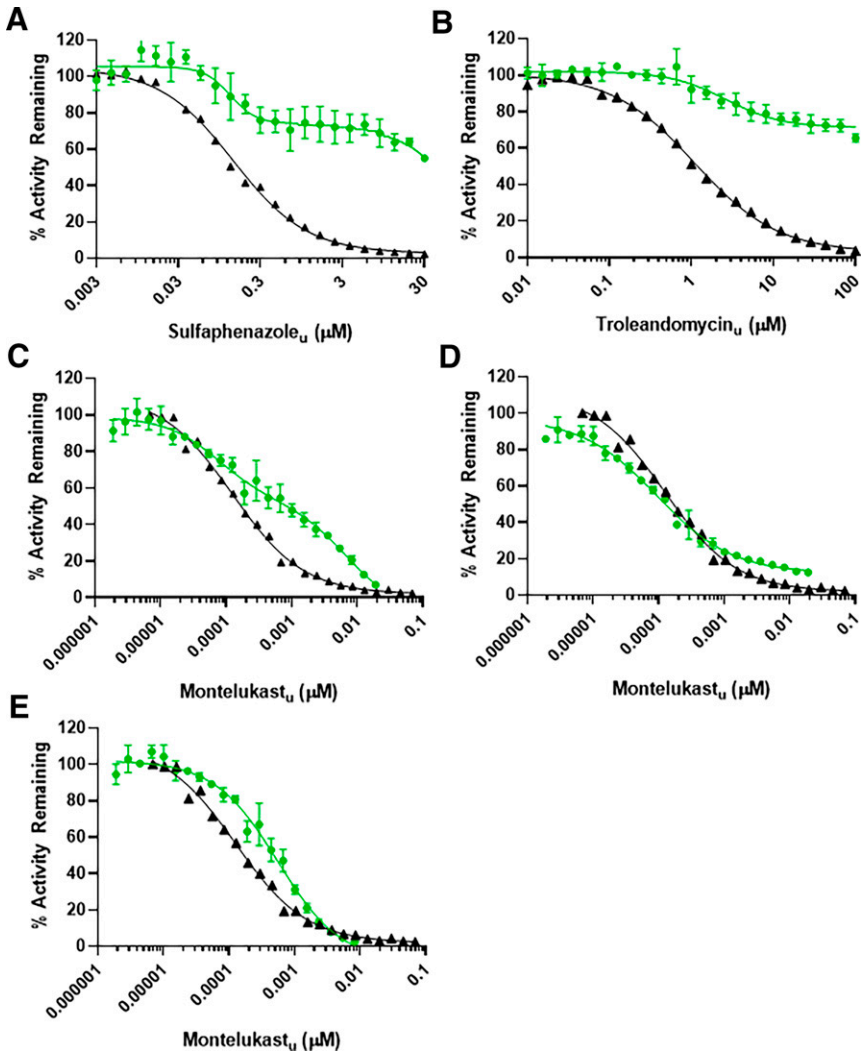

Fig. 4. Inhibition curves for metabolism of pioglitazone. (A) Effect of sulfaphenazole on 2-hydroxylation. (B) Effect of troleandomycin on 5-hydroxylation. (C–E) Effect of Montelukast on 2-. 1'-, and 2'-hydroxylation reactions, respectively. Green curves represent pioglitazone metabolism and black curves represent the positive control reactions for CYP2C9 (diclofenac 4'-hydroxylation), CYP3A (midazolam 1'-hydroxylation), and CYP2C8 (amodiaquine N-deethylation).

Also included in Fig. 2 are previous reports of any in vitro evidence of the involvement of a P450 enzyme in the metabolism of the 48 drugs, which are indicated with open circles. There are a total of 244 instances in which evidence has been reported, using various in vitro methods, that a P450 enzyme was claimed to be involved in the metabolism of a drug. Out of those, 242 were shown using the present approach. The only two not shown were reports of CYP2A6 catalyzed metabolism of atomoxetine (MacKenzie et al., 2020) and CYP2C8 catalyzed metabolism of lansoprazole (Pichard et al., 1995), neither of which has there been any report of clinical relevance.

In addition to the utility of these data in the qualitative-then-quantitative approach to identifying P450 enzymes involved in metabolic clearance of drugs, there are interesting trends that can be noted. The preponderance of CYP2C19 and CYP2D6 in drug metabolism is high (44 of 48 and 47 of 48, respectively). This is not aligned with the frequency of meaningful contributions of these enzymes to in vivo metabolic clearance, likely because in the experimental design employed (i.e., 100 pmol P450/mL) these enzymes are quantitatively over-represented. It is clear that CYP2A6, CYP4A11, and CYP4F2 are least frequently involved in metabolism (16, 17, and nine out of 48 drugs metabolized, respectively). CYP2B6 and CYP2E1 were each shown to metabolize 28 of the 48 drugs, however, in almost all cases this metabolism was detected only by HRMS data; when evaluated by UV data these two enzymes only readily metabolized nine and six drugs, respectively, out of the 48. As anticipated, with few exceptions, CYP3A enzymes were shown to be capable of metabolizing almost all of the drugs. But, unexpectedly, the frequency of CYP1A1, CYP1B1, and CYP2J2 being able to generate metabolites in high enough abundance for UV detection was high. Within the data, there were also instances of less-studied P450 enzymes being able to not only catalyze metabolism of certain drugs, but in high conversion (e.g., CYP3A7 metabolism of fluvastatin, CYP2J2 metabolism of linezolid, and CYP2C18 metabolism of warfarin, to name a few), which poses new questions regarding the possible impact of these enzymes on the pharmacokinetics of these drugs. Examples of the UV chromatograms for extracts of rCYP incubations for fluvastatin, pioglitazone, propranolol, risperidone, and escitalopram are shown in Supplemental Figs. 1–5.

Fluvastatin: Enzyme Kinetics and Reaction Phenotyping. Fluvastatin was metabolized to 5-hydroxy, 6-hydroxy, and N-desisopropyl metabolites in human liver microsomes (Fig. 1). Enzyme kinetic data yielded CL_{int} values for these three pathways that resulted in calculated f_{CL} values of 0.36, 0.42, and 0.21, respectively (Table 1; Supplemental Fig. 6). Single-concentration inhibitor data showed that the P450-selective inhibitors sulfaphenazole (CYP2C9), N-benzylnirvanol (CYP2C19), and TAO (CYP3A4) inhibited fluvastatin overall metabolism by 81%, 11%, and 24%, respectively (Table 2). These values compare favorably with the estimated in vivo contribution by CYP2C9 (f_m = 0.76; Table 6), but overestimate the contribution by CYP3A4. Using the maximum percent

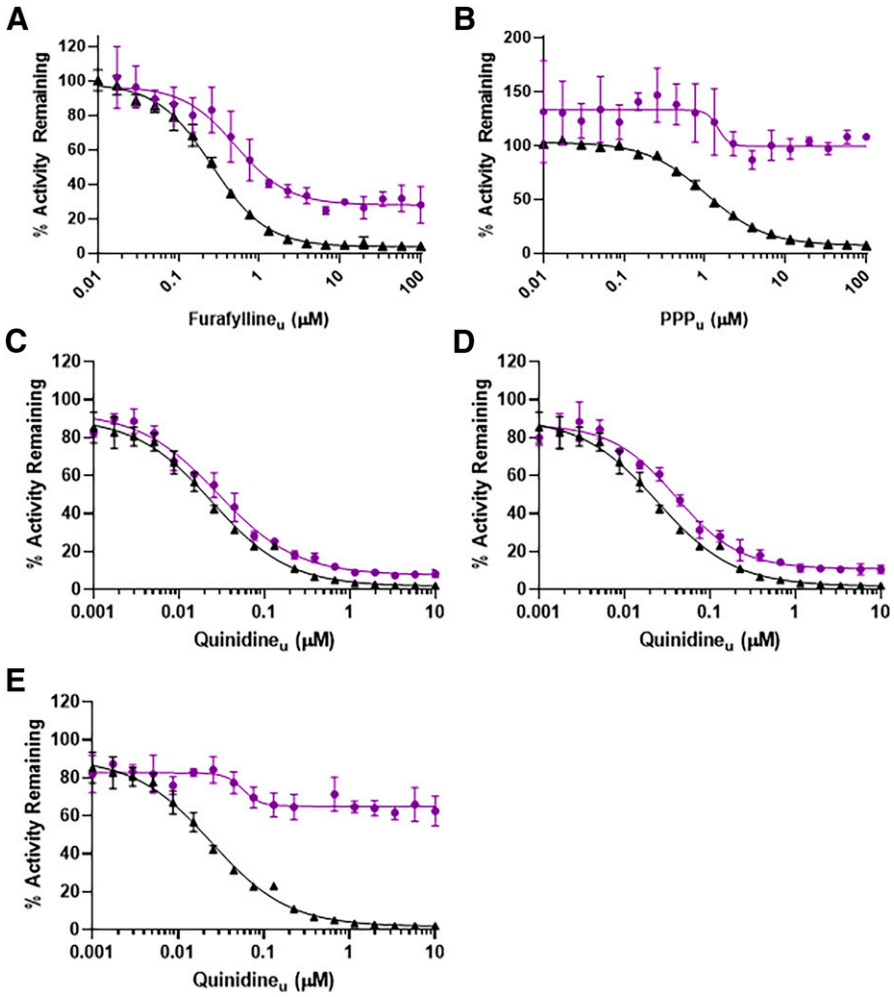

Fig. 5. Inhibition curves for metabolism of propranolol. (A) Effect of furafylline on N-dealkylation. (B) Effect of PPP on N-dealkylation. (C–E) Effect of quindine of 4-hydroxylation, 5-hydroxylation, and N-dealkylation reactions, respectively. Violet curves represent propranolol metabolism and black curves represent the positive control reactions for CYP1A2 (phenacetin O-dethylation), CYP2B6 (bupropion hydroxylation), and CYP2D6 (dextromethorphan O-demethylation).

inhibition values estimated from complex inhibition curve fitting (Fig. 3) yielded f_m values of 0.76 and 0.15 for CYP2C9 and CYP3A4, respectively, while CYP2C19 was concluded to not contribute (Table 3). (It should be noted that in this instance a maximal effect on 5-hydroxylation was not reportable because of assay interference at high concentrations of TAO.)

Recombinant CYP2C8, CYP2C9, CYP2D6, and CYP3A4 were all demonstrated to metabolize fluvastatin at measurable rates (Supplemental Table 10). When adjusting the measured rates for the three reactions by ISEF values for these four enzymes (Table 4), f_m values of 0.67, 0.29, 0.05, and <0.01 were determined for CYP2C9, CYP3A4, CYP2C8, and CYP2D6, respectively (Table 5). Thus, like the inhibition data, the estimated f_m for CYP2C9 matches reasonably well the values estimated from in vivo pharmacogenetic data estimated for CYP2C9 (Table 6). However, the contribution of CYP3A4 is overestimated when compared with the clinical DDI study result (f_m 0.12) shown in Table 6.

Pioglitazone: Enzyme Kinetics and Reaction Phenotyping. Pioglitazone was shown to be metabolized to four hydroxylated metabolites (Fig. 1), and these matched those that had been structurally characterized previously (Shen et al., 2003). Enzyme kinetic analysis of pioglitazone metabolism in human liver microsomes revealed that almost three-quarters of intrinsic clearance arises via 1'- and 2'-hydroxylation of the ethyl side chain (Table 1; Supplemental Fig. 7). Single-concentration inhibitor data supported that CYP2C8, CYP3A, CYP2C9, and CYP1A2 were involved in pioglitazone metabolism with estimated contributions of 0.60, 0.04, 0.04, and 0.04, respectively (Table 2). However, full curve data did not show a contribution from CYP1A2, but showed high involvement of CYP2C8 (f_m = 0.72) along with small contributions from CYP2C9 and CYP3A4 (Table 3; Fig. 4).

Among rCYP enzymes, pioglitazone metabolites were generated by CYP1A2, CYP2C8, CYP2C9, and CYP3A4 (as above) but also CYP2C19 and CYP2D6 (Supplemental Table 10). However, correction of the rates by ISEF and abundance values resulted in an estimated f_m for CYP2C8 of 0.82, with the other enzymes contributing very little (Tables 4 and 5). These values and those from inhibition data can be compared with an estimate of an in vivo value of 0.73 for CYP2C8, based on a gemfibrozil DDI study (Table 6). Thus, the main role for CYP2C8 was identified by all methods, albeit the inhibition curve approach yielded the estimate of f_m that was closest (0.73 versus 0.72; Table 6).

Propranolol: Enzyme Kinetics and Reaction Phenotyping. Propranolol is metabolized by P450-catalyzed oxidations, as well as direct glucuronidation, thus the determination of f_{CL} values required the use of pooled human hepatocytes to accommodate the glucuronidation reactions. Enzyme kinetics (Supplemental Fig. 8) of three oxidative reactions (4-hydroxylation, 5-hydroxylation, and N-deisopropylation), along with two glucuronidation reactions (O- and N-glucuronidations), are listed in Table 1 with estimated f_{CL} values. (There was a fourth oxidative product, 7-hydroxypropranolol, however its f_{CL} value was well under 0.01 and thus it was not measured in subsequent experiments.) 4-Hydroxylation is the dominant pathway (f_{CL} = 0.77). The

glucuronidation reactions accounted for 18% of metabolism in hepatocytes, and this value must be accounted for when estimating f_m values for the oxidation pathways when using liver microsomes and rCYPs. Single point inhibition data suggested a dominating role for CYP2D6 and a minor role for CYP1A2 (Table 3). Full inhibition curves (Fig. 5) showed roles for CYP1A2 and CYP2D6, as well as for CYP2B6 (in N-dealkylation only). Estimated f_m values were 0.68, 0.03, and 0.02 for CYP2D6, CYP1A2, and CYP2B6, respectively. Notably, the minor role for CYP2B6 was revealed with the data-rich full inhibition curve, but the single point data for the effect of PPP on propranolol N-desisopropylation did not achieve statistical significance.

Propranolol metabolism was observed in several rCYPs when measuring metabolites with a sensitive HPLC-MS assay (Supplemental Table 10). Overall, when corrected for ISEF values, few of these enzymes were estimated to have a meaningful contribution to metabolism. The main contribution was from CYP2D6, which is in agreement with the inhibition data, albeit the estimated f_m value was somewhat lower (0.55; Table 5) and was within the range of estimated in vivo f_m values (Table 6). The lower CYP2D6 f_m value estimated from rCYP data as compared with inhibition data are due to an observable contribution by CYP3A4 (f_m = 0.11), which was not identified in TAO inhibition experiments in human liver microsomes. Furthermore, estimates of CYP3A contribution in vivo range as high as 0.39 from DDI data (Table 6), however, it is important to note that these DDI were observed with other drugs that affect cardiovascular functions (i.e., diltiazem and verapamil), and in one of those studies there was no effect observed on exposure to the 4-hydroxy metabolite, which would contradict CYP3A inhibition (since the 4-hydroxy metabolite was the major one formed by recombinant CYP3A4). Thus, the CYP3A4 contribution to propranolol clearance is unclear, but the CYP2D6 contribution was readily identified.

Risperidone: Enzyme Kinetics and Reaction Phenotyping. In human liver microsomes, risperidone was metabolized by three routes: 7-hydroxylation, 9-hydroxylation, and N-dealkylation (Fig. 1). For all three reactions, substrate saturation experiments showed biphasic kinetics (Supplemental Fig. 9). From the summed CL_{int} data, the fraction of metabolic clearance progressing through the 7-hydroxy, 9-hydroxy, and N-dealkylation pathways were calculated at 0.16, 0.67, and 0.17, respectively (Table 1). Using data from single concentrations of P450-selective inhibitors, it was shown that risperidone was metabolized mostly by CYP2D6 and CYP3A4, with minor involvement of CYP2C8 and CYP2C19 (Table 2). Using the approach of complete inhibition curves (Fig. 6) and fitting the data to generate the maximum inhibition value showed that only CYP2D6 and CYP3A4 contribute, with f_m values of 0.60 and 0.34, respectively (Table 3), which compare favorably to values estimated from pharmacogenetic and DDI studies (Table 6).

When using reaction rate data from rCYP enzymes, risperidone was shown to be metabolized by CYP2C8, CYP2C19, CYP2D6, and CYP3A4 (Supplemental Table 10). Adjusting each reaction rate using ISEF values (Table 4) and calculating f_m values for these four enzymes yielded values of 0.07, 0.01, 0.19, and 0.73 for CYP2C8, CYP2C19, CYP2D6, and CYP3A4, respectively (Table 5). With this approach, CYP3A4 is overemphasized at the expense of CYP2D6 and these estimates of f_m do not compare favorably with in vivo estimates (Table 6).

Escitalopram: Enzyme Kinetics and Reaction Phenotyping. Escitalopram is metabolized primarily via two routes at the amine nitrogen: N-demethylation and N-deamination, with the latter pathway initially yielding an aldehyde that undergoes rapid oxidation to a carboxylic acid (Fig. 1). Because of this latter pathway, the enzyme kinetics were measured in pooled human hepatocytes (Table 1; Supplemental Fig. 10) to generate f_{CL} values of 0.80 and 0.20 for N-demethylation and N-deamination, respectively. Evaluation of inhibition data suggested roles for CYP2B6, CYP2C8, CYP2C19, CYP2D6, and CYP3A4 (Tables 2 and 3; Fig. 7). For the N-deamination reaction, inhibition data were generated using pooled human hepatocytes and showed essentially complete inhibition using the CYP2C19 inactivator esomeprazole. Also observed was a partial effect on N-demethylation, suggesting a role for CYP2C19 in this reaction as well. Initial data in human liver microsomes showed little to no effect of N-benzylnirvanol on escitalopram N-demethylation (Supplemental Fig. 11). The hepatocyte data showing a role for CYP2C19 in N-demethylation was aligned with the metabolite profile data in rCYP2C19 (Supplemental Fig. 5), and illustrates leveraging the knowledge gained from the initial qualitative rCYP metabolite profiling data when interpreting the inhibition data. The estimated in vivo

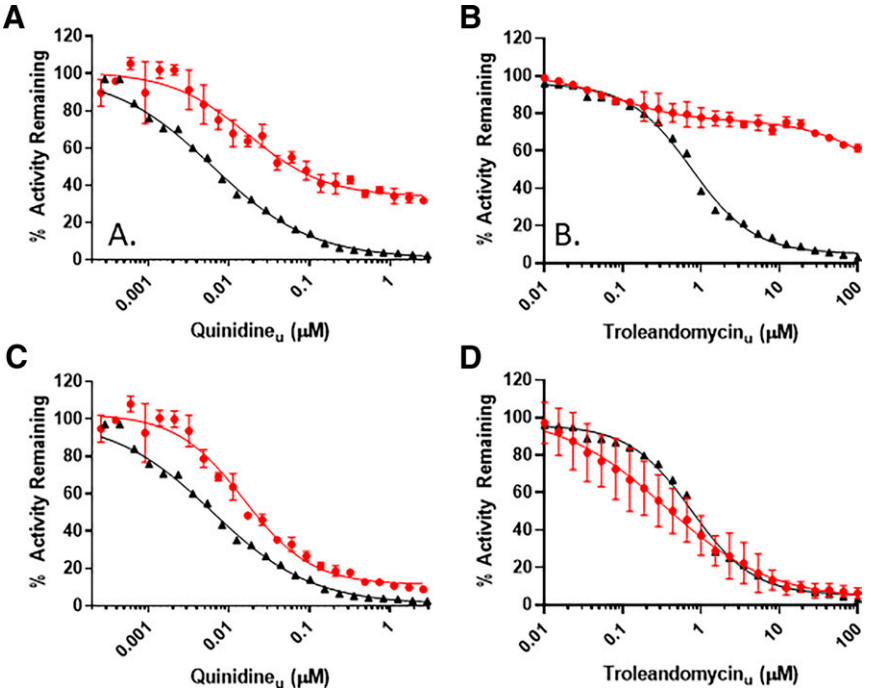

Fig. 6. Inhibition curves for metabolism of risperidone. (A and B) Effect of quinidine and troleandomycin on 9-hydroxylation. (C) Effect of quinidine on 7-hydroxylation. (D) Effect of troleandomycin on N-dealkylation. Red curves represent risperidone metabolism and black curves represent the positive control reactions for CYP2D6 (dextromethorphan O-demethylation), and CYP3A (midazolam 1'-hydroxylation).

values for CYP2C19 contribution to escitalopram clearance from pharmacogenetic studies give a wide range of 0.36–0.82 (Table 6) with a minor contribution from CYP3A and no impact of CYP2D6. Also shown in Fig. 7 is the inhibition curve generated by TAO, which is readily interpretable, and data can be fit to a simple four-parameter inhibition curve. Finally, it should be noted that monoamine oxidase inhibitors were also tested for their effect on escitalopram N-deamination in human hepatocytes, since a previous report described a role for monoamine oxidase in this reaction (Rochat et al., 1998). However, in the present study no effects of monoamine oxidase inhibitors chlorgyline (0.1 μM) or selegiline (1 μM) were observed. It is still possible that monoamine oxidase in extrahepatic tissues contributes to escitalopram clearance in vivo.

In rCYP enzymes, escitalopram N-demethylation was measurable in CYP1A2, CYP2C8, CYP2C19, CYP2D6, and CYP3A4, with CYP2D6 catalyzing this reaction at a very high rate relative to the others (Supplemental Table 10). Only CYP2C19 was able to generate the carboxylic acid metabolite. Following correction for ISEF factors for rate (Table 4), estimations of f_m values for escitalopram total metabolism were 0.22, 0.23, 0.47, and 0.08 for CYP2C8, CYP2C19, CYP2D6, and CYP3A4, respectively, with the contribution by CYP1A2 less than 0.01 (Table 5). This may overemphasize the CYP2D6 contribution relative to CYP2C19, since not all of the enzymes may be able to convert an initial (and undetectable) aldehyde metabolite from N-deamination to the carboxylic acid, but several are able to catalyze formation of the readily detectable N-desmethyl metabolite.

Discussion

The quantitative estimation of the involvement of individual P450 enzymes to metabolic clearance from in vitro data is important in drug research, as the data can inform the need for clinical drug interaction and pharmacogenetic studies. Two orthogonal approaches, effect of specific inhibitors in human liver microsomes or hepatocytes and ISEF-corrected metabolism rates in expressed P450 enzymes, have been recommended in consortia publications and regulatory guidance documents (Bjornsson et al., 2003; EMA, 2012; Bohnert et al., 2016; FDA, 2020: https://www.fda.gov/regulatory-information/search-fda-guidance-documents/in-vitro-drug-interaction-studies-cytochrome-p450-enzyme-and-transporter-mediated-drug-interactions). However, these approaches are not perfect. Selective inhibitors are generally not selective enough, especially when used at single-test concentrations (Lu, et al., 2003; Khojasteh et al., 2011; Nirogi et al., 2015; Doran et al., 2022). The use of rCYP enzymes can be flawed because different marker substrates can yield different ISEFs (Siu and Lai, 2017; Lindmark et al., 2018; Wang et al., 2019; Dantonio et al., 2022). The two methods can frequently yield f_m values that are not in agreement. The objective of the present work was to develop an approach that would yield improved reaction phenotyping data.

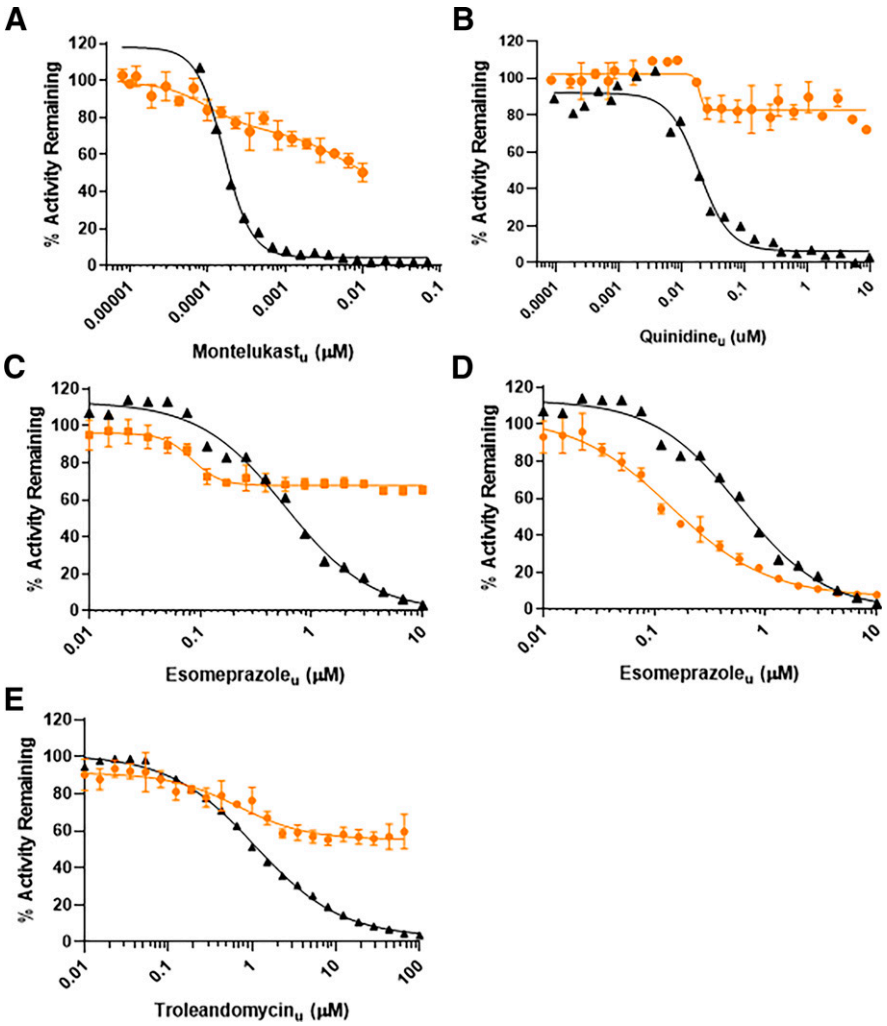

Fig. 7. Inhibition curves for metabolism of escitalopram. (A) Effect of montelukast on N-demethylation in human liver microsomes. (B) Effect of quindine on N-deamination in human liver microsomes. (C) Effect of esomeprazole on N-demethylation in human hepatocytes. (D) Effect of esomeprazole on N-deamination in human hepatocytes. (E) Effect of troleandomycin on N-demethylation in human liver microsomes. Orange curves represent escitalopram metabolism and black curves represent the positive control reactions for CYP2C8 (amodiaquine N-deethylation), CYP2D6 (dextromethorphan O-demethylation), CYP2C19 (mephenytoin 4'-hydroxylation), and CYP3A (midazolam 1'-hydroxylation).

Forty-eight drugs were first evaluated in baculosome-expressed rCYP enzymes using a metabolite profiling approach, and from this set, five were selected for detailed reaction phenotyping using both rCYPs with ISEF and selective inhibitors. These five were selected to ensure that the involvement of different P450 enzymes was evaluated and that they had commercially available or readily biosynthesized metabolite standards needed for quantitative bioanalysis. The estimated f_m values were compared with those estimated from clinical DDI and pharmacogenetic studies (Table 6; Fig. 8). Overall, the use of chemical inhibitors using a full concentration range offered the values of f_m that were closest to clinical data. The merits of this, when integrated into a "qualitative-then-quantitative" reaction phenotyping experimental design (Fig. 9), are described below.

Baculosome-expressed rCYPs are valuable reagents. Although it was not the main objective of the study, some interesting observations into these enzymes can be made from the data in Table 2. As expected, the P450 enzymes that have been a focus of drug metabolism for decades, such as CYP3A4, CYP3A5, CYP1A2, CYP2C8, CYP2C9, CYP2C19, and CYP2D6, show a high prevalence of ability to metabolize drugs (at least from this set of 48). But there were also some unexpected observations, such as the high frequency with which some of the less-studied enzymes, such as CYP1A1, CYP1B1, CYP2J2, CYP2C18, and CYP3A7, demonstrated an ability to catalyze drug metabolism. Some of these latter P450s are not highly expressed in the liver or are extrahepatically expressed. Also, at present, they do not have well-characterized selective inhibitors or marker substrate activities, which makes it difficult to understand their relative contributions to the in vivo metabolism of any given drug. However, despite the overall value of rCYPs in identifying the potential for involvement in metabolism, their use in making quantitative f_m estimates is limited. For pioglitazone, fluvastatin, and propranolol, rCYPs with ISEFs yielded values in agreement with clinical data for their major clearing enzymes CYP2C8, CYP2C9, and CYP2D6, respectively. However, the contribution of CYP2D6 to risperidone metabolism was far underestimated, wherein the low f_m value of 0.19 would not project the important impact of CYP2D6 expression on risperidone pharmacokinetics. A similar finding was made for escitalopram and CYP2C19. From examples like these and others (unpublished data on experimental drug candidates), we conclude that rCYP data

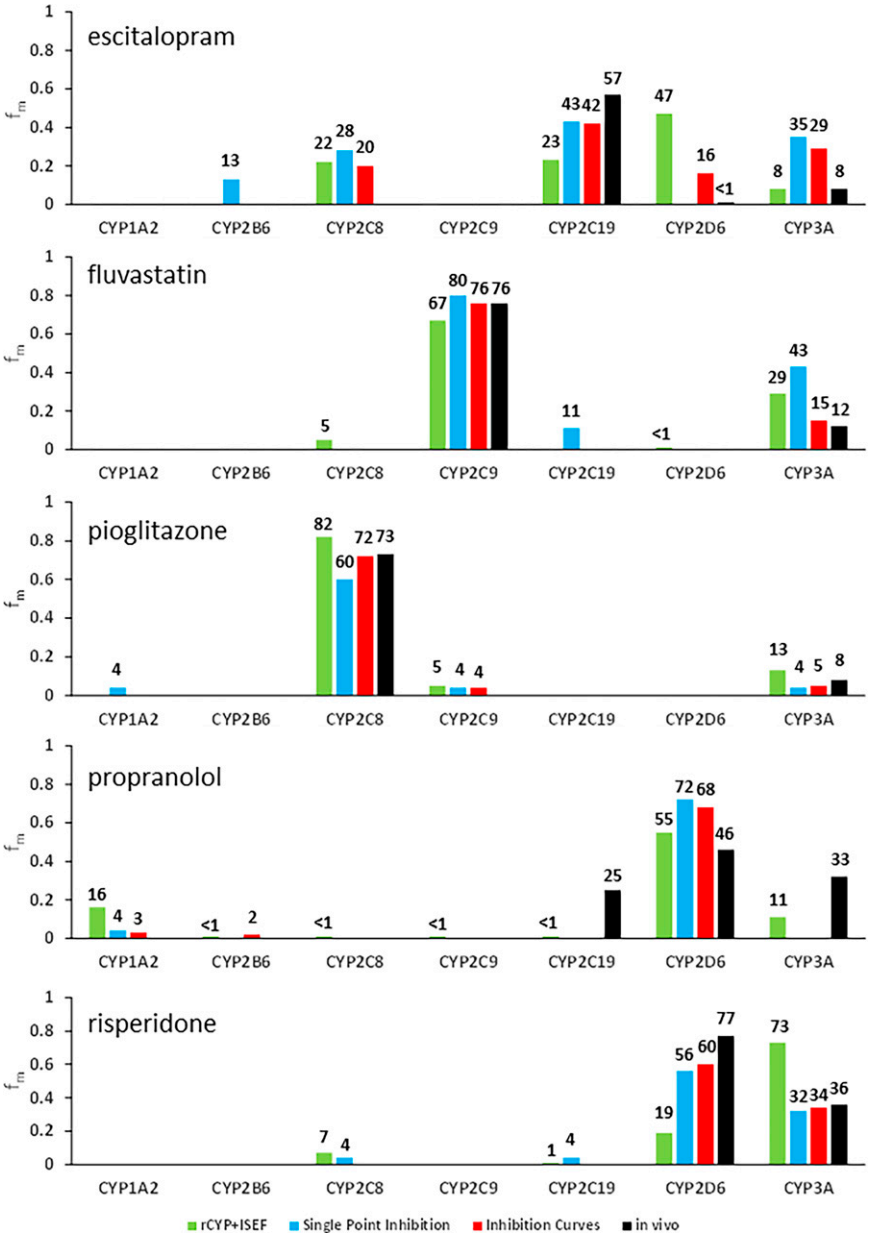

Fig. 8. Comparison of f_m values calculated by different methods and in vivo estimates. For instances in which more than one clinical report was available the median value is shown.

should not be used quantitatively to project f_m values. The observation that some ISEF values vary with the P450 marker substrates used to derive them is proposed as a main factor contributing to this problem (Siu and Lai, 2017; Lindmark et al., 2018; Wang et al., 2019; Dantonio et al., 2022). Reasons underlying substrate-dependent ISEF values at the biochemical level are unknown. However, it has been demonstrated that rCYPs can be useful in an initial qualitative assessment of metabolism, especially when combined with modern methods of metabolite profiling and identification. By following the formation of metabolites, rCYP incubations never failed to identify an enzyme that has importance in drug clearance for all 48 of the drugs evaluated (Fig. 2). In fact, this approach was too sensitive in many cases, as shown by numerous instances in which a given enzyme demonstrated a capability to generate metabolites for a drug even when the enzyme has no demonstrated clinical relevance. But there were no instances of false negatives where an enzyme important in clearance in vivo failed to generate metabolites. As such, this experiment can offer a good first step in a reaction phenotyping cascade (Fig. 9). Any P450 that demonstrates an ability to generate metabolites would move on to subsequent evaluation with inhibitors in liver microsomes (or hepatocytes).

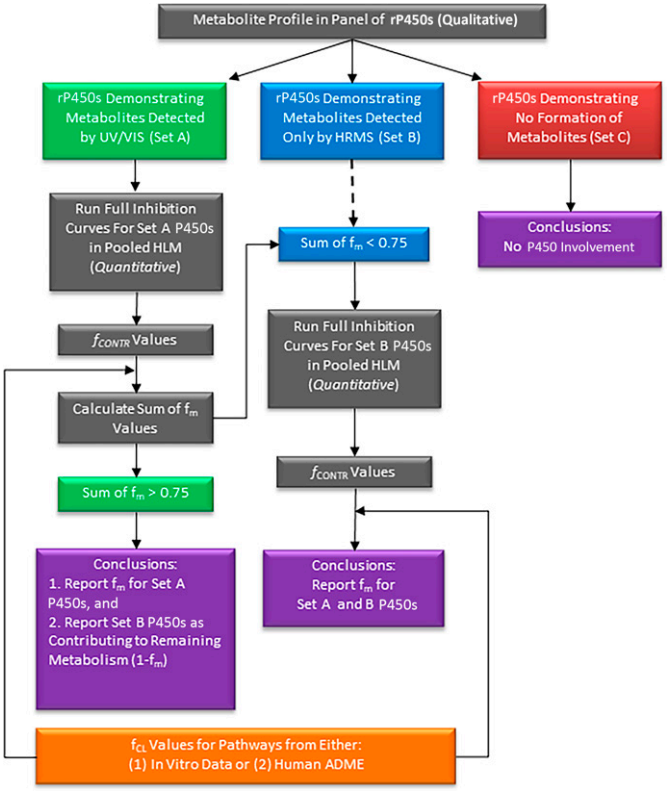

Fig. 9. Overall approach for P450 reaction phenotyping. A qualitative determination of metabolite profiles is conducted across a panel of individually expressed P450 enzymes using HPLC-UV-HRMS. Enzymes that yield no discernable metabolites by UV/VIS or HRMS are eliminated from any further consideration. Those enzymes that demonstrate formation of metabolites detected by UV/VIS are of greatest focus (Set A). Full inhibition curves are generated in human liver microsomes using inhibitors to address only Set A enzymes and generate f_{CONTR} values. The f_{CONTR} values are combined with f_{CL} values, obtained from either quantitative metabolite profiles from human metabolism-excretion studies or from metabolite profile data generated in an appropriate in vitro system, to yield f_m values. If the sum of f_m values across all pathways exceeds 0.75, then the P450 phenotyping is considered complete, and any remaining uninhibited activity (f_m < 0.25) is attributed to the enzymes that generated metabolites only detectable by HRMS (Set B). If the sum of f_m values is less than 0.75, then additional inhibition curves are generated to yield f_{CONTR} values for Set B P450 enzymes. In this latter case, the collective f_m values for both Set A and Set B P450 enzymes are reported.

P450 inhibitors were evaluated in two ways: single concentration versus full inhibition curves. Use of single concentrations of inhibitors is commonly observed in literature reports describing P450 reaction phenotyping. A challenge with this lies in delineating a true contribution of a P450 versus spillover inhibition caused by suboptimal inhibitor selectivity (Doran et al., 2022). In Table 2, there are several instances of low but measurable inhibition, even cases where the standard deviation was lower than the percentage of inhibition. When summed, these small amounts of inhibition can erode the estimation of f_m values for important enzymes. However, application of a more rigorous statistical evaluation (described in Materials and Methods) can eliminate these as artifacts.

To overcome problems of inhibitor spillover we employed a dense 18–22-point inhibition curve design for chemical inhibition experiments (seen in Figs. 3–7), which permits fitting complex functions to the data to reliably capture instances of nonselective inhibition. The power in this design affords a check on the inflection point of the first inhibition curve to verify agreement with the IC_{50} for a known marker substrate activity, and also permits estimation of the maximum inhibition that is due only to effects on the target enzyme and excludes inhibition caused by spillover. Fraction metabolized values for the major P450 enzymes involved in the metabolism of the five example drugs were well-estimated using this approach. Success was realized particularly for escitalopram and risperidone, where the ISEF approach failed. Employing the most selective inhibitors is important. Finally, reaction phenotyping experimental designs, wherein the effects of inhibitors are assessed by measuring formation of metabolites, offer greater levels of sensitivity and granularity because the contribution of each enzyme to the formation of each metabolite is determined. Furthermore, it should be appreciated that following metabolite formation is essential for accurate reaction phenotyping of low intrinsic clearance drugs.

From the results of these studies, a "qualitative-then-quantitative" cascade approach is proposed for reaction phenotyping (Fig. 9). In step 1, a metabolite profile is generated for each rCYP enzyme. Those enzymes that yield the largest amounts of metabolites (especially observed in the UV traces) are selected for evaluation in step 2, which is a full multipoint inhibition curve for each of the enzymes identified in the first step. After step 2, if at least 75% of the total clearance is accounted for, then the study can be considered complete with the f_m values reported from the maximum inhibition data, and the remaining f_m (<25%) described as being catalyzed by a combination of the remaining P450s observed in step 1 and any other non-P450–mediated clearance. If less than 75% is accounted for, step 2 is expanded to the other P450s identified in step 1 that showed less metabolism (including those for which metabolites were only observed by MS). If an rCYP fails to generate any metabolites by MS, it can be concluded that the enzyme is not involved in the metabolism at all, since the first step yielded no instances of false negative outcomes. Such an approach leverages the value in each of the individual experiment types while avoiding their pitfalls.

In conclusion, a sequential "qualitative-then-quantitative" approach to P450 reaction phenotyping is proposed as an alternate to the current standard in-parallel two-orthogonal method approach described in reviews and guidance documents (Bjornsson et al., 2003; EMA, 2012; Bohnert et al., 2016; FDA, 2020: https://www.fda.gov/regulatory-information/search-fda-guidance-documents/in-vitro-drug-interaction-studies-cytochrome-p450-enzyme-and-transporter-mediated-drug-interactions). The approach merges metabolite profiling techniques into reaction phenotyping and leverages the best that each of the individual P450 reaction phenotyping tools have to offer while avoiding confounding factors such as inhibitor spillover and substrate-dependent ISEFs. Further efforts include investigation into roles for some of the P450 enzymes that are extrahepatically expressed, along with continued application of the qualitative-then-quantitative P450 phenotyping approach to drug candidates.

Acknowledgments

The authors express gratitude to Greg Steeno for discussion of statistical approaches, Raeanne Geffert for some preliminary data, and Greg Walker and Raman Sharma for qNMR data for biosynthesized metabolite standards.

Authorship Contributions

Participated in research design: Doran, Dantonio, Goosen, Obach.

Conducted experiments: Dantonio, Gualtieri, Balesano, Landers, Obach.

Performed data analysis: Doran, Dantonio, Gualtieri, Balesano, Landers, Burchett, Obach.

Wrote or contributed to the writing of the manuscript: Doran, Goosen, Obach.

References

Aquilante CL, Kosmiski LA, Bourne DW, Bushman LR, Daily EB, Hammond KP, Hopley CW, Kadam RS, Kanack AT, Kompella UB et al. (2013) Impact of the CYP2C8 *3 polymorphism on the drug-drug interaction between gemfibrozil and pioglitazone. *Br J Clin Pharmacol* **75**:217–226.

Bjornsson TD, Callaghan JT, Einolf HJ, Fischer V, Gan L, Grimm S, Kao J, King SP, Miwa G, Ni L et al.; Pharmaceutical Research and Manufacturers of America Drug Metabolism/Clinical Pharmacology Technical Working Groups (2003) The conduct of in vitro and in vivo drug-drug interaction studies: a PhRMA perspective. *J Clin Pharmacol* **43**:443–469.

Bohnert T, Patel A, Templeton I, Chen Y, Lu C, Lai G, Leung L, Tse S, Einolf HJ, Wang YH et al.; International Consortium for Innovation and Quality in Pharmaceutical Development (IQ) Victim Drug-Drug Interactions Working Group (2016) Evaluation of a New Molecular Entity as a Victim of Metabolic Drug-Drug Interactions-an Industry Perspective. *Drug Metab Dispos* **44**:1399–1423.

Byrne AJ, McNeil JJ, Harrison PM, Louis W, Tonkin AM, and McLean AJ (1984) Stable oral availability of sustained release propranolol when co-administered with hydralazine or food: evidence implicating substrate delivery rate as a determinant of presystemic drug interactions. *Br J Clin Pharmacol* **17**:45S–50S.

Cabaleiro T, Ochoa D, López-Rodríguez R, Román M, Novalbos J, Ayuso C, and Abad-Santos F (2014) Effect of polymorphisms on the pharmacokinetics, pharmacodynamics, and safety of risperidone in healthy volunteers. *Hum Psychopharmacol* **29**:459–469.

Dantonio AL, Doran AC, and Obach RS (2022) Intersystem extrapolation factors are substrate-dependent for CYP3A4: impact on cytochrome P450 reaction phenotyping. *Drug Metab Dispos* **50**:249–257.

Dimmitt DC, Yu DK, Elvin AT, Giesing DH, and Lanman RC (1991) Pharmacokinetics of diltiazem and propranolol when administered alone and in combination. *Biopharm Drug Dispos* **12**:515–523.

Doran AD, Dantoio AL, Gualtieri GM, Balesano A, Landers C, Burchett W, Goosen TC, and Obach RS (2022) Using a multiple concentration chemical inhibition design for improved reaction phenotyping. Manuscript submitted for publication.

EMA (2012) Guideline on the investigation of drug interactions.

Gassó P, Mas S, Papagianni K, Ferrando E, de Bobadilla RF, Arnaiz JA, Bioque M, Bernardo M, and Lafuente A (2014) Effect of CYP2D6 on risperidone pharmacokinetics and extrapyramidal symptoms in healthy volunteers: results from a pharmacogenetic clinical trial. *Pharmacogenomics* **15**:17–28.

Gelboin HV, Park SS, Fujino T, Song BJ, Cheng KC, Miller H, Robinson R, West D, and Friedman FK (1985) Cytochromes P-450, xenobiotic and endobiotic metabolism: monoclonal antibody directed detection, purification and reaction phenotyping, in *Proc. Int. Symp.* pp 390–401, Microsomes Drug Oxid.

Gutierrez MM, Rosenberg J, and Abramowitz W (2003) An evaluation of the potential for pharmacokinetic interaction between escitalopram and the cytochrome P450 3A4 inhibitor ritonavir. *Clin Ther* **25**:1200–1210.

Herrlin K, Yasui-Furukori N, Tybring G, Widén J, Gustafsson LL, and Bertilsson L (2003) Metabolism of citalopram enantiomers in CYP2C19/CYP2D6 phenotyped panels of healthy Swedes. *Br J Clin Pharmacol* **56**:415–421.

Jaakkola T, Backman JT, Neuvonen M, and Neuvonen PJ (2005) Effects of gemfibrozil, itraconazole, and their combination on the pharmacokinetics of pioglitazone. *Clin Pharmacol Ther* **77**:404–414.

Jukić MM, Haslemo T, Molden E, and Ingelman-Sundberg M (2018) Impact of CYP2C19 Genotype on Escitalopram Exposure and Therapeutic Failure: A Retrospective Study Based on 2,087 Patients. *Am J Psychiatry* **175**:463–470.

Khojasteh SC, Prabhu S, Kenny JR, Halladay JS, and Lu AY (2011) Chemical inhibitors of cytochrome P450 isoforms in human liver microsomes: a re-evaluation of P450 isoform selectivity. *Eur J Drug Metab Pharmacokinet* **36**:1–16.

Kirchheiner J, Kudlicz D, Meisel C, Bauer S, Meineke I, Roots I, and Brockmöller J (2003) Influence of CYP2C9 polymorphisms on the pharmacokinetics and cholesterol-lowering activity of (-)-3S,5R-fluvastatin and (+)-3R,5S-fluvastatin in healthy volunteers. *Clin Pharmacol Ther* **74**:186–194.

Kivistö KT, Kantola T, and Neuvonen PJ (1998) Different effects of itraconazole on the pharmacokinetics of fluvastatin and lovastatin. *Br J Clin Pharmacol* **46**:49–53.

Krishnaiah YS, Satyanarayana S, and Visweswaram D (1994) Interaction between tolbutamide and ketoconazole in healthy subjects. *Br J Clin Pharmacol* **37**:205–207.

Lennard MS, Jackson PR, Freestone S, Tucker GT, Ramsay LE, and Woods HF (1984) The relationship between debrisoquine oxidation phenotype and the pharmacokinetics and pharmacodynamics of propranolol. *Br J Clin Pharmacol* **17**:679–685.

Lindh JD, Annas A, Meurling L, Dahl ML, and AL-Shurbaji A (2003) Effect of ketoconazole on venlafaxine plasma concentrations in extensive and poor metabolisers of debrisoquine. *Eur J Clin Pharmacol* **59**:401–406.

Lindmark B, Lundahl A, Kanebratt KP, Andersson TB, and Isin EM (2018) Human hepatocytes and cytochrome P450-selective inhibitors predict variability in human drug exposure more accurately than human recombinant P450s. *Br J Pharmacol* **175**:2116–2129.

Lu AY, Wang RW, and Lin JH (2003) Cytochrome P450 in vitro reaction phenotyping: a re-evaluation of approaches used for P450 isoform identification. *Drug Metab Dispos* **31**:345–350.

MacKenzie KR, Zhao M, Barzi M, Wang J, Bissig K-D, Maletic-Savatic M, Jung SY, and Li F (2020) Metabolic profiling of norepinephrine reuptake inhibitor atomoxetine. *Eur J Pharm Sci* **153**:105488.

Mahatthanatrakul W, Sriwiriyajan S, Ridtitid W, Boonleang J, Wongnawa M, Rujimamahasan N, and Pipatrattanaseree W (2012) Effect of cytochrome P450 3A4 inhibitor ketoconazole on risperidone pharmacokinetics in healthy volunteers. *J Clin Pharm Ther* **37**:221–225.

McCourty JC, Silas JH, Tucker GT, and Lennard MS (1988) The effect of combined therapy on the pharmacokinetics and pharmacodynamics of verapamil and propranolol in patients with angina pectoris. *Br J Clin Pharmacol* **25**:349–357.

McLean AJ, Skews H, Bobik A, and Dudley FJ (1980) Interaction between oral propranolol and hydralazine. *Clin Pharmacol Ther* **27**:726–732.

Nagar S, Argikar UA, and Tweedie DJ (2014) Enzyme kinetics in drug metabolism: fundamentals and applications. *Methods Mol Biol* **1113**:1–6.

Nirogi R, Palacharla RC, Uthukam V, Manoharan A, Srikakolapu SR, Kalaikadhiban I, Boggavarapu RK, Ponnamaneni RK, Ajjala DR, and Bhyrapuneni G (2015) Chemical inhibitors of CYP450 enzymes in liver microsomes: combining selectivity and unbound fractions to guide selection of appropriate concentration in phenotyping assays. *Xenobiotica* **45**:95–106.

O'Reilly RA (1973) Interaction of sodium warfarin and disulfiram (antabuse) in man. *Ann Intern Med* **78**:73–76.

Parkinson A (1996) An overview of current cytochrome P450 technology for assessing the safety and efficacy of new materials. *Toxicol Pathol* **24**:48–57.

Pichard L, Curi-Pedrosa R, Bonfils C, Jacqz-Aigrain E, Domergue J, Joyeux H, Cosme J, Guengerich FP, and Maurel P (1995) Oxidative metabolism of lansoprazole by human liver cytochromes P450. *Mol Pharmacol* **47**:410–418.

Raghuram TC, Koshakji RP, Wilkinson GR, and Wood AJ (1984) Polymorphic ability to metabolize propranolol alters 4-hydroxypropranolol levels but not beta blockade. *Clin Pharmacol Ther* **36**:51–56.

Rochat B, Kosel M, Boss G, Testa B, Gillet M, and Baumann P (1998) Stereoselective biotransformation of the selective serotonin reuptake inhibitor citalopram and its demethylated metabolites by monoamine oxidases in human liver. *Biochem Pharmacol* **56**:15–23.

Rodrigues AD (1999) Integrated cytochrome P450 reaction phenotyping: attempting to bridge the gap between cDNA-expressed cytochromes P450 and native human liver microsomes. *Biochem Pharmacol* **57**:465–480.

Rowland M and Matin SB (1973) Kinetics of drug-drug interactions. *Journal of Pharmacokinetics and Biopharmaceutics* **1**:553–567.

Rudberg I, Mohebi B, Hermann M, Refsum H, and Molden E (2008) Impact of the ultrarapid CYP2C19*17 allele on serum concentration of escitalopram in psychiatric patients. *Clin Pharmacol Ther* **83**:322–327.

Rudberg I, Reubsaet JL, Hermann M, Refsum H, and Molden E (2009) Identification of a novel CYP2C19-mediated metabolic pathway of S-citalopram in vitro. *Drug Metab Dispos* **37**:2340–2348.

Shen Z, Reed JR, Creighton M, Liu DQ, Tang YS, Hora DF, Feeney W, Szewczyk J, Bakhtiar R, Franklin RB et al. (2003) Identification of novel metabolites of pioglitazone in rat and dog. *Xenobiotica* **33**:499–509.

Siu YA and Lai WG (2017) Impact of Probe Substrate Selection on Cytrochrome P450 Reaction Phenotyping Using the Relative Activity Factor. *Drug Metab Dispos* **45**:183–189.

Spence JD, Munoz CE, Hendricks L, Latchinian L, and Khouri HE (1995) Pharmacokinetics of the combination of fluvastatin and gemfibrozil. *Am J Cardiol* **76**:80A–83A.

Tateishi T, Nakashima H, Shitou T, Kumagai Y, Ohashi K, Hosoda S, and Ebihara A (1989) Effect of diltiazem on the pharmacokinetics of propranolol, metoprolol and atenolol. *Eur J Clin Pharmacol* **36**:67–70.

Tateishi T, Ohashi K, Fujimura A, and Ebihara A (1992) The influence of diltiazem versus cimetidine on propranolol metabolism. *J Clin Pharmacol* **32**:1099–1104.

Tsuchimine S, Ochi S, Tajiri M, Suzuki Y, Sugawara N, Inoue Y, and Yasui-Furukori N (2018) Effects of Cytochrome P450 (CYP) 2C19 Genotypes on Steady-State Plasma Concentrations of Escitalopram and its Desmethyl Metabolite in Japanese Patients With Depression. *Ther Drug Monit* **40**:356–361.

Waade RB, Hermann M, Moe HL, and Molden E (2014) Impact of age on serum concentrations of venlafaxine and escitalopram in different CYP2D6 and CYP2C19 genotype subgroups. *Eur J Clin Pharmacol* **70**:933–940.

Walker GS, Bauman JN, Ryder TF, Smith EB, Spracklin DK, and Obach RS (2014) Biosynthesis of drug metabolites and quantitation using NMR spectroscopy for use in pharmacologic and drug metabolism studies. *Drug Metab Dispos* **42**:1627–1639.

Wang S, Tang X, Yang T, Xu J, Zhang J, Liu X, and Liu L (2019) Predicted contributions of cytochrome P450s to drug metabolism in human liver microsomes using relative activity factor were dependent on probes. *Xenobiotica* **49**:161–168.

Ward SA, Walle T, Walle UK, Wilkinson GR, and Branch RA (1989) Propranolol's metabolism is determined by both mephenytoin and debrisoquin hydroxylase activities. *Clin Pharmacol Ther* **45**:72–79.

Yoshida K, Maeda K, and Sugiyama Y (2013) Hepatic and intestinal drug transporters: prediction of pharmacokinetic effects caused by drug-drug interactions and genetic polymorphisms. *Annu Rev Pharmacol Toxicol* **53**:581–612.

Yasuhara M, Yatsuzuka A, Yamada K, Okumura K, Hori R, Sakurai T, and Kawai C (1990) Alteration of propranolol pharmacokinetics and pharmacodynamics by quinidine in man. *J Pharmacobiodyn* **13**:681–687.

Zhou HH, Anthony LB, Roden DM, and Wood AJ (1990) Quinidine reduces clearance of (+)-propranolol more than (-)-propranolol through marked reduction in 4-hydroxylation. *Clin Pharmacol Ther* **47**:686–693.

Address correspondence to: R. Scott Obach, Pfizer Inc., Eastern Point Road, Groton, CT, 06340. E-mail: r.scott.obach@pfizer.com

SUPPLEMENTAL TABLES AND FIGURES

AN IMPROVED METHOD FOR CYTOCHROME P450 REACTION PHENOTYPING USING A SEQUENTIAL QUALITATIVE-THEN-QUANTITATIVE APPROACH

Angela C. Doran, Alyssa L. Dantonio, Gabrielle M. Gualtieri, Amanda Balesano, Connor Landers, Woodrow Burchett, Theunis C. Goosen, and R. Scott Obach

SUPPLEMENTAL TABLE 1. Incubation Conditions for Metabolism of Escitalopram, Fluvastatin, Pioglitazone, Propranolol, and Risperidone in Pooled Human Liver Microsomes.

	Escitalopram	Fluvastatin	Pioglitazone	Propranolol	Risperidone
Human Liver Microsomes (mg/mL)	0.3	0.3	0.1	0.1	0.3
Substrate Concentration (μM)	Inhibition 4	Kinetic 0.01-100 Inhibition 0.1	Kinetic 0.003-300 Inhibition 0.3	Inhibition 0.5	Kinetic 0.003-300 Inhibition 1
Incubation Volume (mL)	Inhibition 0.20	Kinetic 0.30 Inhibition 0.30	Kinetic 0.30 Inhibition 0.40	Inhibition 0.30	Kinetic 0.30 Inhibition 0.30
Incubation Time (min)	15	40	40	10	30
Termination Solvent	Acetonitrile	Acetonitrile	Acetonitrile	Acetonitrile	Acetonitrile
Termination Solvent Volume (mL)	0.20	0.60	0.40	0.60	0.60
Internal Standard	Indomethacin	Diclofenac	Indomethacin	Indomethacin	Indomethacin
Internal Standard Concentration (ng/mL)	50	50	50	100	100

SUPPLEMENTAL TABLE 2. Hepatocyte Conditions

	Escitalopram	Propranolol
Human Hepatocytes (million cells/mL)	0.5	0.1
Substrate Concentration (μM)	Kinetics 0.03-600 Inhibition 25	Kinetics 0.01-300
Incubation Volume (mL)	Kinetics 0.12 Inhibition 0.15	Kinetics 0.12
Incubation Time (min)	120	45
Termination Solvent	Acetonitrile	Acetonitrile
Sample Collection Volume (mL)	Kinetics 0.08 Inhibition 0.1	Kinetics 0.08
Termination Solvent Volume (mL)	Kinetics 0.24 Inhibition 0.3	Kinetics 0.24
Internal Standard	Kinetics Terfenadine Inhibition Indomethacin	Diclofenac
Internal Standard Concentration (ng/mL)	5 50	25

SUPPLEMENTAL TABLE 3 rCYP Incubation Conditions

Substrate	Fluvastatin				
Substrate Concentration (μM)	0.1				
Incubation Volume (mL)	0.4				
Termination Solvent	Acetonitrile				
Sampling Volume (mL)	0.04				
Termination Solvent Volume (mL)	0.16				
Internal Standard	Diclofenac				
Internal Standard Concentration (ng/mL)	25				
Metabolite	5-Hydroxy	6-Hydroxy			N-Dealkyl
Enzyme	CYP2C9	CYP2C8 CYP2D6	CYP2C9	CYP3A4	CYP2C9
Enzyme Concentration (pmol/mL)	10	100	100	100	100
Incubation Time (min)	60	60	40	20	60

Substrate	Pioglitazone						
Substrate Concentration (μM)	0.3						
Incubation Volume (mL)	0.4						
Termination Solvent	Acetonitrile						
Sampling Volume (mL)	0.04						
Termination Solvent Volume (mL)	0.16						
Internal Standard	Indomethacin						
Internal Standard Concentration (ng/mL)	50						
Metabolite	2-Hydroxy		1'-Hydroxy			2'-Hydroxy	5-Hydroxy
Enzyme	CYP2C8	CYP2C9	CYP1A2 CYP2C8	CYP2C9 CYP2C19 CYP3A4	CYP2D6	CYP2C8	CYP2C8 CYP3A4
Enzyme Concentration (pmol/mL)	10	100	10	100	100	10	100
Incubation Time (min)	60	60	60	60	40	60	60

Supplemental Table 3 (continued)

Substrate	Escitalopram			
Substrate Concentration (μM)	0.3			
Incubation Volume (mL)	0.4			
Termination Solvent	Acetonitrile			
Sampling Volume (mL)	0.04			
Termination Solvent Volume (mL)	0.16			
Internal Standard	Indomethacin			
Internal Standard Concentration (ng/mL)	50			
Metabolite	N-desmethyl			N-Deamination
Enzyme	CYP1A2	CYP2C8 CYP2C19 CYP3A4	CYP2D6	CYP2C19
Enzyme Concentration (pmol/mL)	100	10	1	100
Incubation Time (min)	16	60	12	60

Substrate	Risperidone					
Substrate Concentration (μM)	1					
Incubation Volume (mL)	0.4					
Termination Solvent	Acetonitrile					
Sampling Volume (mL)	0.04					
Termination Solvent Volume (mL)	0.16					
Internal Standard	Indomethacin					
Internal Standard Concentration (ng/mL)	100					
Metabolite	9-OH			7-OH		N-Dealkyl
Enzyme	CYP2C8 CYP2C19	CYP2D6	CYP3A4	CYP2C8 CYP2C19 CYP3A4	CYP2D6	CYP3A4
Enzyme Concentration (pmol/mL)	100	10	10	100	10	10
Incubation Time (min)	60	20	60	60	20	20

Supplemental Table 3 (continued)

Substrate	Propranolol															
Substrate Concentration (μM)	0.5															
Incubation Volume (mL)	400															
Termination Solvent	Acetonitrile + 1% formic acid															
Sampling Volume (mL)	0.04															
Termination Solvent Volume (mL)	0.16															
Internal Standard	Diclofenac															
Internal Standard Concentration (ng/mL)	25															
Metabolite	4-OH					5-OH					N-Dealkyl					
CYP Enzyme	2B6 2C8 2C9	2C19	3A4	1A2	2D6	2C8	2C9	3A4	1A2	2D6	2C8 2C9	2B6	3A4	2C19	1A2	2D6
Enzyme Concentration (pmol/mL)	100	100	10	1	0.1	100	100	100	1	0.1	100	100	10	10	1	0.1
Incubation Time (min)	60	40	20	8	8	60	40	20	8	8	60	40	60	40	8	8

SUPPLEMENTAL TABLE 4. HPLC Conditions for Metabolites of Escitalopram, Fluvastatin, Pioglitazone, Propranolol, and Risperidone.

	Escitalopram		Fluvastatin		Pioglitazone		Propranolol		Risperidone	
Column	Kinetex C18		Waters Acquity HSS T3		Waters Acquity BEH C18		Kinetex C18		Kinetex C18	
Column Dimensions (mm)	2.1x50		2.1x100		2.1x50		2.1x50		2.1x100	
Particle Size (µm)	1.7		1.8		1.7		1.7		1.7	
Temperature (^{o}C)	20		20		20		50		20	
Mobile Phase A	0.1% formic acid in water		0.1% formic acid in water		0.1% formic acid in water		0.1% formic acid in water		0.1% Formic acid in 10 mM ammonium acetate in water	
Mobile Phase B	0.1% formic acid on acetonitrile		0.1% formic acid on acetonitrile		0.1% formic acid in acetonitrile		0.1% formic acid in acetonitrile		0.1% Formic acid in acetonitrile	
Flow Rate (mL/min)	0.5		0.5		0.4		0.55		0.5	
Gradient	Time (min)	%B	Time (min)	% B	Time (min)	% B	Time (min)	% B	Time (min)	% B
	0.00	5	0.00	2	0.00	10	0.00	2	0.00	2
	0.50	5	0.25	2	0.50	10	1.00	2	0.50	2
	2.00	95	3.50	55	5.50	23	3.20	30	3.00	40
	2.50	95	4.50	95	5.60	95	4.00	90	3.10	95
	2.60	5	5.00	95	6.20	95	4.80	90	3.50	95
	3.00	5	5.10	2	6.21	10	4.85	2	3.51	2
	-	-	5.50	2	7.21	10	5.15	2	4.00	2
Injection Volume (µL)	10		10		10		10		10	

SUPPLEMENTAL TABLE 5. Mass Spectrometer Conditions for Metabolites of Escitalopram, Fluvastatin, Pioglitazone, Propranolol, and Risperidone.

	Escitalopram	Fluvastatin	Pioglitazone	Propranolol	Risperidone
Metabolite	N-Demethylation	5-Hydroxylation	2-Hydroxylation	N-Dealkylation	9-Hydroxylation
Mass Transition (*m/z*)	311 → 262	428 → 240	373 → 239	218 → 74	427 → 110
Collision Energy (V)	22	40	36	18	50
Dwell Time (ms)	25	25	50	25	50
Standard Curve Range (nM)	0.25-500	0.25-500	0.4-500	0.25-100	1-500
Metabolite	N-Deamination	6-Hydroxylation	1'-Hydroxylation	4-Hydroxylation	7-Hydroxylation
Mass Transition (*m/z*)	311 → 237	428 → 282	373 → 150	276 → 116	427 → 207
Collision Energy (V)	-30	26	37	24	38
Dwell Time (ms)	25	25	50	25	40
Standard Curve Range (nM)	0.25-500	0.25-500	0.4-500	0.25-100	1-500
Metabolite	-	N-Dealkylation	2'-Hydroxylation	5-Hydroxylation	N-Dealkylation
Mass Transition (*m/z*)	-	352 → 334	373 → 132	276 → 116	220 → 94
Collision Energy (V)	-	20	48	24	28
Dwell Time (ms)	-	25	50	25	40
Standard Curve Range (nM)	-	0.25-500	0.4-500	0.25-100	1-500
Metabolite	-	-	5-Hydroxylation	Glucuronidation	-
Mass Transition (*m/z*)	-	-	373.0 → 313.0	436.3 → 260.0	-
Collision Energy (V)	-	-	27	31	-
Dwell Time (ms)	-	-	50	30	-
Standard Curve Range (nM)	-	-	0.4-500	0.25-100	-
Internal Standard	Indomethacin	Diclofenac	Indomethacin	Indomethacin	Indomethacin
Mass Transition (*m/z*)	358 → 139	297 → 216	358 → 139	258 → 139	358 → 139
Collision Energy (V)	22	30	22	22	22
Dwell Time (ms)	25	50	25	50	50

SUPPLEMENTAL TABLE 6. Incubation Conditions for Positive Control Probe Substrates.

CYP Isoform	Inhibitor	Inhibitor Concentration Range (µM)	Selective Probe Substrate	Substrate Concentration (µM)	Selective Reaction Monitored	Protein Concentration[a]	Incubation Time (min)
1A2	Furafylline	0.002-20	Phenacetin	6.0	Acetaminophen	0.03	15
2B6	PPP	0.01-100	Bupropion	18	hydroxybupropion	0.03	15
2C8	Montelukast	0.001-10	Amodiaquine	0.33	N-desethylamodiaquine	0.03	15
2C9	Sulfaphenazole	0.003-30	Diclofenac	1.3	hydroxydiclofenac	0.03	15
2C19	N-Benzylnirvanol	0.002-20	*S*-Mephenytoin	7.9	4'OHmephenytoin	0.03	15-20
	Esomeprazole	0.01-10		10		0.25	30
2D6	Quinidine	0.0003-3	Dextromethorphan	0.36	Dextrorphan	0.03	15
3A4/5	TAO	0.01-100	Midazolam	0.42	Midazolam 1′-hydroxylation	0.03	15

[a]For esomeprazole incubation conducted in HHEPs, protein concentration is in units of million cells/mL; for all other inhibitors incubations were conducted in HLM and protein concentration units are in mg/mL.

SUPPLEMENTAL TABLE 7. HPLC and Mass Spectrometer Conditions for Positive Control Probe Substrates.

	1A2		2B6		2C8		2C9		2C19		2D6		3A4	
Column	Waters HSS T3		Halo C18		Kinetex C18		Halo C18		Halo C18		Halo C18		Halo C18	
Column Dimensions (mm)	50x2.1		2.1x30		50x2.1		2.1x30		2.1x30		2.1x30		2.1x30	
Particle Size (µm)	1.8		2.7		1.7		2.7		2.7		2.7		2.7	
Temperature (^{o}C)	20		20		20		20		20		20		20	
Mobile Phase A	0.1% formic acid in water		0.1% formic acid in water		0.1% formic acid in water		0.1% formic acid in water		0.1% formic acid in water		0.1% formic acid in water		0.1% formic acid in water	
Mobile Phase B	0.1% formic acid in acetonitrile		0.1% formic acid in acetonitrile		0.1% formic acid in acetonitrile		0.1% formic acid in acetonitrile		0.1% formic acid in acetonitrile		0.1% formic acid in acetonitrile		0.1% formic acid in acetonitrile	
Flow Rate (mL/min)	0.3		0.5		0.5		0.5		0.5		0.5		0.5	
Gradient	Time	%B	Time	%B	Time	%B	Time	%B	Time	%B	Time	%B	Time	%B
	0	2	0	5	0	2	0	10	0	2	0	5	0	10
	0.5	2	0.3	5	0.5	2	0.8	10	0.5	2	0.4	5	0.8	10
	2	70	1.2	95	2.5	95	1.3	95	1.7	32	1.3	95	1.3	90
	2.1	90	1.5	95	3	95	1.8	95	1.9	95	1.8	95	1.8	90
	2.5	90	1.6	5	3.1	2	1.81	10	2.2	95	1.9	5	1.85	10
	2.55	2	2.1	5	3.5	2	2.2	10	2.25	2	2.4	5	2.3	10
	3	2							2.5	2				
Injection Volume (µL)	10		10		10		10		10		10		10	
Retention Time (min)	1.24		0.62		1.09		1.79		1.39		1.06		1.23	
Mass Transition (*m/z*)	152→110		256→139		328→283		312→266		235.2→150		258.1→201		342.2→324	
Collision Energy (V)	22		26		30		20		26		31		30	
Internal standard	[D_7]-Acetaminophen		[$^{2}H_6$]-Hydroxybupropion		[$^{2}H_5$]-N-Desethyl-amodiaquine		[$^{13}C_6$]-4′-Hydroxydiclofenac		[$^{2}H_3$]4'-Hydroxymephenytoin		[$^{2}H_3$]-Dextrorphan		[$^{2}H_4$]-Hydroxymidazolam	
IS (*m/z*)	159→115		262→139		333.2→283		318→272		238.2→150		261.1→201		346.2→328	

SUPPLEMENTAL TABLE 8. Fraction unbound values of inhibitors in liver microsomes[a]

Inhibitor	Fraction Unbound at Varying Microsomal Protein Concentrations					
	0.01 mg/mL	**0.03 mg/mL**	**0.1 mg/mL**	**0.3 mg/mL**	**1 mg/mL**	**3 mg/mL**
Ketoconazole				0.240 ± 0.0163[b]		
N-Benzylnirvanol	0.965 ± 0.0874	0.925 ± 0.0341	0.911 ± 0.0135	0.822 ± 0.0635	0.758 ± 0.0317	0.490 ± 0.0621
Quinidine	0.971 ± 0.0110	0.964 ± 0.0136	0.967 ± 0.0179	0.864 ± 0.0167	0.789 ± 0.0300	0.593 ± 0.0367
Sulfaphenazole	0.949 ± 0.118	0.985 ± 0.0294	1.057 ± 0.0409	1.034 ± 0.123	0.949 ± 0.0880	0.764 ± 0.0307
PPP	0.925 ± 0.0557	0.967 ± 0.0349	0.999 ± 0.0240	0.918 ± 0.0681	0.875 ± 0.0389	0.787 ± 0.0248
Furafylline	0.910 ± 0.189	0.980 ± 0.0845	1.004 ± 0.0666	0.935 ± 0.111	0.903 ± 0.0738	0.890 ± 0.0378
Montelukast	0.057 ± 0.026	0.00691 ± 0.0015	0.00193 ± 0.0009	0.00101 ± 0.00040	0.000302 ± 0.00009	0.000170 ± 0.00001
TAO	unbound at all concentrations					

[a]Mean ±, N=3

[b]ketoconazole only used for escitalopram at a liver microsome concentration of 0.3 mg/mL

SUPPLEMENTAL TABLE 9. Inhibitor concentrations used (μM) in single point inhibition experiments.

	Substrate				
Inhibitor	Escitalopram	Fluvastatin	Pioglitazone	Propranolol	Risperidone
Furafylline (1A2)	8.1	11.5	8.7	11.5	8.1
PPP (2B6)	8.1	11.5	8.1	11.5	8.1
Montelukast (2C8)	1.87	1.69	0.53	1.69	1.87
Sulfaphenazole (2C9)	8.1	11.5	8.54	11.5	8.1
N-Benzylnirvanol (2C19)	2.67	3.33	2.67	3.33	2.67
Esomeprazole (2C19)	2.96	NA	NA	NA	NA
Quinidine (2D6)	1.2	1.15	0.90	1.15	0.854
TAO (3A4)	18.7	19.7	18.7	19.7	18.7

NA = not applicable.

SUPPLEMENTAL TABLE 10. rCYP Rate Data for Escitalopram, Fluvastatin, Pioglitazone, Propranolol, and Risperidone[a]

	CYP1A2	CYP2B6	CYP2C8	CYP2C9	CYP2C19	CYP2D6	CYP3A4
Escitalopram							
N-Demethylation	0.460 (0.12)	ND	37.0 (1.3)	ND	53.3 (1.6)	7970 (380)	21.8 (0.93)
N-Deamination	ND	ND	ND	ND	3.47 (0.34)	ND	ND
Fluvastatin							
5- Hydroxylation	ND	ND	ND	237 (12)	ND	ND	ND
6- Hydroxylation	ND	ND	66.0 (5.3)	190 (11)	ND	37.5 (1.9)	645 (20)
N-Dealkylation	ND	ND	ND	21.3 (1.2)	ND	ND	ND
Pioglitazone							
1'-Hydroxylation	49.4 (2.2)	ND	238 (3)	14.7 (0.5)	18.0 (0.6)	55.6 (1.7)	3.74 (0.23)
2-Hydroxylation	ND	ND	25.2 (0.4)	13.2 (0.3)	ND	ND	ND
2'-Hydroxylation	ND	ND	43.5 (1.3)	ND	ND	ND	ND
5-Hydroxylation	ND	ND	4.83 (0.20)	ND	ND	ND	30.8 (1.1)
Propranolol							
4-Hydroxylation	590 (29.3)	0.0772 (0.0675)	1.43 (0.17)	0.204 (0.036)	0.962 (0.145)	16560 (688)	55.4 (5.0)
5-Hydroxylation	126 (6)	ND	0.174 (0.010)	0.350 (0.022)	ND	1458 (80)	0.984 (0.069)
N-Dealkylation	1170 (57)	2.46 (0.13)	0.562 (0.046)	0.682 (0.039)	137 (8)	1744 (105)	4.52 (0.38)
Risperidone							
7-Hydroxylation	ND	ND	0.861 (0.013)	ND	1.12 (0.05)	183 (2)	0.436 (0.051)
9-Hydroxylation	ND	ND	3.83 (0.11)	ND	4.82 (0.26)	1310 (9)	126 (5)
N-Dealkylation	ND	ND	ND	ND	ND	ND	115 (36)

[a]Rate data are expressed in intrinsic clearance terms (v/[S]) and in units of μL/min/nmol P450. Values are mean (SEM). ND = not detected

SUPPLEMENTAL TABLE 11. Unbound $IC_{50,A}$ Values (μM) from Multiple Concentration Inhibition Experiments for the Metabolism of Escitalopram, Fluvastatin, Pioglitazone, Propranolol, and Risperidone[a,c]

	Furafylline	PPP	Montelukast	Sulfaphenazole	N-Benzylnirvanol	Quinidine	TAO
	CYP1A2	CYP2B6	CYP2C8	CYP2C9	CYP2C19	CYP2D6	CYP3A
Escitalopram							
N-Demethylation	-	-	9.66e-005 (1.68e-005 - 0.000176)	-	0.0841 (0.0685 - 0.0997)	0.0194 (0.0128 - 0.0260)	0.677 (0.388 - 0.967)
N-Deamination	-	-	-	-	0.141 (0.111 - 0.171)	-	-
Positive Control Activity	-	-	0.000163 (0.000148 - 0.000177)	-	0.581 (0.426 - 0.736)	0.0192 (0.0141 - 0.0244)	1.09 (0.95 - 1.23)
Fluvastatin							
5- Hydroxylation	-	-	-	0.467 (0.445 - 0.489)	-	-	-
6- Hydroxylation	-	-	-	0.380 (0.320 - 0.454)	-	-	1.41 (1.11 - 1.82)
N-Dealkylation	-	-	-	0.488 (0.458 - 0.521)	-	-	-
Positive Control Activity	-	-	-	0.911 (0.875 - 0.949)	-	-	3.83 (3.42 - 4.35)
Pioglitazone							
1'-Hydroxylation	-	-	9.46e-005 (7.96e-005 - 0.000110)	-	-	-	-
2-Hydroxylation	-	-	0.00157 (0.00000 - 0.00325)	0.129 (0.0901 - 0.168)	-	-	-
2'-Hydroxylation	-	-	0.000555 (0.000410 - 0.000700)	-	-	-	-

5-Hydroxylation	-	-	-	-	-	-	2.66 (1.74 - 3.57)
Positive Control Activity	-	-	0.000126 (9.32e-005 - 0.000158)	0.140 (0.121 - 0.159)	-	-	1.10 (0.96 - 1.23)
Propranolol[d]							
4-Hydroxylation	-	-	-	-	-	0.0285 (0.0229 - 0.0346)	-
5-Hydroxylation	-	-	-	-	-	0.0398 (0.0328 - 0.0480)	-
N-Dealkylation	0.508 (0.328 - 0.688)	1.46 (0.63 - 2.29)	-	-	-	0.0574 (0.0387 - 0.0887)	-
Positive Control Activity	0257 (0.230 - 0.283)	1.03 (0.96 - 1.10)	-	-	-	0.0245 (0.0204 - 0.0290)	-
Risperidone							
7-Hydroxylation	-	-	-	-	-	0.0152 (0.0125 - 0.0179	-
9-Hydroxylation	-	-	-	-	-	0.0171 (0.0112 - 0.0229)	0.0760 (0.0365 - 0.116)
N-Dealkylation	-	-	-	-	-	-	0.349 (0.186 - 0.513)
Positive Control Activity	-	-	-	-	-	0.00620 (0.00531 - 0.00709)	0.751 (0.642 - 0.859)

[a]$IC_{50,A}$ data are mean (SE).

[b]Human hepatocyte values for escitalopram and propranolol, all others in HLM.

[c]Positive control activities are phenacetin O-deethylation (CYP1A2), bupropion hydroxylation (CYP2B6), amodiaquine N-deethylase (CYP2C8), diclofenac 4'-hydroxylase (CYP2C9), S-mephenytoin 4'-hydroxylase (CYP2C19), dextromethorphan O-demethylase (CYP2D6) and midazolam 1'-hydroxylase (CYP3A).

Supplemental Figure 1. HPLC-UV Chromatograms of Metabolite Profiles for Escitalopram (λ = 239 nm)

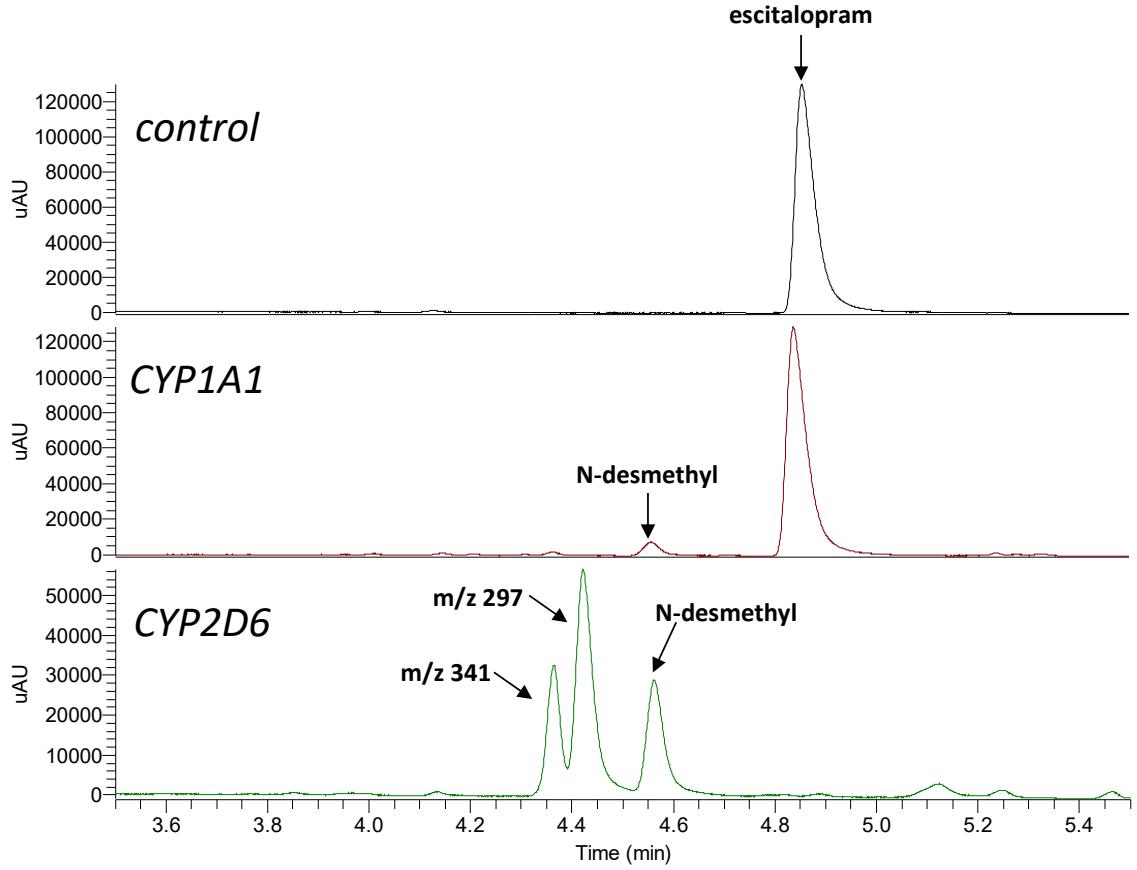

***m/z* 297 is the didesmethyl secondary metabolite. *m/z* 341 represents an addition of oxygen, but this metabolite was not seen in hepatocyte incubations**

Supplemental Figure 1 (continued)

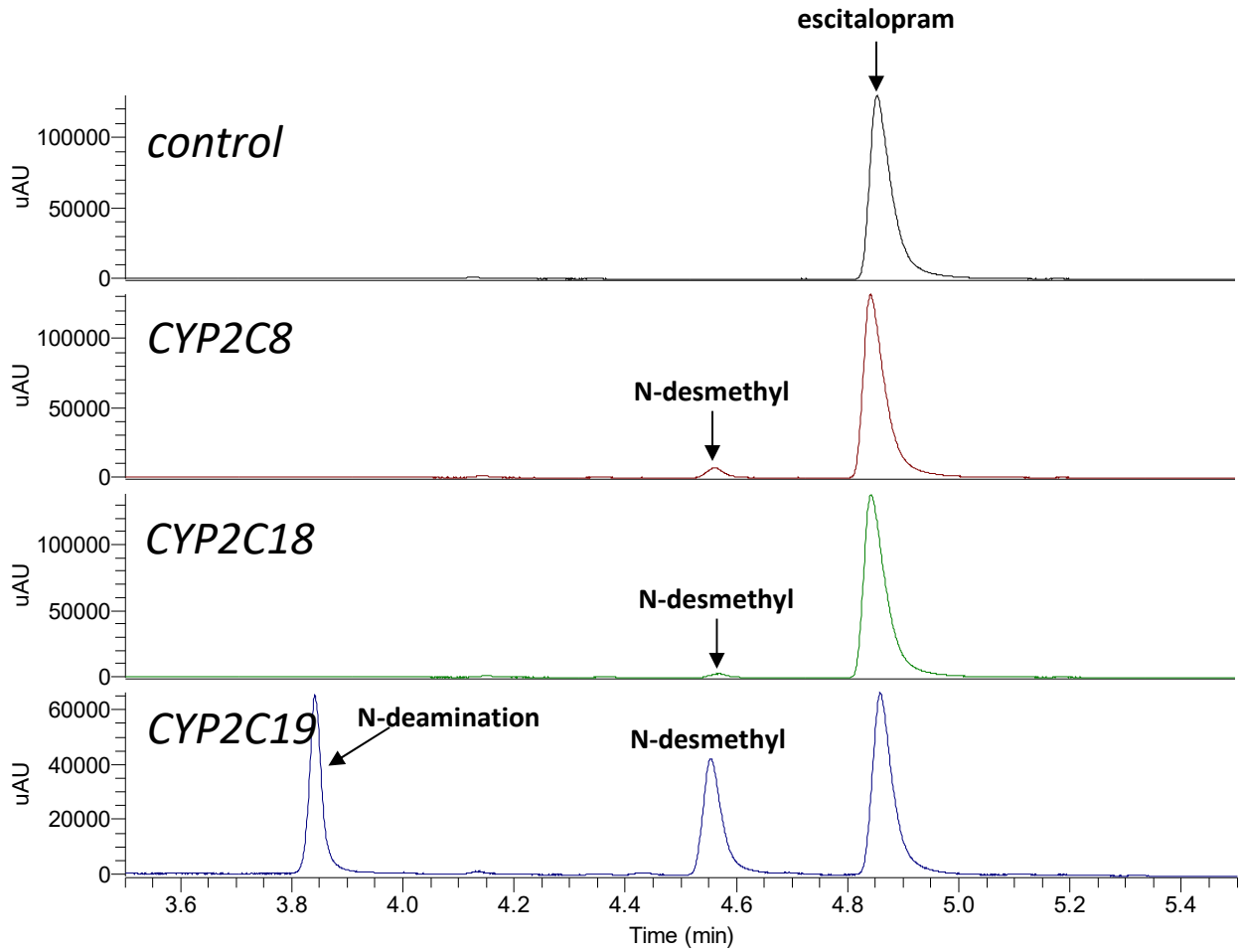

Supplemental Figure 1 (continued)

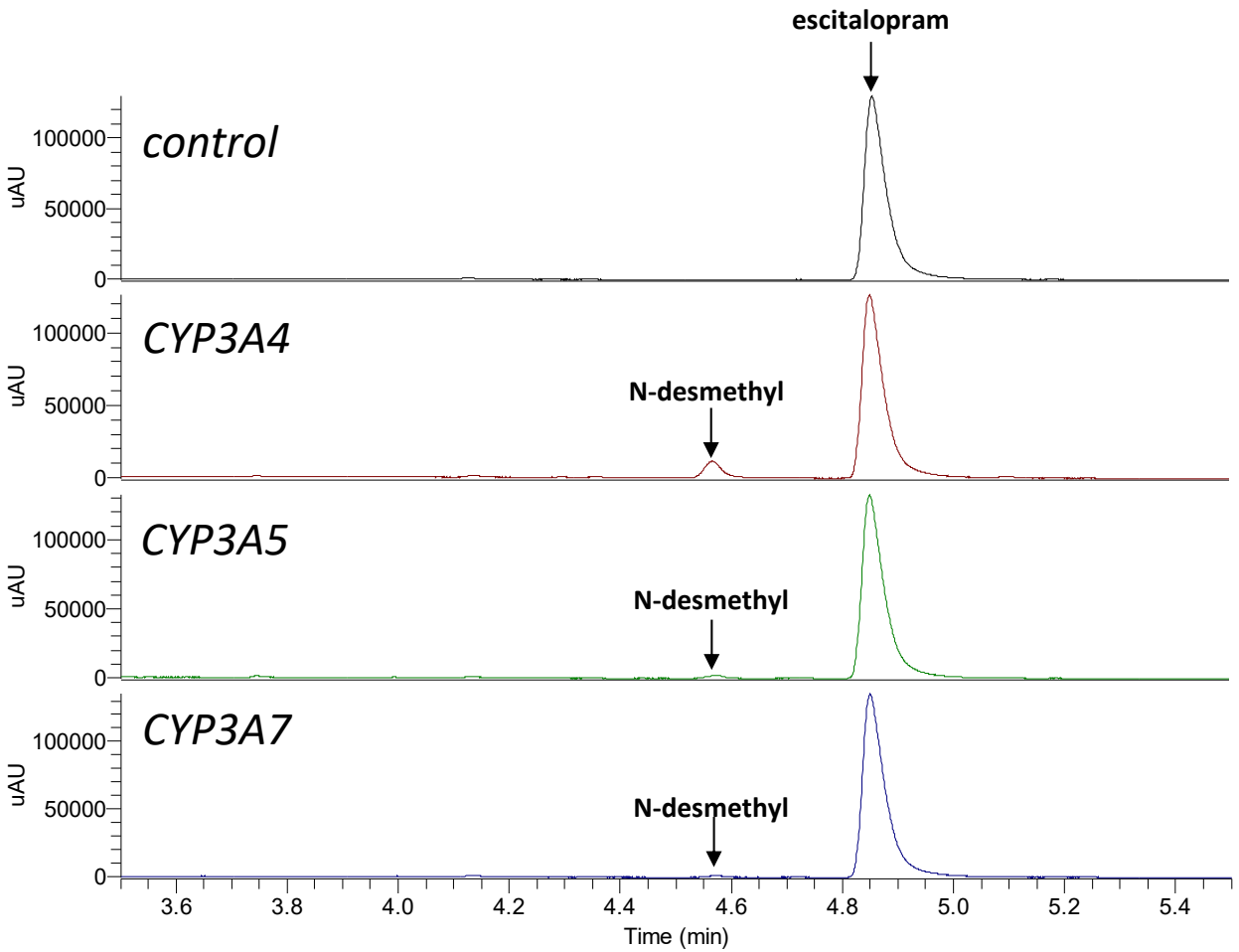

Supplemental Figure 2. HPLC-UV Chromatograms of Metabolite Profiles for Fluvastatin (λ = 304 nm)

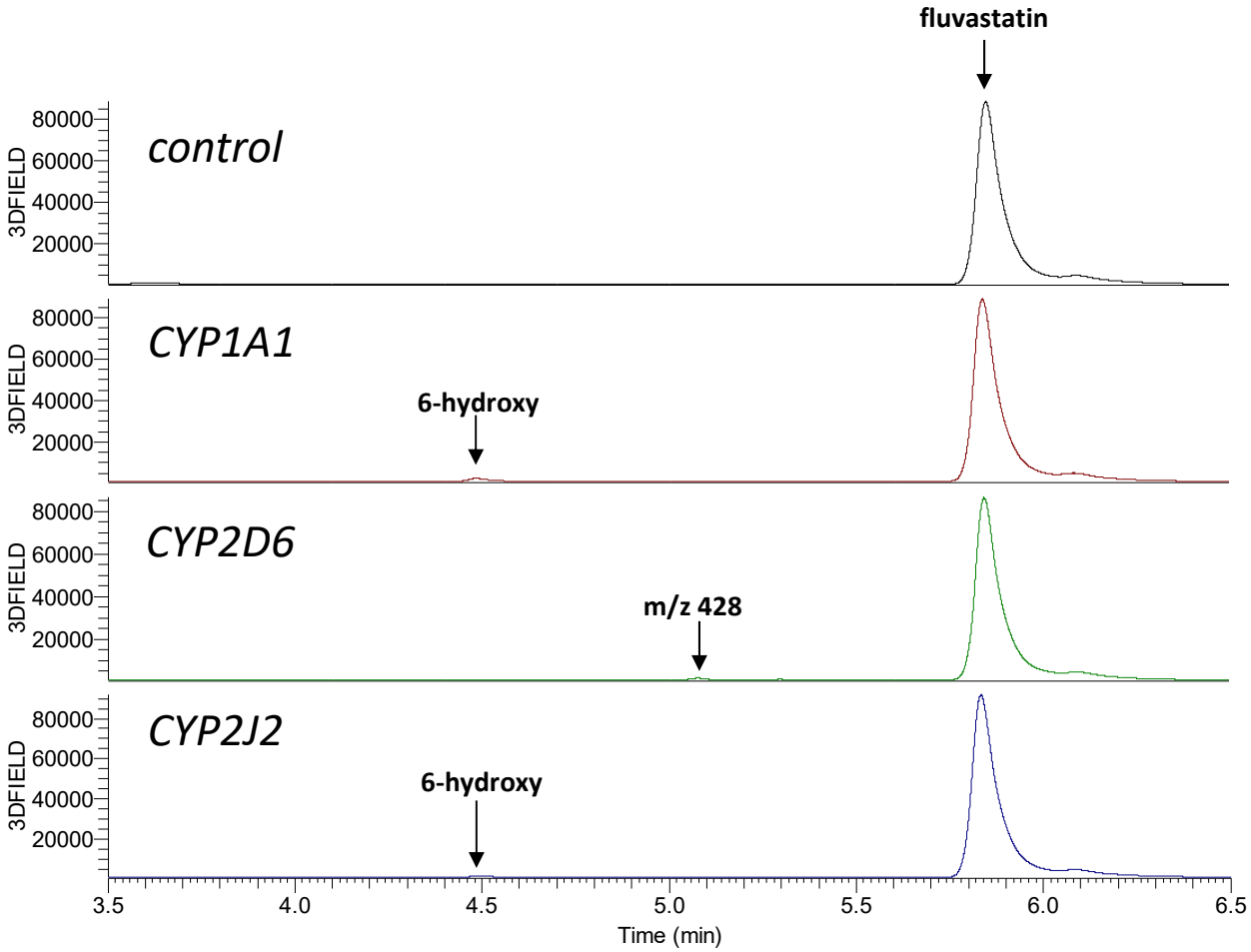

***m/z* 428 is an additional hydroxy metabolite not observed elsewhere.**

Supplemental Figure 2 (continued)

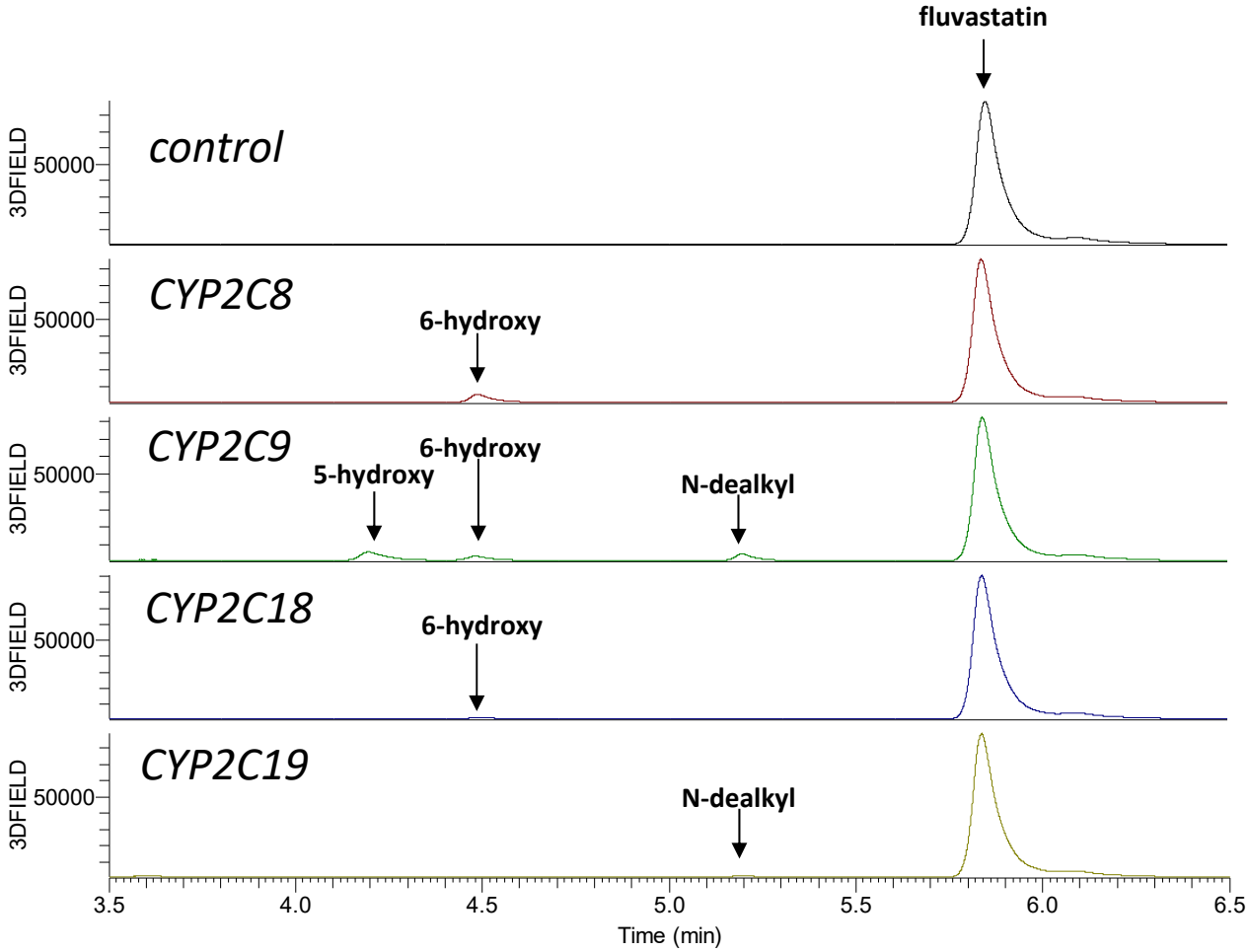

Supplemental Figure 2 (continued)

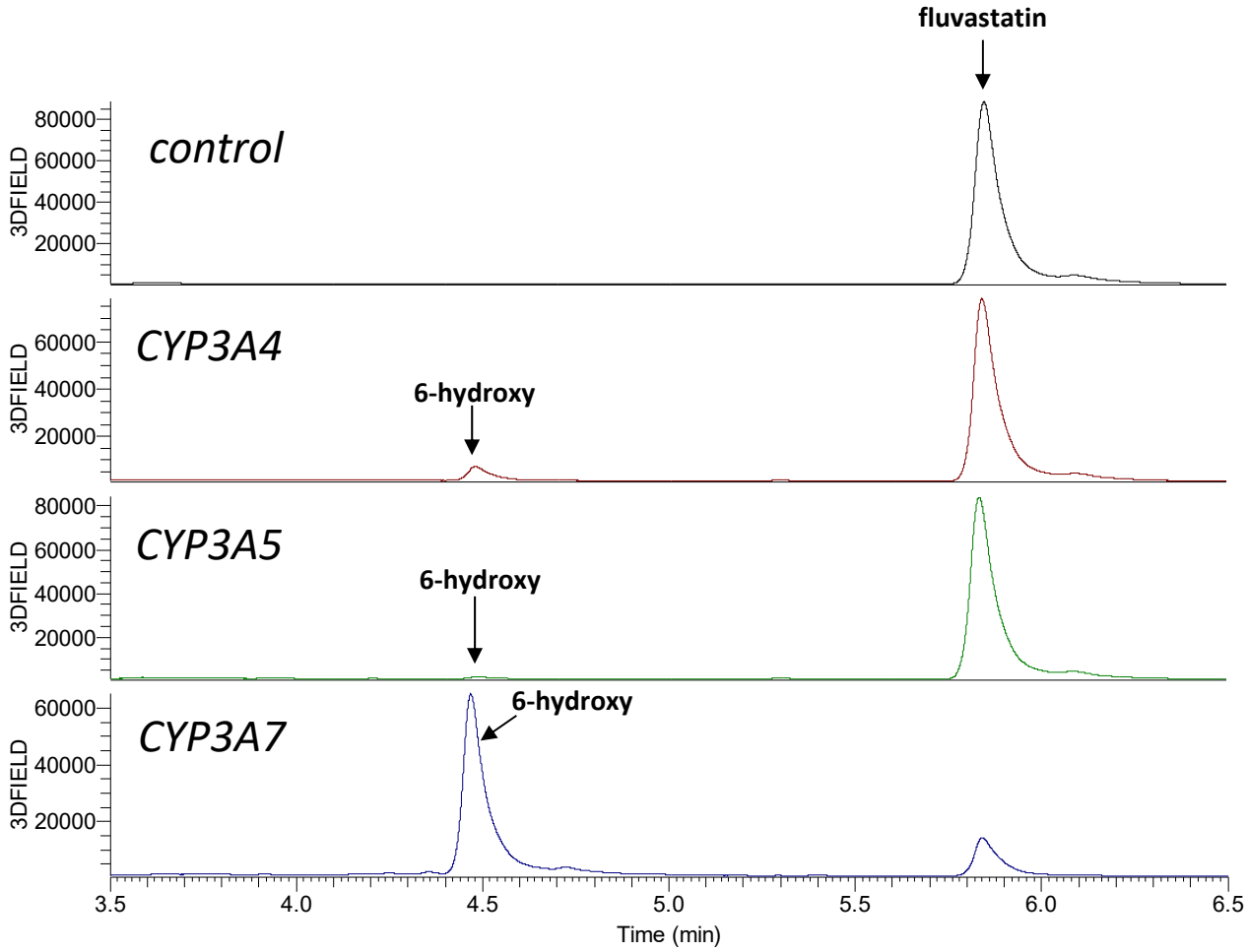

Supplemental Figure 3. HPLC-UV Chromatograms of Metabolite Profiles for Pioglitazone (λ = 264 nm)

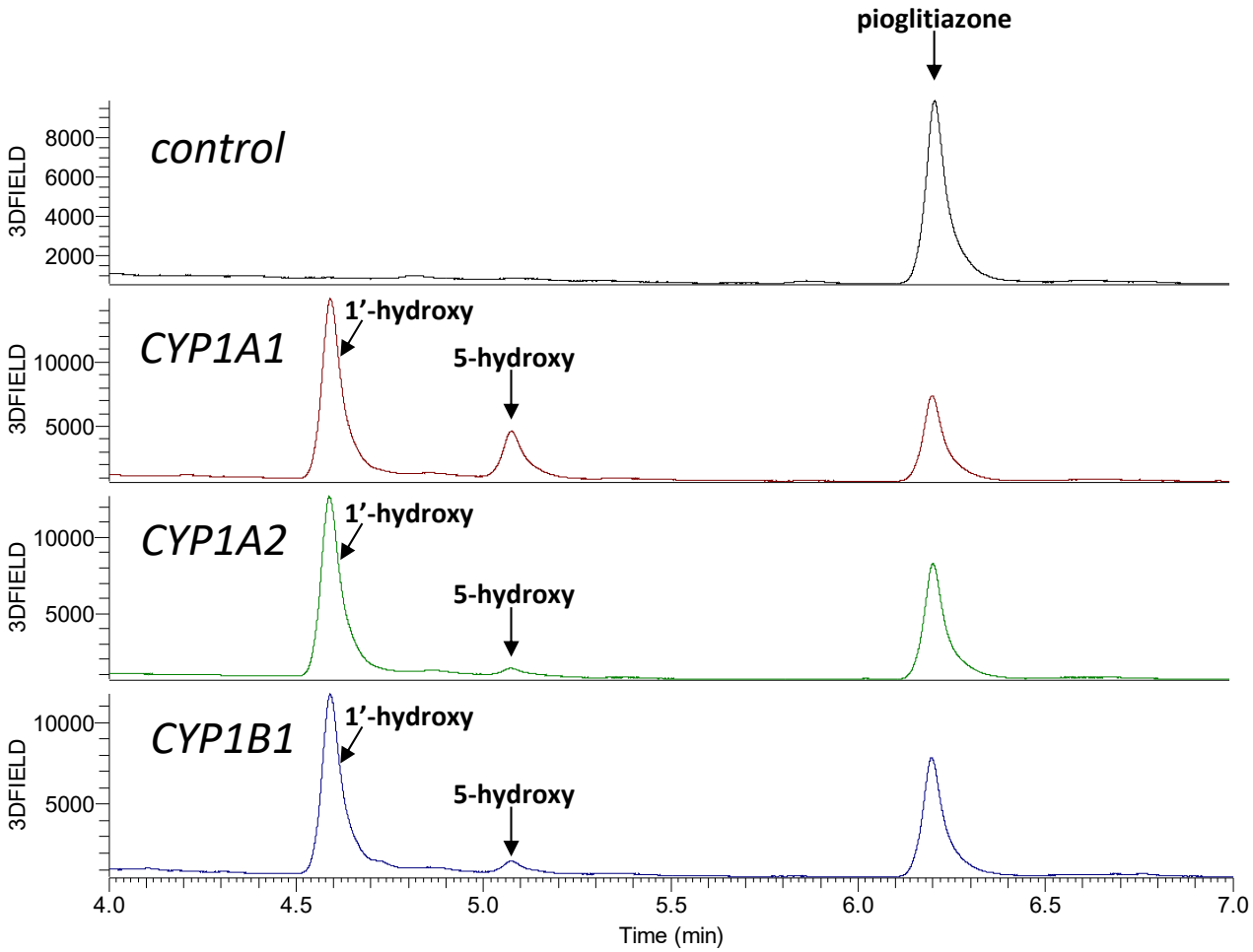

Supplemental Figure 3 (continued)

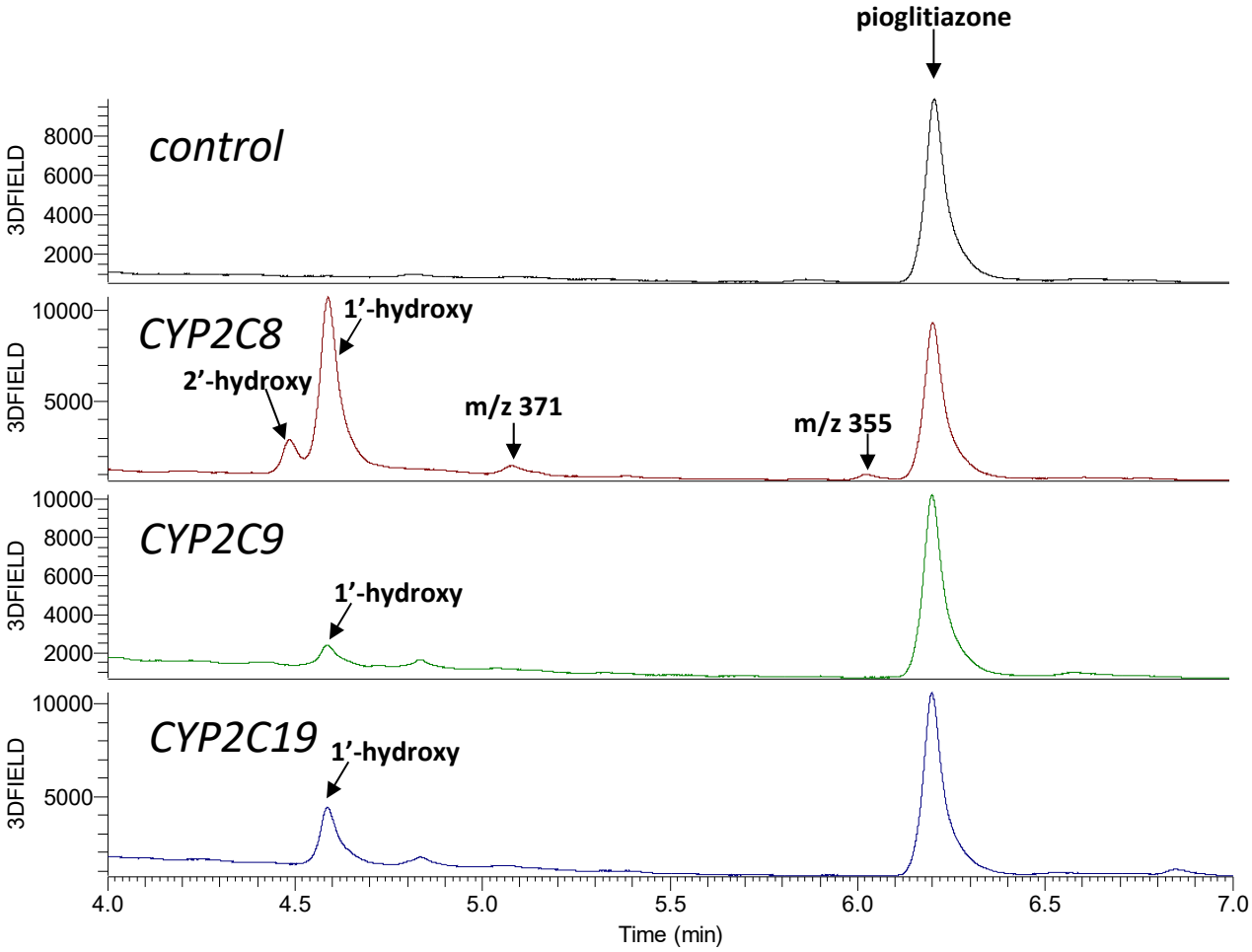

***m/z* 371 is likely a ketone secondary metabolite while *m/z* 355 is a metabolite likely arises from a dehydrogenation reaction.**

Supplemental Figure 3 (continued)

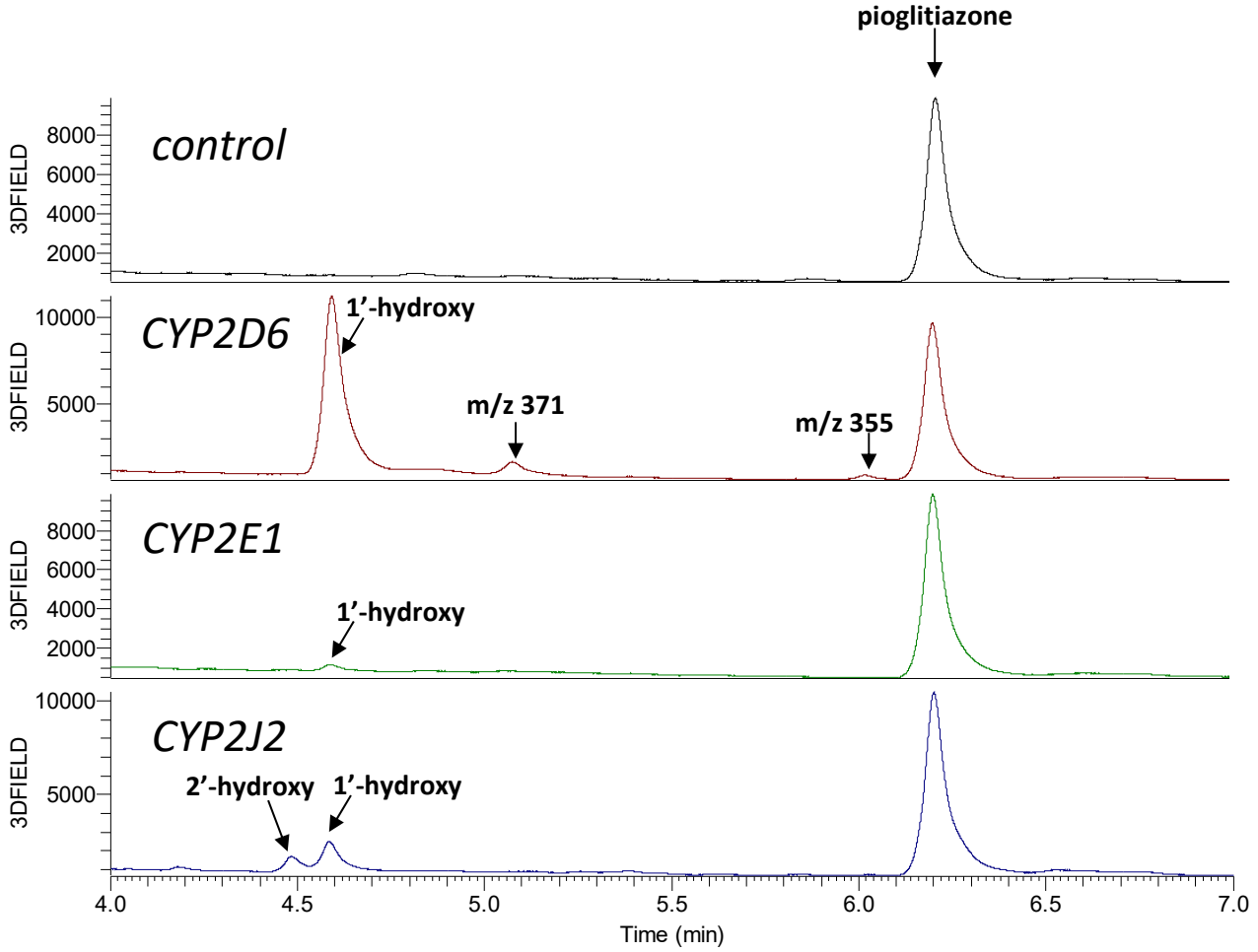

***m/z* 371 is likely a ketone secondary metabolite while *m/z* 355 is a metabolite likely arises from a dehydrogenation reaction.**

Supplemental Figure 3 (continued)

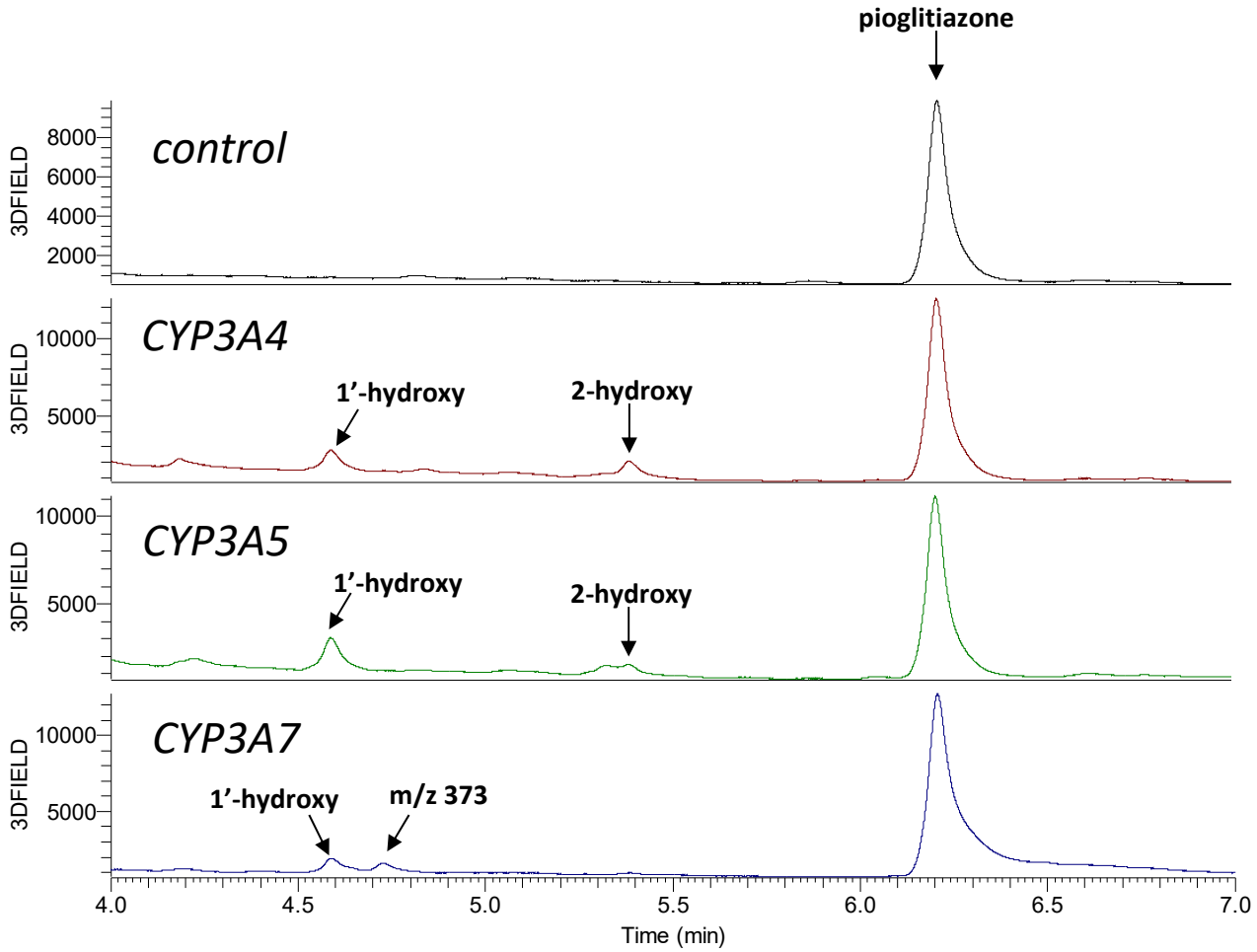

***m/z* 373 is another hydroxy metabolite observed only in CYP3A7 incubations and does not match any of the hydroxy metabolites observed in human liver microsomes.**

Supplemental Figure 3 (continued)

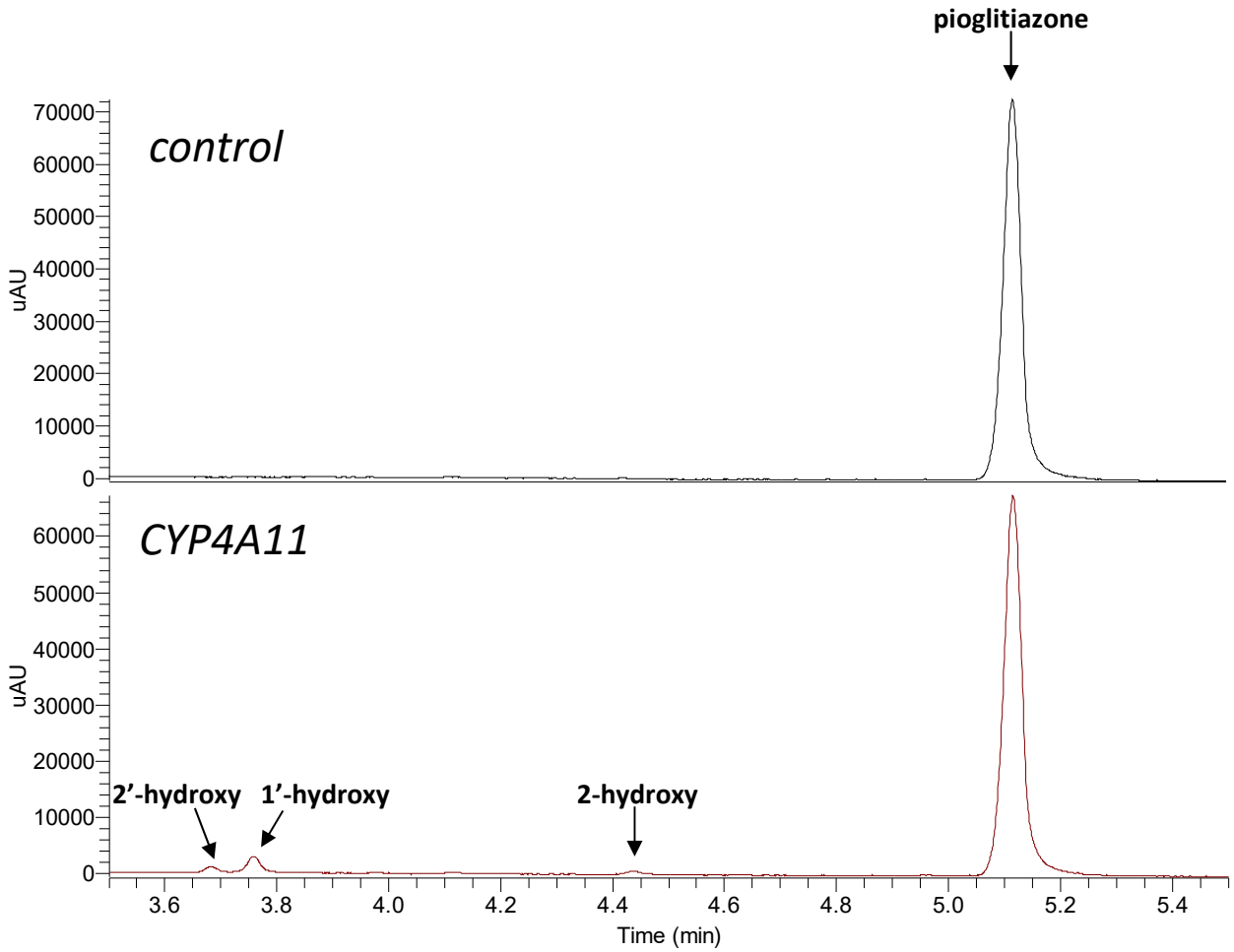

Supplemental Figure 4. HPLC-UV Chromatograms of Metabolite Profiles for Propranolol (λ = 291 nm)

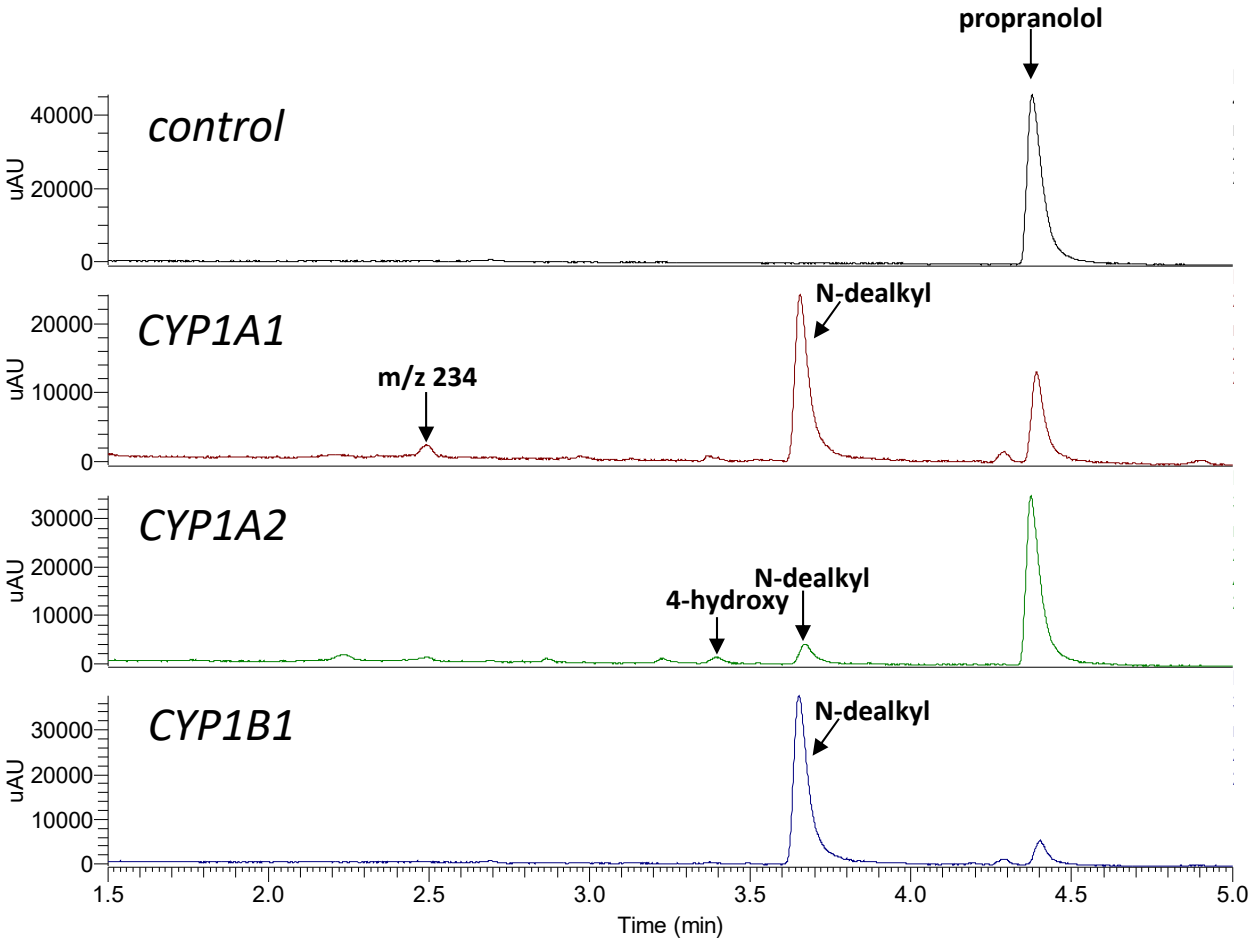

***m/z* 234 represents a likely secondary metabolite arising from hydroxylation of the N-dealkyl metabolite.**

Supplemental Figure 4 (continued)

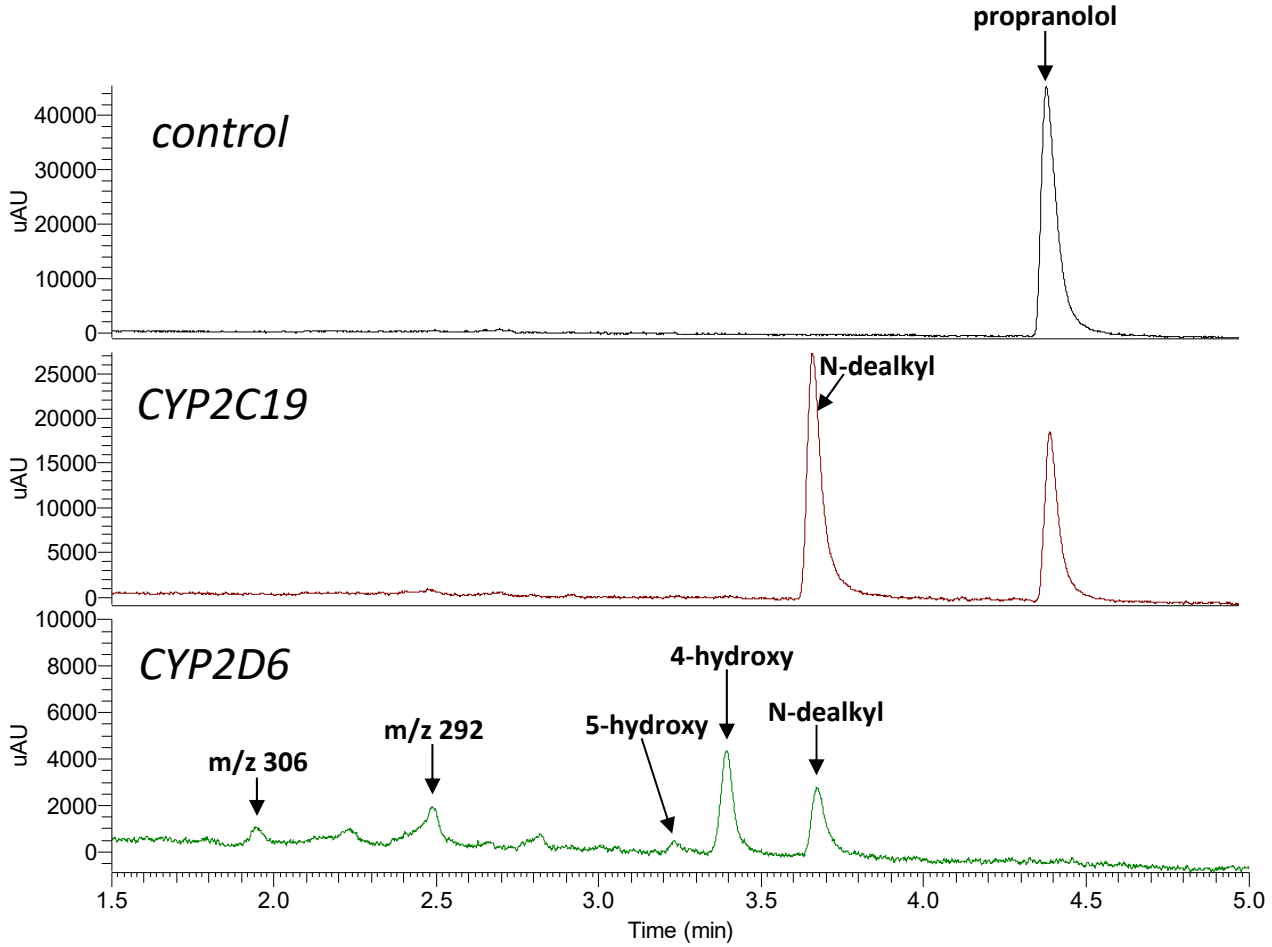

***m/z* 306 and 292 are further oxidations (secondary metabolites).**

Supplemental Figure 5. HPLC-UV Chromatograms of Metabolite Profiles for Risperidone (λ = 278 nm)

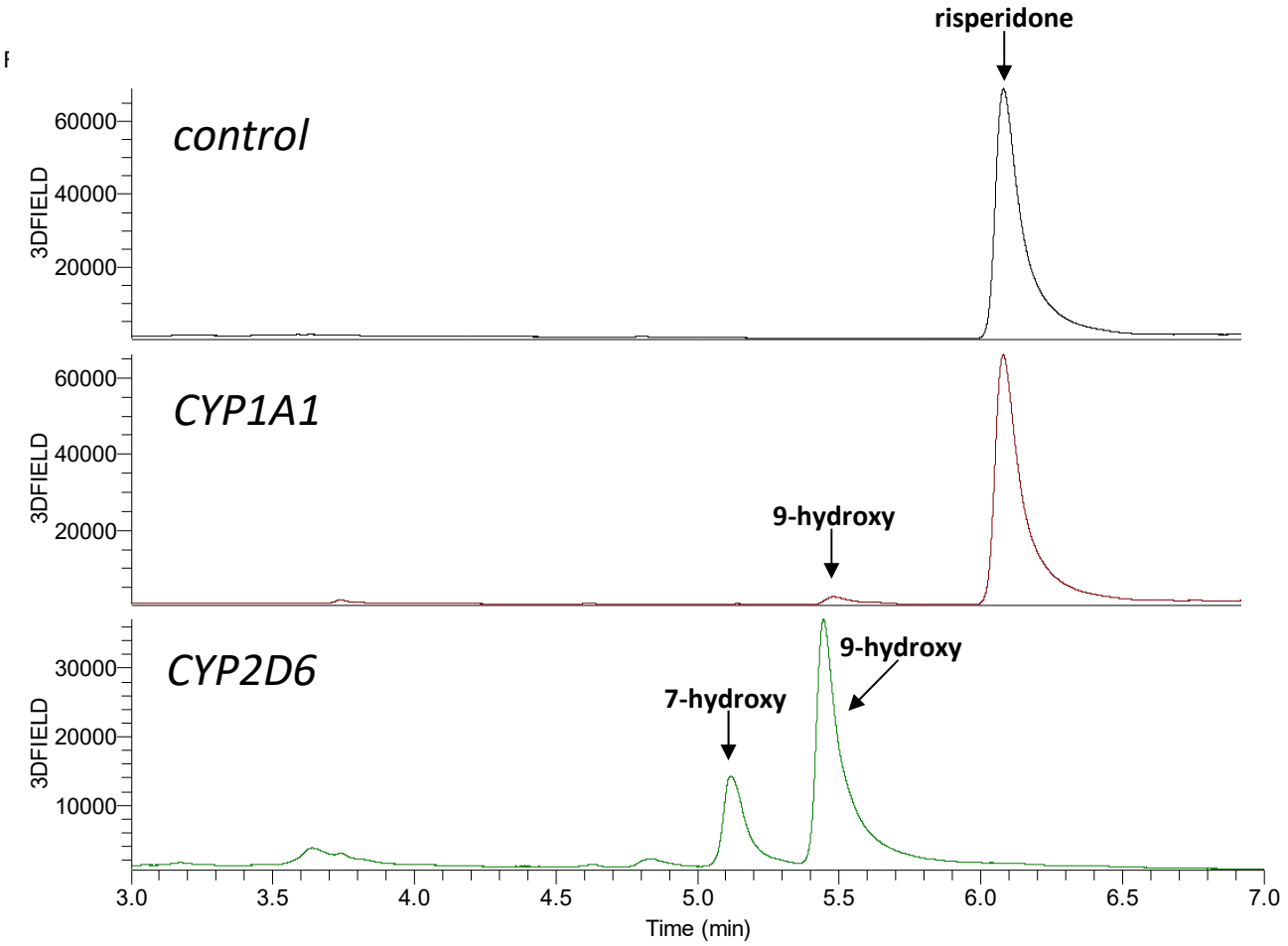

Supplemental Figure 5 (continued)

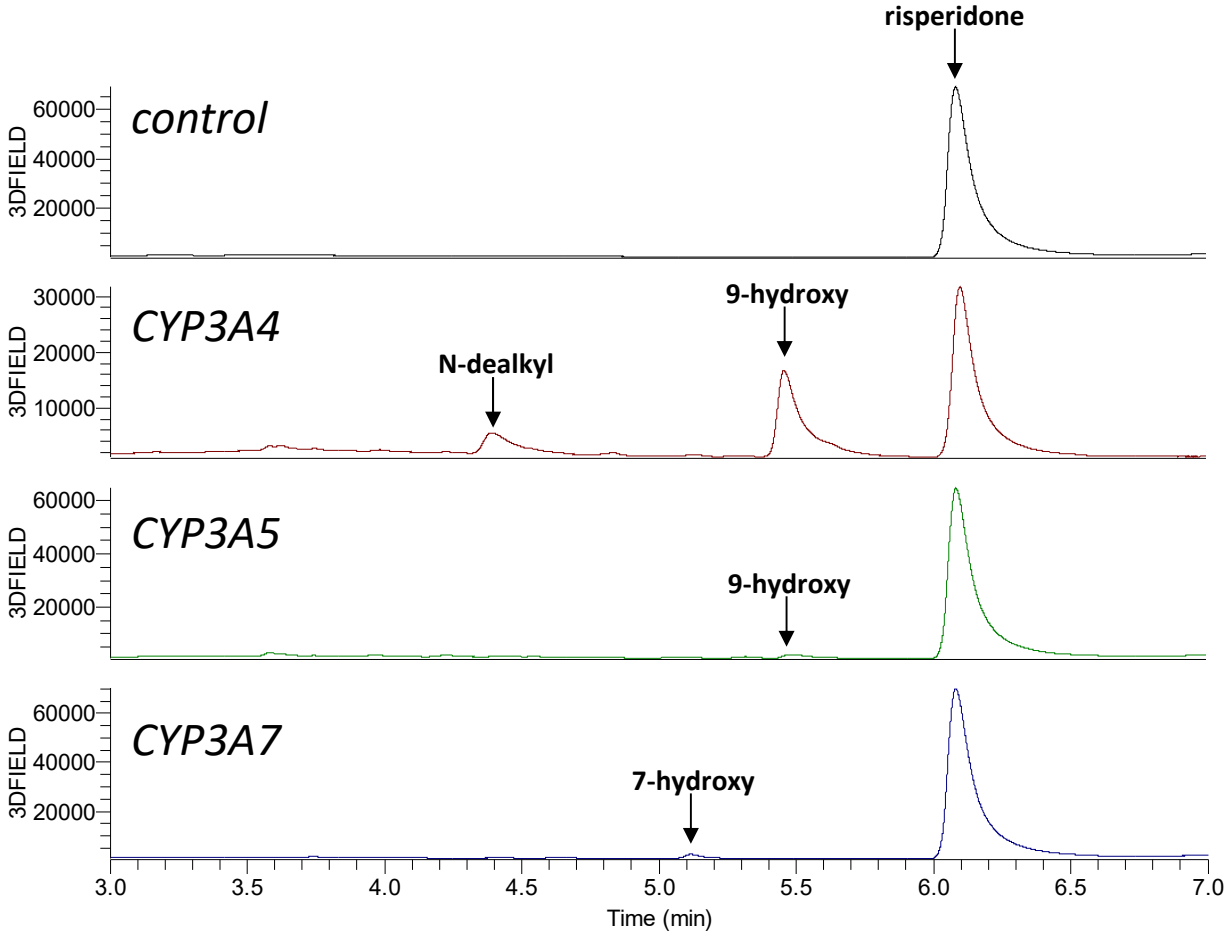

Supplemental Figure 6 - Substrate Saturation Plots for Metabolism of Fluvastatin in Pooled Human Liver Microsomes. Panel A: 5-Hydroxylation; Panel B: 6-Hydroxylation; Panel C: N-Dealkylation

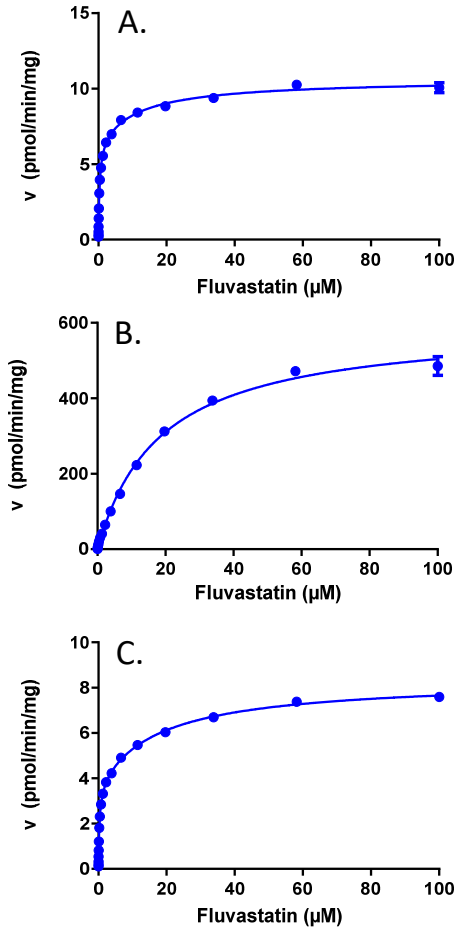

Supplemental Figure 7. Substrate Saturation Plots for Metabolism of Pioglitazone in Pooled Human Liver Microsomes. Panel A: 1'-Hydroxylation; Panel B: 2-Hydroxylation; Panel C: 2'-Hydroxylation; Panel D: 5-Hydroxylation

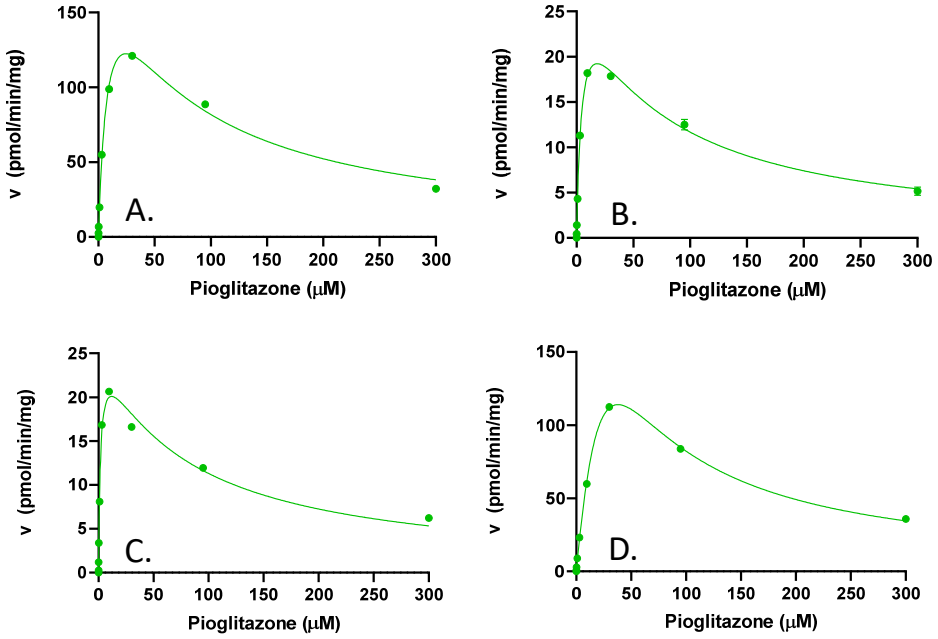

Supplemental Figure 8. Substrate Saturation Plots for Metabolism of Propranolol in Pooled Human Hepatocytes. Panel A: 4-Hydroxylation; Panel B: 5-Hydroxylation; Panel C: N-Dealkylation; Panel D: Glucuronidation. In panel D, the solid line represents one glucuronidation reaction and the dashed line represents the other.

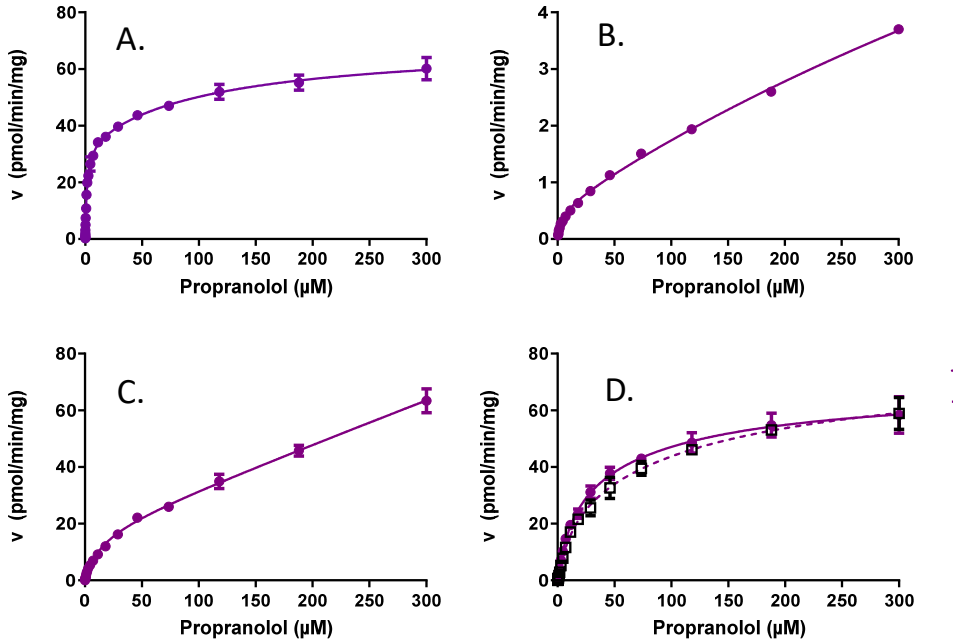

Supplemental Figure 9. Substrate Saturation Plots for Metabolism of Risperidone in Pooled Human Liver Microsomes. Panel A: 9-Hydroxylation; Panel B: 7-Hydroxylation; Panel C: N-Dealkylation

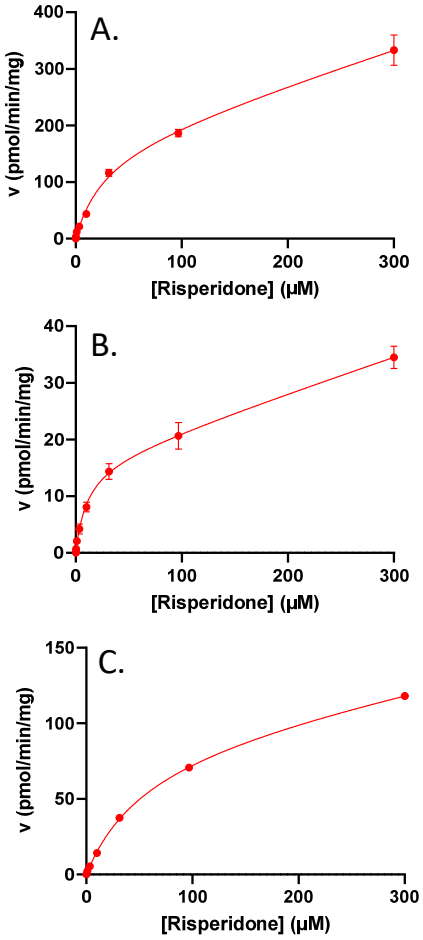

Supplemental Figure 10. Substrate Saturation Plots for Metabolism of Escitalopram in Pooled Human Hepatocytes. Panel A: N-Demethylation; Panel B: N-Deamination

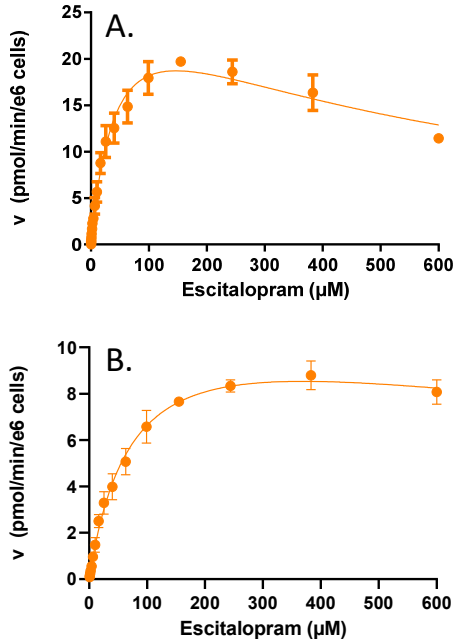

Supplemental Figure 11. Inhibition of Escitalopram N-Demethylation by N-Benzylnirvanol in Human Liver Microsomes. The orange line is the curve for escitalopram N-demethylation and the black curve is for S-mephenytoin 4-hydroxylase as the positive control.

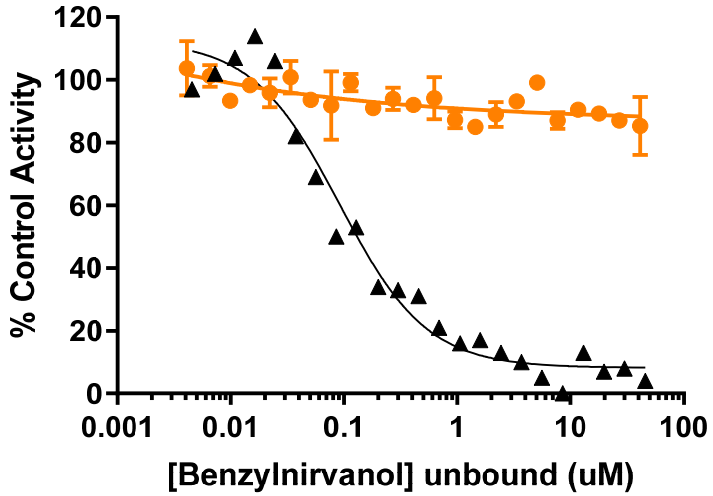

References in Support of Figure 2

Amitriptyline:

Attia TZ, Yamashita T, Hammad MA, Hayasaki A, Sato T, Miyamoto M, Yasuhara Y, Nakamura T, Kagawa Y, Tsujino H, Omar MA, Abdelmageed OH, Derayea SM, Uno T. Effect of cytochrome P450 2C19 and 2C9 amino acid residues 72 and 241 on metabolism of tricyclic antidepressant drugs. Chem Pharm Bull (Tokyo). 2014;62(2):176-81

el-Yazigi A, Chaleby K, Gad A, Raines DA. Steady-state kinetics of fluoxetine and amitriptyline in patients treated with a combination of these drugs as compared with those treated with amitriptyline alone. J Clin Pharmacol. 1995 Jan;35(1):17-21.

Ghahramani P, Ellis SW, Lennard MS, Ramsay LE, Tucker GT. Cytochromes P450 mediating the N-demethylation of amitriptyline. Br J Clin Pharmacol. 1997 Feb;43(2):137-44.

Leucht S, Hackl HJ, Steimer W, Angersbach D, Zimmer R. Effect of adjunctive paroxetine on serum levels and side-effects of tricyclic antidepressants in depressive inpatients. Psychopharmacology (Berl). 2000 Jan;147(4):378-83.

Ryu S, Park S, Lee JH, Kim YR, Na HS, Lim HS, Choi HY, Hwang IY, Lee JG, Park ZW, Oh WY, Kim JM, Choi SE. A Study on CYP2C19 and CYP2D6 Polymorphic Effects on Pharmacokinetics and Pharmacodynamics of Amitriptyline in Healthy Koreans. Clin Transl Sci. 2017 Mar;10(2):93-101

Venkatakrishnan K, Schmider J, Harmatz JS, Ehrenberg BL, von Moltke LL, Graf JA, Mertzanis P, Corbett KE, Rodriguez MC, Shader RI, Greenblatt DJ. Relative contribution of CYP3A to amitriptyline clearance in humans: in vitro and in vivo studies. J Clin Pharmacol. 2001 Oct;41(10):1043-54.

Wagmann L, Meyer MR, Maurer HH. What is the contribution of human FMO3 in the N-oxygenation of selected therapeutic drugs and drugs of abuse? Toxicol Lett. 2016 Sep 6;258:55-70.

Yamaori S, Yamazaki H, Suzuki A, Yamada A, Tani H, Kamidate T, Fujita Ki, Kamataki T. Effects of cytochrome b(5) on drug oxidation activities of human cytochrome P450 (CYP) 3As: similarity of CYP3A5 with CYP3A4 but not CYP3A7. Biochem Pharmacol. 2003 Dec 15;66(12):2333-40.

Amlodipine:

Glesby MJ, Aberg JA, Kendall MA, Fichtenbaum CJ, Hafner R, Hall S, Grosskopf N, Zolopa AR, Gerber JG; Adult AIDS Clinical Trials Group A5159 Protocol Team. Pharmacokinetic interactions between indinavir plus ritonavir and calcium channel blockers. Clin Pharmacol Ther. 2005 Aug;78(2):143-53.

Lee JE, van Heeswijk R, Alves K, Smith F, Garg V. Effect of the hepatitis C virus protease inhibitor telaprevir on the pharmacokinetics of amlodipine and atorvastatin. Antimicrob Agents Chemother. 2011 Oct;55(10):4569-74.

Sasaki M, Maeda A, Fujimura A. Influence of diltiazem on the pharmacokinetics of amlodipine in elderly hypertensive patients. Eur J Clin Pharmacol. 2001 Apr;57(1):85-6.

Zuo XC, Zhou YN, Zhang BK, Yang GP, Cheng ZN, Yuan H, Ouyang DS, Liu SK, Barrett JS, Li PJ, Liu Z, Tan HY, Guo R, Zhou LY, Xie YL, Li ZJ, Li J, Wang CJ, Wang JL. Effect of CYP3A5*3 polymorphism on pharmacokinetic drug interaction between tacrolimus and amlodipine. Drug Metab Pharmacokinet. 2013;28(5):398-405.

Amodiaquine:

Li XQ, Björkman A, Andersson TB, Ridderström M, Masimirembwa CM. Amodiaquine clearance and its metabolism to N-desethylamodiaquine is mediated by CYP2C8: a new high affinity and turnover enzyme-specific probe substrate. J Pharmacol Exp Ther. 2002 Feb;300(2):399-407.

Aripiprazole:

ABILITY Product Label. label (fda.gov)

Azuma J, Hasunuma T, Kubo M, Miyatake M, Koue T, Higashi K, Fujiwara T, Kitahara S, Katano T, Hara S. The relationship between clinical pharmacokinetics of aripiprazole and CYP2D6 genetic polymorphism: effects of CYP enzyme inhibition by coadministration of paroxetine or fluvoxamine. Eur J Clin Pharmacol. 2012 Jan;68(1):29-37.

Kubo M, Koue T, Inaba A, Takeda H, Maune H, Fukuda T, Azuma J. Influence of itraconazole co-administration and CYP2D6 genotype on the pharmacokinetics of the new antipsychotic ARIPIPRAZOLE. Drug Metab Pharmacokinet. 2005 Feb;20(1):55-64.

Atomoxetine:

Belle DJ, Ernest CS, Sauer JM, Smith BP, Thomasson HR, Witcher JW. Effect of potent CYP2D6 inhibition by paroxetine on atomoxetine pharmacokinetics. J Clin Pharmacol. 2002 Nov;42(11):1219-27.

Jung EH, Lee YJ, Kim DH, Kang P, Lim CW, Cho CK, Jang CG, Lee SY, Bae JW. Effects of paroxetine on the pharmacokinetics of atomoxetine and its metabolites in different CYP2D6 genotypes. Arch Pharm Res. 2020 Dec;43(12):1356-1363.

MacKenzie KR, Zhao M, Barzi M, Wang J, Bissig KD, Maletic-Savatic M, Jung SY, Li F. Metabolic profiling of norepinephrine reuptake inhibitor atomoxetine. Eur J Pharm Sci. 2020 Oct 1;153:105488

Ring BJ, Gillespie JS, Eckstein JA, Wrighton SA. Identification of the human cytochromes P450 responsible for atomoxetine metabolism. Drug Metab Dispos. 2002 Mar;30(3):319-23.

Todor I, Popa A, Neag M, Muntean D, Bocsan C, Buzoianu A, Vlase L, Gheldiu AM, Briciu C. Evaluation of a Potential Metabolism-Mediated Drug-Drug Interaction Between Atomoxetine and Bupropion in Healthy Volunteers. J Pharm Pharm Sci. 2016 Apr-Jun;19(2):198-207.

Todor I, Popa A, Neag M, Muntean D, Bocsan C, Buzoianu A, Vlase L, Gheldiu AM, Briciu C. Evaluation of the Potential Pharmacokinetic Interaction between Atomoxetine and Fluvoxamine in Healthy Volunteers. Pharmacology. 2017;99(1-2):84-88.

Bufuralol:

Dayer P, Balant L, Kupfer A, Striberni R, Leemann T. Effect of oxidative polymorphism (debrisoquine/sparteine type) on hepatic first-pass metabolism of bufuralol. Eur J Clin Pharmacol. 1985;28(3):317-20.

Mankowski DC. The role of CYP2C19 in the metabolism of (+/-) bufuralol, the prototypic substrate of CYP2D6. Drug Metab Dispos. 1999 Sep;27(9):1024-8.

Shimada T, Tsumura F, Yamazaki H, Guengerich FP, Inoue K. Characterization of (+/-)-bufuralol hydroxylation activities in liver microsomes of Japanese and Caucasian subjects genotyped for CYP2D6. Pharmacogenetics. 2001 Mar;11(2):143-56.

Bupropion:

Bosilkovska M, Samer CF, Déglon J, Rebsamen M, Staub C, Dayer P, Walder B, Desmeules JA, Daali Y. Geneva cocktail for cytochrome p450 and P-glycoprotein activity assessment using dried blood spots. Clin Pharmacol Ther. 2014 Sep;96(3):349-59.

Chen Y, Liu HF, Liu L, Nguyen K, Jones EB, Fretland AJ. The in vitro metabolism of bupropion revisited: concentration dependent involvement of cytochrome P450 2C19. Xenobiotica. 2010 Aug;40(8):536-46.

Faucette SR, Hawke RL, Shord SS, Lecluyse EL, Lindley CM. Evaluation of the contribution of cytochrome P450 3A4 to human liver microsomal bupropion hydroxylation. Drug Metab Dispos. 2001 Aug;29(8):1123-9.

Turpeinen M, Tolonen A, Uusitalo J, Jalonen J, Pelkonen O, Laine K. Effect of clopidogrel and ticlopidine on cytochrome P450 2B6 activity as measured by bupropion hydroxylation. Clin Pharmacol Ther. 2005 Jun;77(6):553-9

Chlorzoxazone:

Frye RF, Tammara B, Cowart TD, Bramer SL. Effect of disulfiram-mediated CYP2E1 inhibition on the disposition of vesnarinone. J Clin Pharmacol. 1999 Nov;39(11):1177-83.

Gorski JC, Jones DR, Wrighton SA, Hall SD. Contribution of human CYP3A subfamily members to the 6-hydroxylation of chlorzoxazone. Xenobiotica. 1997 Mar;27(3):243-56

Leclercq I, Desager JP, Horsmans Y. Inhibition of chlorzoxazone metabolism, a clinical probe for CYP2E1, by a single ingestion of watercress. Clin Pharmacol Ther. 1998 Aug;64(2):144-9.

Yamamura Y, Koyama N, Umehara K. Comprehensive kinetic analysis and influence of reaction components for chlorzoxazone 6-hydroxylation in human liver microsomes with CYP antibodies. Xenobiotica. 2015 Apr;45(4):353-60.

Desipramine:

Alderman J, Preskorn SH, Greenblatt DJ, Harrison W, Penenberg D, Allison J, Chung M. Desipramine pharmacokinetics when coadministered with paroxetine or sertraline in extensive metabolizers. J Clin Psychopharmacol. 1997 Aug;17(4):284-91.

Ayesh R, Dawling S, Hayler A, Oates NS, Cholerton S, Widdop B, Idle JR, Smith RL. Comparative effects of the diastereoisomers, quinine and quinidine in producing phenocopy debrisoquine poor metabolisers (PMs) in healthy volunteers. Chirality. 1991;3(1):14-8.

Bergstrom RF, Peyton AL, Lemberger L. Quantification and mechanism of the fluoxetine and tricyclic antidepressant interaction. Clin Pharmacol Ther. 1992 Mar;51(3):239-48.

Brøsen K, Gram LF. Quinidine inhibits the 2-hydroxylation of imipramine and desipramine but not the demethylation of imipramine. Eur J Clin Pharmacol. 1989;37(2):155-60.

Madani S, Barilla D, Cramer J, Wang Y, Paul C. Effect of terbinafine on the pharmacokinetics and pharmacodynamics of desipramine in healthy volunteers identified as cytochrome P450 2D6 (CYP2D6) extensive metabolizers. J Clin Pharmacol. 2002 Nov;42(11):1211-8.

Spina E, Steiner E, Ericsson O, Sjöqvist F. Hydroxylation of desmethylimipramine: dependence on the debrisoquin hydroxylation phenotype. Clin Pharmacol Ther. 1987 Mar;41(3):314-9.

Dextromethorphan:

Capon DA, Bochner F, Kerry N, Mikus G, Danz C, Somogyi AA. The influence of CYP2D6 polymorphism and quinidine on the disposition and antitussive effect of dextromethorphan in humans. Clin Pharmacol Ther. 1996 Sep;60(3):295-307.

Huang W, Lin YS, McConn DJ 2nd, Calamia JC, Totah RA, Isoherranen N, Glodowski M, Thummel KE. Evidence of significant contribution from CYP3A5 to hepatic drug metabolism. Drug Metab Dispos. 2004 Dec;32(12):1434-45

McGinnity DF, Parker AJ, Soars M, Riley RJ. Automated definition of the enzymology of drug oxidation by the major human drug metabolizing cytochrome P450s. Drug Metab Dispos. 2000 Nov;28(11):1327-34.

Sager JE, Lutz JD, Foti RS, Davis C, Kunze KL, Isoherranen N. Fluoxetine- and norfluoxetine-mediated complex drug-drug interactions: in vitro to in vivo correlation of effects on CYP2D6, CYP2C19, and CYP3A4. Clin Pharmacol Ther. 2014 Jun;95(6):653-62.

Schmider J, Greenblatt DJ, Fogelman SM, von Moltke LL, Shader RI. Metabolism of dextromethorphan in vitro: involvement of cytochromes P450 2D6 and 3A3/4, with a possible role of 2E1. Biopharm Drug Dispos. 1997 Apr;18(3):227-40.

Storelli F, Matthey A, Lenglet S, Thomas A, Desmeules J, Daali Y. Impact of CYP2D6 Functional Allelic Variations on Phenoconversion and Drug-Drug Interactions. Clin Pharmacol Ther. 2018 Jul;104(1):148-157.

von Moltke LL, Greenblatt DJ, Grassi JM, Granda BW, Venkatakrishnan K, Schmider J, Harmatz JS, Shader RI. Multiple human cytochromes contribute to biotransformation of dextromethorphan in-vitro: role of CYP2C9, CYP2C19, CYP2D6, and CYP3A. J Pharm Pharmacol. 1998 Sep;50(9):997-1004.

Diclofenac:

Bort R, Macé K, Boobis A, Gómez-Lechón MJ, Pfeifer A, Castell J. Hepatic metabolism of diclofenac: role of human CYP in the minor oxidative pathways. Biochem Pharmacol. 1999 Sep 1;58(5):787-96

den Braver MW, den Braver-Sewradj SP, Vermeulen NP, Commandeur JN. Characterization of cytochrome P450 isoforms involved in sequential two-step bioactivation of diclofenac to reactive p-benzoquinone imines. Toxicol Lett. 2016 Jun 24;253:46-54.

Hynninen VV, Olkkola KT, Leino K, Lundgren S, Neuvonen PJ, Rane A, Valtonen M, Laine K. Effect of voriconazole on the pharmacokinetics of diclofenac. Fundam Clin Pharmacol. 2007 Dec;21(6):651-6.

Kovarik JM, Kurki P, Mueller E, Guerret M, Markert E, Alten R, Zeidler H, Genth-Stolzenburg S. Diclofenac combined with cyclosporine in treatment refractory rheumatoid arthritis: longitudinal safety assessment and evidence of a pharmacokinetic/dynamic interaction. J Rheumatol. 1996 Dec;23(12):2033-8.

Ohyama K, Murayama N, Shimizu M, Yamazaki H. Drug interactions of diclofenac and its oxidative metabolite with human liver microsomal cytochrome P450 1A2-dependent drug oxidation. Xenobiotica. 2014 Jan;44(1):10-6.

Transon C, Leemann T, Vogt N, Dayer P. In vivo inhibition profile of cytochrome P450TB (CYP2C9) by (+/-)-fluvastatin. Clin Pharmacol Ther. 1995 Oct;58(4):412-7.

Escitalopram:

Bondolfi G, Lissner C, Kosel M, Eap CB, Baumann P. Fluoxetine augmentation in citalopram non-responders: pharmacokinetic and clinical consequences. Int J Neuropsychopharmacol. 2000 Mar;3(1):55-60.

Malling D, Poulsen MN, Søgaard B. The effect of cimetidine or omeprazole on the pharmacokinetics of escitalopram in healthy subjects. Br J Clin Pharmacol. 2005 Sep;60(3):287-90.

Olesen OV, Linnet K. Studies on the stereoselective metabolism of citalopram by human liver microsomes and cDNA-expressed cytochrome P450 enzymes. Pharmacology. 1999 Dec;59(6):298-309.

Rocha A, Coelho EB, Sampaio SA, Lanchote VL. Omeprazole preferentially inhibits the metabolism of (+)-(S)-citalopram in healthy volunteers. Br J Clin Pharmacol. 2010 Jul;70(1):43-51.

Rochat B, Amey M, Gillet M, Meyer UA, Baumann P. Identification of three cytochrome P450 isozymes involved in N-demethylation of citalopram enantiomers in human liver microsomes. Pharmacogenetics. 1997 Feb;7(1):1-10.

von Moltke LL, Greenblatt DJ, Giancarlo GM, Granda BW, Harmatz JS, Shader RI. Escitalopram (S-citalopram) and its metabolites in vitro: cytochromes mediating biotransformation, inhibitory effects, and comparison to R-citalopram. Drug Metab Dispos. 2001 Aug;29(8):1102-9.

Esomeprazole:

Abelö A, Andersson TB, Antonsson M, Naudot AK, Skånberg I, Weidolf L. Stereoselective metabolism of omeprazole by human cytochrome P450 enzymes. Drug Metab Dispos. 2000 Aug;28(8):966-72.

Hassan-Alin M, Andersson T, Niazi M, Liljeblad M, Persson BA, Röhss K. Studies on drug interactions between esomeprazole, amoxicillin and clarithromycin in healthy subjects. Int J Clin Pharmacol Ther. 2006 Mar;44(3):119-27.

Shiohira H, Yasui-Furukori N, Yamada S, Tateishi T, Akamine Y, Uno T. Hydroxylation of R(+)- and S(-)-omeprazole after racemic dosing are different among the CYP2C19 genotypes. Pharm Res. 2012 Aug;29(8):2310-6.

Febuxostat:

Mukoyoshi M, Nishimura S, Hoshide S, Umeda S, Kanou M, Taniguchi K, Muroga H. In vitro drug-drug interaction studies with febuxostat, a novel non-purine selective inhibitor of xanthine oxidase: plasma protein binding, identification of metabolic enzymes and cytochrome P450 inhibition. Xenobiotica. 2008 May;38(5):496-510.

Fluoxetine:

Fang P, He JY, Han AX, Lan T, Dai DP, Cai JP, Hu GX. Effects of CYP2C19 Variants on Fluoxetine Metabolism in vitro. Pharmacology. 2017;100(1-2):91-97.

Hamelin BA, Turgeon J, Vallée F, Bélanger PM, Paquet F, LeBel M. The disposition of fluoxetine but not sertraline is altered in poor metabolizers of debrisoquin. Clin Pharmacol Ther. 1996 Nov;60(5):512-21.

Llerena A, Dorado P, Berecz R, González AP, Peñas-LLedó EM. Effect of CYP2D6 and CYP2C9 genotypes on fluoxetine and norfluoxetine plasma concentrations during steady-state conditions. Eur J Clin Pharmacol. 2004 Feb;59(12):869-73.

Margolis JM, O'Donnell JP, Mankowski DC, Ekins S, Obach RS. (R)-, (S)-, and racemic fluoxetine N-demethylation by human cytochrome P450 enzymes. Drug Metab Dispos. 2000 Oct;28(10):1187-91.

Scordo MG, Spina E, Dahl ML, Gatti G, Perucca E. Influence of CYP2C9, 2C19 and 2D6 genetic polymorphisms on the steady-state plasma concentrations of the enantiomers of fluoxetine and norfluoxetine. Basic Clin Pharmacol Toxicol. 2005 Nov;97(5):296-301.

Wang Z, Wang S, Huang M, Hu H, Yu L, Zeng S. Characterizing the effect of cytochrome P450 (CYP) 2C8, CYP2C9, and CYP2D6 genetic polymorphisms on stereoselective N-demethylation of fluoxetine. Chirality. 2014 Mar;26(3):166-73.

Fluvastatin:

Fischer V, Johanson L, Heitz F, Tullman R, Graham E, Baldeck JP, Robinson WT. The 3-hydroxy-3-methylglutaryl coenzyme A reductase inhibitor fluvastatin: effect on human cytochrome P-450 and implications for metabolic drug interactions. Drug Metab Dispos. 1999 Mar;27(3):410-6.

Kirchheiner J, Kudlicz D, Meisel C, Bauer S, Meineke I, Roots I, Brockmöller J. Influence of CYP2C9 polymorphisms on the pharmacokinetics and cholesterol-lowering activity of (-)-3S,5R-fluvastatin and (+)-3R,5S-fluvastatin in healthy volunteers. Clin Pharmacol Ther. 2003 Aug;74(2):186-94.

Glyburide:

Lilja JJ, Niemi M, Fredrikson H, Neuvonen PJ. Effects of clarithromycin and grapefruit juice on the pharmacokinetics of glibenclamide. Br J Clin Pharmacol. 2007 Jun;63(6):732-40.

Naritomi Y, Terashita S, Kagayama A. Identification and relative contributions of human cytochrome P450 isoforms involved in the metabolism of glibenclamide and lansoprazole: evaluation of an approach based on the in vitro substrate disappearance rate. Xenobiotica. 2004 May;34(5):415-27.

Niemi M, Cascorbi I, Timm R, Kroemer HK, Neuvonen PJ, Kivistö KT. Glyburide and glimepiride pharmacokinetics in subjects with different CYP2C9 genotypes. Clin Pharmacol Ther. 2002 Sep;72(3):326-32.

Semple CG, Omile C, Buchanan KD, Beastall GH, Paterson KR. Effect of oral verapamil on glibenclamide stimulated insulin secretion. Br J Clin Pharmacol. 1986 Aug;22(2):187-90.

Shuster DL, Risler LJ, Prasad B, Calamia JC, Voellinger JL, Kelly EJ, Unadkat JD, Hebert MF, Shen DD, Thummel KE, Mao Q. Identification of CYP3A7 for glyburide metabolism in human fetal livers. Biochem Pharmacol. 2014 Dec 15;92(4):690-700.

Zharikova OL, Fokina VM, Nanovskaya TN, Hill RA, Mattison DR, Hankins GD, Ahmed MS. Identification of the major human hepatic and placental enzymes responsible for the biotransformation of glyburide. Biochem Pharmacol. 2009 Dec 15;78(12):1483-90.

Zhou L, Naraharisetti SB, Liu L, Wang H, Lin YS, Isoherranen N, Unadkat JD, Hebert MF, Mao Q. Contributions of human cytochrome P450 enzymes to glyburide metabolism. Biopharm Drug Dispos. 2010 May;31(4):228-42.

Granisetron:

Bustos ML, Zhao Y, Chen H, Caritis SN, Venkataramanan R. Polymorphisms in CYP1A1 and CYP3A5 Genes Contribute to the Variability in Granisetron Clearance and Exposure in Pregnant Women with Nausea and Vomiting. Pharmacotherapy. 2016 Dec;36(12):1238-1244.

Lang D, Radtke M, Bairlein M. Highly Variable Expression of CYP1A1 in Human Liver and Impact on Pharmacokinetics of Riociguat and Granisetron in Humans. Chem Res Toxicol. 2019 Jun 17;32(6):1115-1122.

Lansoprazole:

Ieiri I, Kishimoto Y, Okochi H, Momiyama K, Morita T, Kitano M, Morisawa T, Fukushima Y, Nakagawa K, Hasegawa J, Otsubo K, Ishizaki T. Comparison of the kinetic disposition of and serum gastrin change by lansoprazole versus rabeprazole during an 8-day dosing scheme in relation to CYP2C19 polymorphism. Eur J Clin Pharmacol. 2001 Sep;57(6-7):485-92

Itagaki F, Homma M, Yuzawa K, Nishimura M, Naito S, Ueda N, Ohkohchi N, Kohda Y. Effect of lansoprazole and rabeprazole on tacrolimus pharmacokinetics in healthy volunteers with CYP2C19 mutations. J Pharm Pharmacol. 2004 Aug;56(8):1055-9.

Niioka T, Yasui-Furukori N, Uno T, Sugawara K, Kaneko S, Tateishi T. Identification of a single time-point for plasma lansoprazole measurement that adequately reflects area under the concentration-time curve. Ther Drug Monit. 2006 Jun;28(3):321-5.

Pichard L, Curi-Pedrosa R, Bonfils C, Jacqz-Aigrain E, Domergue J, Joyeux H, Cosme J, Guengerich FP, Maurel P. Oxidative metabolism of lansoprazole by human liver cytochromes P450. Mol Pharmacol. 1995 Feb;47(2):410-8.

Vlase L, Popa A, Neag M, Muntean D, Leucuta SE. Effect of fluoxetine on the pharmacokinetics of lansoprazole: a two-treatment period study in healthy male subjects. Clin Drug Investig. 2011 Oct 1;31(10):727-33.

Linezolid:

Bolhuis MS, van Altena R, Uges DR, van der Werf TS, Kosterink JG, Alffenaar JW. Clarithromycin significantly increases linezolid serum concentrations. Antimicrob Agents Chemother. 2010 Dec;54(12):5418-9.

Mephenytoin:

Heyn H, White RB, Stevens JC. Catalytic role of cytochrome P4502B6 in the N-demethylation of S-mephenytoin. Drug Metab Dispos. 1996 Sep;24(9):948-54.

Ko JW, Desta Z, Flockhart DA. Human N-demethylation of (S)-mephenytoin by cytochrome P450s 2C9 and 2B6. Drug Metab Dispos. 1998 Aug;26(8):775-8

Wedlund PJ, Aslanian WS, Jacqz E, McAllister CB, Branch RA, Wilkinson GR. Phenotypic differences in mephenytoin pharmacokinetics in normal subjects. J Pharmacol Exp Ther. 1985 Sep;234(3):662-9.

Metoprolol:

Berger B, Bachmann F, Duthaler U, Krähenbühl S, Haschke M. Cytochrome P450 Enzymes Involved in Metoprolol Metabolism and Use of Metoprolol as a CYP2D6 Phenotyping Probe Drug. Front Pharmacol. 2018 Jul 24;9:774

Goryachkina K, Burbello A, Boldueva S, Babak S, Bergman U, Bertilsson L. Inhibition of metoprolol metabolism and potentiation of its effects by paroxetine in routinely treated patients with acute myocardial infarction (AMI). Eur J Clin Pharmacol. 2008 Mar;64(3):275-82.

Leemann TD, Devi KP, Dayer P. Similar effect of oxidation deficiency (debrisoquine polymorphism) and quinidine on the apparent volume of distribution of (+/-)-metoprolol. Eur J Clin Pharmacol. 1993;45(1):65-71.

Lennard MS, Tucker GT, Silas JH, Freestone S, Ramsay LE, Woods HF. Differential stereoselective metabolism of metoprolol in extensive and poor debrisoquin metabolizers. Clin Pharmacol Ther. 1983 Dec;34(6):732-7.

McLean AJ, Knight R, Harrison PM, Harper RW. Clearance-based oral drug interaction between verapamil and metoprolol and comparison with atenolol. Am J Cardiol. 1985 Jun 1;55(13 Pt 1):1628-9.

Midazolam:

Ekins S, Vandenbranden M, Ring BJ, Gillespie JS, Yang TJ, Gelboin HV, Wrighton SA. Further characterization of the expression in liver and catalytic activity of CYP2B6. J Pharmacol Exp Ther. 1998 Sep;286(3):1253-9.

Emoto C, Iwasaki K. Relative roles of CYP2C19 and CYP3A4/5 in midazolam 1'-hydroxylation. Xenobiotica. 2007 Jun;37(6):592-603.

Goh BC, Lee SC, Wang LZ, Fan L, Guo JY, Lamba J, Schuetz E, Lim R, Lim HL, Ong AB, Lee HS. Explaining interindividual variability of docetaxel pharmacokinetics and pharmacodynamics in Asians through phenotyping and genotyping strategies. J Clin Oncol. 2002 Sep 1;20(17):3683-90.

Gorski JC, Jones DR, Haehner-Daniels BD, Hamman MA, O'Mara EM Jr, Hall SD. The contribution of intestinal and hepatic CYP3A to the interaction between midazolam and clarithromycin. Clin Pharmacol Ther. 1998 Aug;64(2):133-43.

Huang W, Lin YS, McConn DJ 2nd, Calamia JC, Totah RA, Isoherranen N, Glodowski M, Thummel KE. Evidence of significant contribution from CYP3A5 to hepatic drug metabolism. Drug Metab Dispos. 2004 Dec;32(12):1434-45.

Williams JA, Ring BJ, Cantrell VE, Jones DR, Eckstein J, Ruterbories K, Hamman MA, Hall SD, Wrighton SA. Comparative metabolic capabilities of CYP3A4, CYP3A5, and CYP3A7. Drug Metab Dispos. 2002 Aug;30(8):883-91.

Nevirapine:

Erickson DA, Mather G, Trager WF, Levy RH, Keirns JJ. Characterization of the in vitro biotransformation of the HIV-1 reverse transcriptase inhibitor nevirapine by human hepatic cytochromes P-450. Drug Metab Dispos. 1999 Dec;27(12):1488-95.

Olagunju A, Khoo S, Owen A. Pharmacogenetics of nevirapine excretion into breast milk and infants' exposure through breast milk versus postexposure prophylaxis. Pharmacogenomics. 2016 Jun;17(8):891-906.

Saitoh A, Sarles E, Capparelli E, Aweeka F, Kovacs A, Burchett SK, Wiznia A, Nachman S, Fenton T, Spector SA. CYP2B6 genetic variants are associated with nevirapine pharmacokinetics and clinical response in HIV-1-infected children. AIDS. 2007 Oct 18;21(16):2191-9.

Nifedipine:

Bowles SK, Reeves RA, Cardozo L, Edwards DJ. Evaluation of the pharmacokinetic and pharmacodynamic interaction between quinidine and nifedipine. J Clin Pharmacol. 1993 Aug;33(8):727-31.

Karlsson FH, Bouchene S, Hilgendorf C, Dolgos H, Peters SA. Utility of in vitro systems and preclinical data for the prediction of human intestinal first-pass metabolism during drug discovery and preclinical development. Drug Metab Dispos. 2013 Dec;41(12):2033-46.

Ohashi K, Tateishi T, Sudo T, Sakamoto K, Toyosaki N, Hosoda S, Toyo-oka T, Sugimoto K, Kumagai Y, Ebihara A. Effects of diltiazem on the pharmacokinetics of nifedipine. J Cardiovasc Pharmacol. 1990 Jan;15(1):96-101.

Soons PA, van den Berg G, Danhof M, van Brummelen P, Jansen JB, Lamers CB, Breimer DD. Influence of single- and multiple-dose omeprazole treatment on nifedipine pharmacokinetics and effects in healthy subjects. Eur J Clin Pharmacol. 1992;42(3):319-24.

Tateishi T, Ohashi K, Sudo T, Sakamoto K, Toyosaki N, Hosoda S, Toyo-oka T, Kumagai Y, Sugimoto K, Fujimura A, et al. Dose dependent effect of diltiazem on the pharmacokinetics of nifedipine. J Clin Pharmacol. 1989 Nov;29(11):994-7.

Williams JA, Ring BJ, Cantrell VE, Jones DR, Eckstein J, Ruterbories K, Hamman MA, Hall SD, Wrighton SA. Comparative metabolic capabilities of CYP3A4, CYP3A5, and CYP3A7. Drug Metab Dispos. 2002 Aug;30(8):883-91.

Ondansetron:

Sanwald P, David M, Dow J. Characterization of the cytochrome P450 enzymes involved in the in vitro metabolism of dolasetron. Comparison with other indole-containing 5-HT3 antagonists. Drug Metab Dispos. 1996 May;24(5):602-9.

Stamer UM, Lee EH, Rauers NI, Zhang L, Kleine-Brueggeney M, Fimmers R, Stuber F, Musshoff F. CYP2D6- and CYP3A-dependent enantioselective plasma concentrations of ondansetron in postanesthesia care. Anesth Analg. 2011 Jul;113(1):48-54.

Phenacetin:

Dong SX, Ping ZZ, Xiao WZ, Shu CC, Bartoli A, Gatti G, D'Urso S, Perucca E. Effect of active and passive cigarette smoking on CYP1A2-mediated phenacetin disposition in Chinese subjects. Ther Drug Monit. 1998 Aug;20(4):371-5.

Kobayashi K, Nakajima M, Oshima K, Shimada N, Yokoi T, Chiba K. Involvement of CYP2E1 as A low-affinity enzyme in phenacetin O-deethylation in human liver microsomes. Drug Metab Dispos. 1999 Aug;27(8):860-5.

Tassaneeyakul W, Birkett DJ, Veronese ME, McManus ME, Tukey RH, Quattrochi LC, Gelboin HV, Miners JO. Specificity of substrate and inhibitor probes for human cytochromes P450 1A1 and 1A2. J Pharmacol Exp Ther. 1993 Apr;265(1):401-7.

Venkatakrishnan K, von Moltke LL, Greenblatt DJ. Human cytochromes P450 mediating phenacetin O-deethylation in vitro: validation of the high affinity component as an index of CYP1A2 activity. J Pharm Sci. 1998 Dec;87(12):1502-7.

Pioglitazone:

Aquilante CL, Kosmiski LA, Bourne DW, Bushman LR, Daily EB, Hammond KP, Hopley CW, Kadam RS, Kanack AT, Kompella UB, Le M, Predhomme JA, Rower JE, Sidhom MS. Impact of the CYP2C8 *3 polymorphism on the drug-drug interaction between gemfibrozil and pioglitazone. Br J Clin Pharmacol. 2013 Jan;75(1):217-26.

Muschler E, Lal J, Jetter A, Rattay A, Zanger U, Zadoyan G, Fuhr U, Kirchheiner J. The role of human CYP2C8 and CYP2C9 variants in pioglitazone metabolism in vitro. Basic Clin Pharmacol Toxicol. 2009 Dec;105(6):374-9.

Tornio A, Niemi M, Neuvonen PJ, Backman JT. Trimethoprim and the CYP2C8*3 allele have opposite effects on the pharmacokinetics of pioglitazone. Drug Metab Dispos. 2008 Jan;36(1):73-80.

Propafenone:

Afshar M, Thormann W. Capillary electrophoretic investigation of the enantioselective metabolism of propafenone by human cytochrome P-450 SUPERSOMES: Evidence for atypical kinetics by CYP2D6 and CYP3A4. Electrophoresis. 2006 Apr;27(8):1526-36.

Cai WM, Chen B, Zhou Y, Zhang YD. Fluoxetine impairs the CYP2D6-mediated metabolism of propafenone enantiomers in healthy Chinese volunteers. Clin Pharmacol Ther. 1999 Nov;66(5):516-21.

Dilger K, Greiner B, Fromm MF, Hofmann U, Kroemer HK, Eichelbaum M. Consequences of rifampicin treatment on propafenone disposition in extensive and poor metabolizers of CYP2D6. Pharmacogenetics. 1999 Oct;9(5):551-9

Funck-Brentano C, Kroemer HK, Pavlou H, Woosley RL, Roden DM. Genetically-determined interaction between propafenone and low dose quinidine: role of active metabolites in modulating net drug effect. Br J Clin Pharmacol. 1989 Apr;27(4):435-44.

Rouini MR, Afshar M. Effect of CYP2D6 polymorphisms on the pharmacokinetics of propafenone and its two main metabolites. Therapie. 2017 Jun;72(3):373-382.

Uehara S, Murayama N, Yamazaki H, Suemizu H. Regioselective hydroxylation of an antiarrhythmic drug, propafenone, mediated by rat liver cytochrome P450 2D2 differs from that catalyzed by human P450 2D6. Xenobiotica. 2019 Nov;49(11):1323-1331.

Propranolol:

Lennard MS, Jackson PR, Freestone S, Tucker GT, Ramsay LE, Woods HF. The relationship between debrisoquine oxidation phenotype and the pharmacokinetics and pharmacodynamics of propranolol. Br J Clin Pharmacol. 1984 Jun;17(6):679-85

McCourty JC, Silas JH, Tucker GT, Lennard MS. The effect of combined therapy on the pharmacokinetics and pharmacodynamics of verapamil and propranolol in patients with angina pectoris. Br J Clin Pharmacol. 1988 Mar;25(3):349-57.

McGinnity DF, Parker AJ, Soars M, Riley RJ. Automated definition of the enzymology of drug oxidation by the major human drug metabolizing cytochrome P450s. Drug Metab Dispos. 2000 Nov;28(11):1327-34.

Raghuram TC, Koshakji RP, Wilkinson GR, Wood AJ. Polymorphic ability to metabolize propranolol alters 4-hydroxypropranolol levels but not beta blockade. Clin Pharmacol Ther. 1984 Jul;36(1):51-6.

Ward SA, Walle T, Walle UK, Wilkinson GR, Branch RA. Propranolol's metabolism is determined by both mephenytoin and debrisoquin hydroxylase activities. Clin Pharmacol Ther. 1989 Jan;45(1):72-9.

Yasuhara M, Yatsuzuka A, Yamada K, Okumura K, Hori R, Sakurai T, Kawai C. Alteration of propranolol pharmacokinetics and pharmacodynamics by quinidine in man. J Pharmacobiodyn. 1990 Nov;13(11):681-7.

Zhou HH, Anthony LB, Roden DM, Wood AJ. Quinidine reduces clearance of (+)-propranolol more than (-)-propranolol through marked reduction in 4-hydroxylation. Clin Pharmacol Ther. 1990 Jun;47(6):686-93.

Quinidine:

Damkier P, Hansen LL, Brosen K. Effect of diclofenac, disulfiram, itraconazole, grapefruit juice and erythromycin on the pharmacokinetics of quinidine. Br J Clin Pharmacol. 1999 Dec;48(6):829-38.

Kaukonen KM, Olkkola KT, Neuvonen PJ. Itraconazole increases plasma concentrations of quinidine. Clin Pharmacol Ther. 1997 Nov;62(5):510-7

Spinler SA, Cheng JW, Kindwall KE, Charland SL. Possible inhibition of hepatic metabolism of quinidine by erythromycin. Clin Pharmacol Ther. 1995 Jan;57(1):89-94.

Tseng E, Walsky RL, Luzietti RA Jr, Harris JJ, Kosa RE, Goosen TC, Zientek MA, Obach RS. Relative contributions of cytochrome CYP3A4 versus CYP3A5 for CYP3A-cleared drugs assessed in vitro using a CYP3A4-selective inactivator (CYP3cide). Drug Metab Dispos. 2014 Jul;42(7):1163-73.

Ramelteon

ROZEREM Product Label. label (fda.gov)

Risperidone:

Bondolfi G, Eap CB, Bertschy G, Zullino D, Vermeulen A, Baumann P. The effect of fluoxetine on the pharmacokinetics and safety of risperidone in psychotic patients. Pharmacopsychiatry. 2002 Mar;35(2):50-6.

Cabaleiro T, Ochoa D, López-Rodríguez R, Román M, Novalbos J, Ayuso C, Abad-Santos F. Effect of polymorphisms on the pharmacokinetics, pharmacodynamics, and safety of risperidone in healthy volunteers. Hum Psychopharmacol. 2014 Sep;29(5):459-69.

Fang J, Bourin M, Baker GB. Metabolism of risperidone to 9-hydroxyrisperidone by human cytochromes P450 2D6 and 3A4. Naunyn Schmiedebergs Arch Pharmacol. 1999 Feb;359(2):147-51

Gassó P, Mas S, Papagianni K, Ferrando E, de Bobadilla RF, Arnaiz JA, Bioque M, Bernardo M, Lafuente A. Effect of CYP2D6 on risperidone pharmacokinetics and extrapyramidal symptoms in healthy volunteers: results from a pharmacogenetic clinical trial. Pharmacogenomics. 2014 Jan;15(1):17-28.

Mahatthanatrakul W, Sriwiriyajan S, Ridtitid W, Boonleang J, Wongnawa M, Rujimamahasan N, Pipatrattanaseree W. Effect of cytochrome P450 3A4 inhibitor ketoconazole on risperidone pharmacokinetics in healthy volunteers. J Clin Pharm Ther. 2012 Apr;37(2):221-5.

Nakagami T, Yasui-Furukori N, Saito M, Tateishi T, Kaneo S. Effect of verapamil on pharmacokinetics and pharmacodynamics of risperidone: in vivo evidence of involvement of P-glycoprotein in risperidone disposition. Clin Pharmacol Ther. 2005 Jul;78(1):43-51.

Spina E, Avenoso A, Facciolà G, Scordo MG, Ancione M, Madia A. Plasma concentrations of risperidone and 9-hydroxyrisperidone during combined treatment with paroxetine. Ther Drug Monit. 2001 Jun;23(3):223-7.

Rosiglitazone:

Bazargan M, Foster DJ, Davey AK, Muhlhausler BS. Rosiglitazone Metabolism in Human Liver Microsomes Using a Substrate Depletion Method. Drugs R D. 2017 Mar;17(1):189-198.

Niemi M, Backman JT, Granfors M, Laitila J, Neuvonen M, Neuvonen PJ. Gemfibrozil considerably increases the plasma concentrations of rosiglitazone. Diabetologia. 2003 Oct;46(10):1319-23

Park JY, Kim KA, Shin JG, Lee KY. Effect of ketoconazole on the pharmacokinetics of rosiglitazone in healthy subjects. Br J Clin Pharmacol. 2004 Oct;58(4):397-402.

Yeo CW, Lee SJ, Lee SS, Bae SK, Kim EY, Shon JH, Rhee BD, Shin JG. Discovery of a novel allelic variant of CYP2C8, CYP2C8*11, in Asian populations and its clinical effect on the rosiglitazone disposition in vivo. Drug Metab Dispos. 2011 Apr;39(4):711-6.

Saquinavir:

Grub S, Bryson H, Goggin T, Lüdin E, Jorga K. The interaction of saquinavir (soft gelatin capsule) with ketoconazole, erythromycin and rifampicin: comparison of the effect in healthy volunteers and in HIV-infected patients. Eur J Clin Pharmacol. 2001 May;57(2):115-21.

Mouly SJ, Matheny C, Paine MF, Smith G, Lamba J, Lamba V, Pusek SN, Schuetz EG, Stewart PW, Watkins PB. Variation in oral clearance of saquinavir is predicted by CYP3A5*1 genotype but not by enterocyte content of cytochrome P450 3A5. Clin Pharmacol Ther. 2005 Dec;78(6):605-18.

Sertraline:

Gjestad C, Westin AA, Skogvoll E, Spigset O. Effect of proton pump inhibitors on the serum concentrations of the selective serotonin reuptake inhibitors citalopram, escitalopram, and sertraline. Ther Drug Monit. 2015 Feb;37(1):90-7.

Kobayashi K, Ishizuka T, Shimada N, Yoshimura Y, Kamijima K, Chiba K. Sertraline N-demethylation is catalyzed by multiple isoforms of human cytochrome P-450 in vitro. Drug Metab Dispos. 1999 Jul;27(7):763-6.

Lee AJ, Chan WK, Harralson AF, Buffum J, Bui BC. The effects of grapefruit juice on sertraline metabolism: an in vitro and in vivo study. Clin Ther. 1999 Nov;21(11):1890-9.

Saiz-Rodríguez M, Belmonte C, Román M, Ochoa D, Koller D, Talegón M, Ovejero-Benito MC, López-Rodríguez R, Cabaleiro T, Abad-Santos F. Effect of Polymorphisms on the Pharmacokinetics, Pharmacodynamics and Safety of Sertraline in Healthy Volunteers. Basic Clin Pharmacol Toxicol. 2018 May;122(5):501-511.

Ueda N, Yoshimura R, Umene-Nakano W, Ikenouchi-Sugita A, Hori H, Hayashi K, Kodama Y, Nakamura J. Grapefruit juice alters plasma sertraline levels after single ingestion of sertraline in healthy volunteers. World J Biol Psychiatry. 2009;10(4 Pt 3):832-5

Wang JH, Liu ZQ, Wang W, Chen XP, Shu Y, He N, Zhou HH. Pharmacokinetics of sertraline in relation to genetic polymorphism of CYP2C19. Clin Pharmacol Ther. 2001 Jul;70(1):42-7.

Yuce-Artun N, Baskak B, Ozel-Kizil ET, Ozdemir H, Uckun Z, Devrimci-Ozguven H, Suzen HS. Influence of CYP2B6 and CYP2C19 polymorphisms on sertraline metabolism in major depression patients. Int J Clin Pharm. 2016 Apr;38(2):388-94.

Sildenafil:

Hedaya MA, El-Afify DR, El-Maghraby GM. The effect of ciprofloxacin and clarithromycin on sildenafil oral bioavailability in human volunteers. Biopharm Drug Dispos. 2006 Mar;27(2):103-10.

Hesse C, Siedler H, Burhenne J, Riedel KD, Haefeli WE. Fluvoxamine affects sildenafil kinetics and dynamics. J Clin Psychopharmacol. 2005 Dec;25(6):589-92.

Hyland R, Roe EG, Jones BC, Smith DA. Identification of the cytochrome P450 enzymes involved in the N-demethylation of sildenafil. Br J Clin Pharmacol. 2001 Mar;51(3):239-48.

Karlsson FH, Bouchene S, Hilgendorf C, Dolgos H, Peters SA. Utility of in vitro systems and preclinical data for the prediction of human intestinal first-pass metabolism during drug discovery and preclinical development. Drug Metab Dispos. 2013 Dec;41(12):2033-46

Ku HY, Ahn HJ, Seo KA, Kim H, Oh M, Bae SK, Shin JG, Shon JH, Liu KH. The contributions of cytochromes P450 3A4 and 3A5 to the metabolism of the phosphodiesterase type 5 inhibitors sildenafil, udenafil, and vardenafil. Drug Metab Dispos. 2008 Jun;36(6):986-90.

Lee S, Kim AH, Yoon S, Lee J, Lee Y, Ji SC, Yoon SH, Lee S, Yu KS, Jang IJ, Cho JY. The utility of CYP3A activity endogenous markers for evaluating drug-drug interaction between sildenafil and CYP3A inhibitors in healthy subjects. Drug Metab Pharmacokinet. 2021 Feb;36:100368.

Muirhead GJ, Wulff MB, Fielding A, Kleinermans D, Buss N. Pharmacokinetic interactions between sildenafil and saquinavir/ritonavir. Br J Clin Pharmacol. 2000 Aug;50(2):99-107.

Muirhead GJ, Faulkner S, Harness JA, Taubel J. The effects of steady-state erythromycin and azithromycin on the pharmacokinetics of sildenafil in healthy volunteers. Br J Clin Pharmacol. 2002;53 Suppl 1(Suppl 1):37S-43S.

Takahiro R, Nakamura S, Kohno H, Yoshimura N, Nakamura T, Ozawa S, Hirono K, Ichida F, Taguchi M. Contribution of CYP3A isoforms to dealkylation of PDE5 inhibitors: a comparison between sildenafil N-demethylation and tadalafil demethylenation. Biol Pharm Bull. 2015;38(1):58-65.

Warrington JS, Shader RI, von Moltke LL, Greenblatt DJ. In vitro biotransformation of sildenafil (Viagra): identification of human cytochromes and potential drug interactions. Drug Metab Dispos. 2000 Apr;28(4):392-7.

Tacrine:

Becquemont L, Ragueneau I, Le Bot MA, Riche C, Funck-Brentano C, Jaillon P. Influence of the CYP1A2 inhibitor fluvoxamine on tacrine pharmacokinetics in humans. Clin Pharmacol Ther. 1997 Jun;61(6):619-27.

Terfenadine:

Evangelista EA, Kaspera R, Mokadam NA, Jones JP 3rd, Totah RA. Activity, inhibition, and induction of cytochrome P450 2J2 in adult human primary cardiomyocytes. Drug Metab Dispos. 2013 Dec;41(12):2087-94

Honig PK, Woosley RL, Zamani K, Conner DP, Cantilena LR Jr. Changes in the pharmacokinetics and electrocardiographic pharmacodynamics of terfenadine with concomitant administration of erythromycin. Clin Pharmacol Ther. 1992 Sep;52(3):231-8.

Honig PK, Wortham DC, Zamani K, Conner DP, Mullin JC, Cantilena LR. Terfenadine-ketoconazole interaction. Pharmacokinetic and electrocardiographic consequences. JAMA. 1993 Mar 24-31;269(12):1513-8. Erratum in: JAMA 1993 Apr 28;269(16):2088.

Huang W, Lin YS, McConn DJ 2nd, Calamia JC, Totah RA, Isoherranen N, Glodowski M, Thummel KE. Evidence of significant contribution from CYP3A5 to hepatic drug metabolism. Drug Metab Dispos. 2004 Dec;32(12):1434-45.

Jeong D, Park HG, Lim YR, Lee Y, Kim V, Cho MA, Kim D. Terfenadine metabolism of human cytochrome P450 2J2 containing genetic variations (G312R, P351L and P115L). Drug Metab Pharmacokinet. 2018 Feb;33(1):61-66

Jones BC, Hyland R, Ackland M, Tyman CA, Smith DA. Interaction of terfenadine and its primary metabolites with cytochrome P450 2D6. Drug Metab Dispos. 1998 Sep;26(9):875-82.

Testosterone:

Ekins S, Vandenbranden M, Ring BJ, Gillespie JS, Yang TJ, Gelboin HV, Wrighton SA. Further characterization of the expression in liver and catalytic activity of CYP2B6. J Pharmacol Exp Ther. 1998 Sep;286(3):1253-9.

Huang W, Lin YS, McConn DJ 2nd, Calamia JC, Totah RA, Isoherranen N, Glodowski M, Thummel KE. Evidence of significant contribution from CYP3A5 to hepatic drug metabolism. Drug Metab Dispos. 2004 Dec;32(12):1434-45.

Kandel SE, Han LW, Mao Q, Lampe JN. Digging Deeper into CYP3A Testosterone Metabolism: Kinetic, Regioselectivity, and Stereoselectivity Differences between CYP3A4/5 and CYP3A7. Drug Metab Dispos. 2017 Dec;45(12):1266-1275.

Yamazaki H, Shimada T. Progesterone and testosterone hydroxylation by cytochromes P450 2C19, 2C9, and 3A4 in human liver microsomes. Arch Biochem Biophys. 1997 Oct 1;346(1):161-9.

Theophylline:

Loi CM, Day JD, Jue SG, Bush ED, Costello P, Dewey LV, Vestal RE. Dose-dependent inhibition of theophylline metabolism by disulfiram in recovering alcoholics. Clin Pharmacol Ther. 1989 May;45(5):476-86.

Nafziger AN, May JJ, Bertino JS Jr. Inhibition of theophylline elimination by diltiazem therapy. J Clin Pharmacol. 1987 Nov;27(11):862-5.

Sirmans SM, Pieper JA, Lalonde RL, Smith DG, Self TH. Effect of calcium channel blockers on theophylline disposition. Clin Pharmacol Ther. 1988 Jul;44(1):29-34.

Sörgel F, Mahr G, Granneman GR, Stephan U, Nickel P, Muth P. Effects of 2 quinolone antibacterials, temafloxacin and enoxacin, on theophylline pharmacokinetics. Clin Pharmacokinet. 1992;22 Suppl 1:65-74.

Wijnands WJ, Vree TB, van Herwaarden CL. The influence of quinolone derivatives on theophylline clearance. Br J Clin Pharmacol. 1986 Dec;22(6):677-83.

Zhang ZY, Kaminsky LS. Characterization of human cytochromes P450 involved in theophylline 8-hydroxylation. Biochem Pharmacol. 1995 Jul 17;50(2):205-11.

Timolol:

Lennard MS, Lewis RV, Brawn LA, Tucker GT, Ramsay LE, Jackson PR, Woods HF. Timolol metabolism and debrisoquine oxidation polymorphism: a population study. Br J Clin Pharmacol. 1989 Apr;27(4):429-34.

Lewis RV, Lennard MS, Jackson PR, Tucker GT, Ramsay LE, Woods HF. Timolol and atenolol: relationships between oxidation phenotype, pharmacokinetics and pharmacodynamics. Br J Clin Pharmacol. 1985 Mar;19(3):329-33.

Mäenpää J, Volotinen-Maja M, Kautiainen H, Neuvonen M, Niemi M, Neuvonen PJ, Backman JT. Paroxetine markedly increases plasma concentrations of ophthalmic timolol; CYP2D6 inhibitors may increase the risk of cardiovascular adverse effects of 0.5% timolol eye drops. Drug Metab Dispos. 2014 Dec;42(12):2068-76.

McGourty JC, Silas JH, Fleming JJ, McBurney A, Ward JW. Pharmacokinetics and beta-blocking effects of timolol in poor and extensive metabolizers of debrisoquin. Clin Pharmacol Ther. 1985 Oct;38(4):409-13.

Volotinen M, Turpeinen M, Tolonen A, Uusitalo J, Mäenpää J, Pelkonen O. Timolol metabolism in human liver microsomes is mediated principally by CYP2D6. Drug Metab Dispos. 2007 Jul;35(7):1135-41.

Tizanidine:

Granfors MT, Backman JT, Neuvonen M, Neuvonen PJ. Ciprofloxacin greatly increases concentrations and hypotensive effect of tizanidine by inhibiting its cytochrome P450 1A2-mediated presystemic metabolism. Clin Pharmacol Ther. 2004 Dec;76(6):598-606.

Granfors MT, Backman JT, Neuvonen M, Ahonen J, Neuvonen PJ. Fluvoxamine drastically increases concentrations and effects of tizanidine: a potentially hazardous interaction. Clin Pharmacol Ther. 2004 Apr;75(4):331-41.

Granfors MT, Backman JT, Laitila J, Neuvonen PJ. Tizanidine is mainly metabolized by cytochrome p450 1A2 in vitro. Br J Clin Pharmacol. 2004 Mar;57(3):349-53.

Tolbutamide:

Chen K, Wang R, Wen SY, Li J, Wang SQ. Relationship of P450 2C9 genetic polymorphisms in Chinese and the pharmacokinetics of tolbutamide. J Clin Pharm Ther. 2005 Jun;30(3):241-9.

Jayasagar G, Dixit AA, Kishan V, Rao YM. Effect of clarithromycin on the pharmacokinetics of tolbutamide. Drug Metabol Drug Interact. 2000;16(3):207-15.

Kirchheiner J, Bauer S, Meineke I, Rohde W, Prang V, Meisel C, Roots I, Brockmöller J. Impact of CYP2C9 and CYP2C19 polymorphisms on tolbutamide kinetics and the insulin and glucose response in healthy volunteers. Pharmacogenetics. 2002 Mar;12(2):101-9.

Komatsu K, Ito K, Nakajima Y, Kanamitsu Si, Imaoka S, Funae Y, Green CE, Tyson CA, Shimada N, Sugiyama Y. Prediction of in vivo drug-drug interactions between tolbutamide and various sulfonamides in humans based on in vitro experiments. Drug Metab Dispos. 2000 Apr;28(4):475-81

Krishnaiah YS, Satyanarayana S, Visweswaram D. Interaction between tolbutamide and ketoconazole in healthy subjects. Br J Clin Pharmacol. 1994 Feb;37(2):205-7.

Madsen H, Enggaard TP, Hansen LL, Klitgaard NA, Brøsen K. Fluvoxamine inhibits the CYP2C9 catalyzed biotransformation of tolbutamide. Clin Pharmacol Ther. 2001 Jan;69(1):41-7.

McGinnity DF, Parker AJ, Soars M, Riley RJ. Automated definition of the enzymology of drug oxidation by the major human drug metabolizing cytochrome P450s. Drug Metab Dispos. 2000 Nov;28(11):1327-34.

Veronese ME, Miners JO, Randles D, Gregov D, Birkett DJ. Validation of the tolbutamide metabolic ratio for population screening with use of sulfaphenazole to produce model phenotypic poor metabolizers. Clin Pharmacol Ther. 1990 Mar;47(3):403-11.

Tolterodine:

Brynne N, Svanström C, Aberg-Wistedt A, Hallén B, Bertilsson L. Fluoxetine inhibits the metabolism of tolterodine-pharmacokinetic implications and proposed clinical relevance. Br J Clin Pharmacol. 1999 Oct;48(4):553-63.

Brynne N, Forslund C, Hallén B, Gustafsson LL, Bertilsson L. Ketoconazole inhibits the metabolism of tolterodine in subjects with deficient CYP2D6 activity. Br J Clin Pharmacol. 1999 Oct;48(4):564-72.

Malhotra B, Darsey E, Crownover P, Fang J, Glue P. Comparison of pharmacokinetic variability of fesoterodine vs. tolterodine extended release in cytochrome P450 2D6 extensive and poor metabolizers. Br J Clin Pharmacol. 2011 Aug;72(2):226-34.

Oishi M, Chiba K, Malhotra B, Suwa T. Effect of the CYP2D6*10 genotype on tolterodine pharmacokinetics. Drug Metab Dispos. 2010 Sep;38(9):1456-63

Postlind H, DanielsonA, Lindgren A, Andersson SH. Tolterodine, a new muscarinic receptor antagonist, is metabolized by cytochromes P450 2D6 and 3A in human liver microsomes. Drug Metab Dispos. 1998 Apr;26(4):289-93.

Venlafaxine:

Fogelman SM, Schmider J, Venkatakrishnan K, von Moltke LL, Harmatz JS, Shader RI, Greenblatt DJ. O- and N-demethylation of venlafaxine in vitro by human liver microsomes and by microsomes from cDNA-transfected cells: effect of metabolic inhibitors and SSRI antidepressants. Neuropsychopharmacology. 1999 May;20(5):480-90.

Hynninen VV, Olkkola KT, Bertilsson L, Kurkinen K, Neuvonen PJ, Laine K. Effect of terbinafine and voriconazole on the pharmacokinetics of the antidepressant venlafaxine. Clin Pharmacol Ther. 2008 Feb;83(2):342-8.

Jiang F, Kim HD, Na HS, Lee SY, Seo DW, Choi JY, Ha JH, Shin HJ, Kim YH, Chung MW. The influences of CYP2D6 genotypes and drug interactions on the pharmacokinetics of venlafaxine: exploring predictive biomarkers for treatment outcomes. Psychopharmacology (Berl). 2015 Jun;232(11):1899-909.

Kringen MK, Bråten LS, Haslemo T, Molden E. The Influence of Combined CYP2D6 and CYP2C19 Genotypes on Venlafaxine and O-Desmethylvenlafaxine Concentrations in a Large Patient Cohort. J Clin Psychopharmacol. 2020 Mar/Apr;40(2):137-144.

Lessard E, Yessine MA, Hamelin BA, O'Hara G, LeBlanc J, Turgeon J. Influence of CYP2D6 activity on the disposition and cardiovascular toxicity of the antidepressant agent venlafaxine in humans. Pharmacogenetics. 1999 Aug;9(4):435-43.

Lindh JD, Annas A, Meurling L, Dahl ML, AL-Shurbaji A. Effect of ketoconazole on venlafaxine plasma concentrations in extensive and poor metabolisers of debrisoquine. Eur J Clin Pharmacol. 2003 Sep;59(5-6):401-6.

Preskorn S, Patroneva A, Silman H, Jiang Q, Isler JA, Burczynski ME, Ahmed S, Paul J, Nichols AI. Comparison of the pharmacokinetics of venlafaxine extended release and desvenlafaxine in extensive and poor cytochrome P450 2D6 metabolizers. J Clin Psychopharmacol. 2009 Feb;29(1):39-43.

Verapamil:

Busse D, Cosme J, Beaune P, Kroemer HK, Eichelbaum M. Cytochromes of the P450 2C subfamily are the major enzymes involved in the O-demethylation of verapamil in humans. Naunyn Schmiedebergs Arch Pharmacol. 1995 Dec;353(1):116-21.

Ekins S, Bravi G, Ring BJ, Gillespie TA, Gillespie JS, Vandenbranden M, Wrighton SA, Wikel JH. Three-dimensional quantitative structure activity relationship analyses of substrates for CYP2B6. J Pharmacol Exp Ther. 1999 Jan;288(1):21-9.

Fuhr U, Müller-Peltzer H, Kern R, Lopez-Rojas P, Jünemann M, Harder S, Staib AH. Effects of grapefruit juice and smoking on verapamil concentrations in steady state. Eur J Clin Pharmacol. 2002 Apr;58(1):45-53.

Jin Y, Wang YH, Miao J, Li L, Kovacs RJ, Marunde R, Hamman MA, Philips S, Hilligoss J, Hall SD. Cytochrome P450 3A5 genotype is associated with verapamil response in healthy subjects. Clin Pharmacol Ther. 2007 Nov;82(5):579-85

Karlsson FH, Bouchene S, Hilgendorf C, Dolgos H, Peters SA. Utility of in vitro systems and preclinical data for the prediction of human intestinal first-pass metabolism during drug discovery and preclinical development. Drug Metab Dispos. 2013 Dec;41(12):2033-46.

Kroemer HK, Gautier JC, Beaune P, Henderson C, Wolf CR, Eichelbaum M. Identification of P450 enzymes involved in metabolism of verapamil in humans. Naunyn Schmiedebergs Arch Pharmacol. 1993 Sep;348(3):332-7.

Shen L, Fitzloff JF, Cook CS. Differential enantioselectivity and product-dependent activation and inhibition in metabolism of verapamil by human CYP3As. Drug Metab Dispos. 2004 Feb;32(2):186-96.

Warfarin:

Bavisotto LM, Ellis DJ, Milner PG, Combs DL, Irwin I, Canafax DM. Tecarfarin, a novel vitamin K reductase antagonist, is not affected by CYP2C9 and CYP3A4 inhibition following concomitant administration of fluconazole in healthy participants. J Clin Pharmacol. 2011 Apr;51(4):561-74.

Flora DR, Rettie AE, Brundage RC, Tracy TS. CYP2C9 Genotype-Dependent Warfarin Pharmacokinetics: Impact of CYP2C9 Genotype on R- and S-Warfarin and Their Oxidative Metabolites. J Clin Pharmacol. 2017 Mar;57(3):382-393.

Jones DR, Kim SY, Boysen G, Yun CH, Miller GP. Contribution of three CYP3A isoforms to metabolism of R- and S-warfarin. Drug Metab Lett. 2010 Dec;4(4):213-9.

Ngui JS, Chen Q, Shou M, Wang RW, Stearns RA, Baillie TA, Tang W. In vitro stimulation of warfarin metabolism by quinidine: increases in the formation of 4'- and 10-hydroxywarfarin. Drug Metab Dispos. 2001 Jun;29(6):877-86

O'Reilly RA. Interaction of sodium warfarin and disulfiram (antabuse) in man. Ann Intern Med. 1973 Jan;78(1):73-6.

O'Reilly RA. Ticrynafen-racemic warfarin interaction: hepatotoxic or stereoselective? Clin Pharmacol Ther. 1982 Sep;32(3):356-61.

Uno T, Sugimoto K, Sugawara K, Tateishi T. The role of cytochrome P2C19 in R-warfarin pharmacokinetics and its interaction with omeprazole. Ther Drug Monit. 2008 Jun;30(3):276-81.

Zhang Z, Fasco MJ, Huang Z, Guengerich FP, Kaminsky LS. Human cytochromes P4501A1 and P4501A2: R-warfarin metabolism as a probe. Drug Metab Dispos. 1995 Dec;23(12):1339-46